An Experimental Investigation for the Effect of Pulsation on Heat Transfer Characteristics in Pipes

by

Salem Ahmed Aldini

A Thesis Presented to the

FACULTY OF THE COLLEGE OF GRADUATE STUDIES

KING FAHD UNIVERSITY OF PETROLEUM & MINERALS

DHAHRAN, SAUDI ARABIA

In Partial Fulfillment of the
Requirements for the Degree of

MASTER OF SCIENCE

In

MECHANICAL ENGINEERING

August, 1997

INFORMATION TO USERS

This manuscript has been reproduced from the microfilm master. UMI films the text directly from the original or copy submitted. Thus, some thesis and dissertation copies are in typewriter face, while others may be from any type of computer printer.

The quality of this reproduction is dependent upon the quality of the copy submitted. Broken or indistinct print, colored or poor quality illustrations and photographs, print bleedthrough, substandard margins, and improper alignment can adversely affect reproduction.

In the unlikely event that the author did not send UMI a complete manuscript and there are missing pages, these will be noted. Also, if unauthorized copyright material had to be removed, a note will indicate the deletion.

Oversize materials (e.g., maps, drawings, charts) are reproduced by sectioning the original, beginning at the upper left-hand corner and continuing from left to right in equal sections with small overlaps. Each original is also photographed in one exposure and is included in reduced form at the back of the book.

Photographs included in the original manuscript have been reproduced xerographically in this copy. Higher quality 6" x 9" black and white photographic prints are available for any photographs or illustrations appearing in this copy for an additional charge. Contact UMI directly to order.

UMI

A Bell & Howell Information Company
300 North Zeeb Road, Ann Arbor MI 48106-1346 USA
313/761-4700 800/521-0600

AN EXPERIMENTAL INVESTIGATION FOR THE EFFECT OF PULSATION ON HEAT TRANSFER CHARACTERISTICS IN PIPES

BY

SALEM AHMED ALDINI

A Thesis Presented to the

FACULTY OF THE COLLEGE OF GRADUATE STUDIES

KING FAHD UNIVERSITY OF PETROLEUM & MINERALS

DHAHRAN, SAUDI ARABIA

In Partial Fulfillment of the
Requirements for the Degree of

MASTER OF SCIENCE

In

MECHANICAL ENGINEERING

AUGUST, 1997

UMI Number: 1390022

UMI Microform 1390022
Copyright 1998, by UMI Company. All rights reserved.

This microform edition is protected against unauthorized copying under Title 17, United States Code.

UMI
300 North Zeeb Road
Ann Arbor, MI 48103

KING FAHD UNIVERSITY OF PETROLEUM AND MINERALS
DHAHRAN 31261, SAUDI ARABIA

COLLEGE OF GRADUATE STUDIES

This thesis, written by ***SALEM AHMED ALDINI*** *under the direction of his Thesis Advisor and approved by his Thesis Committee, has been presented to and accepted by the Dean of the College of Graduate Studies, in partial fulfillment of the requirements for the degree of* ***MASTER OF SCIENCE*** *in Mechanical Engineering.*

Thesis Committee

Dr. S.A.M Said
(Chairman)

Dr. Muhammed Habib
(Co-Chairman)

Dr. Abdul-Ghani Al-Farayedhi

Saad Ahmed
Dr. Saad Ahmed

Dr. M. O. Budair
Chairman, Mechanical Engineering Dept.

Dr. Abdullah M. Al-Shehri
Dean, College of Graduate Studies

11/5/98
Date

Dedicated

To

my beloved parents

&

my immediate family members

whose patience, forbearance and courage are

instrumental to this accomplishment

Acknowledgment

First and foremost, all praise to Almighty Allah who gave me the courage and patience to carry out this work. I am happy to have a chance to glorify His name in the sincerest way through this small accomplishment and ask Him to accept my efforts.

Acknowledgement is due to King Fahd University of Petroleum and Minerals for providing support to this work.

My deep appreciation goes to my major thesis advisor Dr. Syed Said for his constant help, guidance and the countless hours of attention he devoted throughout the course of this work . His priceless suggestions made this work interesting and challenging for me. He was always kind, understanding and encouraging. Working with him was indeed a wonderful and learning experience which I thoroughly enjoyed.

Thanks are also due to my thesis committee members Dr. Mohamed Habib, Dr. Saad Ahmed and Dr. Abdul-Ghani Al-Farayedhi for their interest, cooperation, advice and constructive criticism.

I am also indebted to the department chairman, Dr. Mohammad O. Budair and other faculty members for their support.

Contents

List of Tables

List of Figures

Abstract

Name: Salem Al-Dini

Title: An Experimental Investigation For The Effect of Pulsation on Heat Transfer Characteristics in Pipes.

Major Field: Mechanical Engineering

Date of Degree: August 1997

Heat transfer characteristics of pulsated turbulent pipe flow under different conditions of pulsation frequency, amplitude and Reynolds number was experimentally investigated. The pipe wall was kept at uniform heat flux. Reynolds number was varied from 5032 to 28,984 while frequency of pulsation ranged from 1 to 8 Hz. The displacement amplitude of pulsation inducing mechanism was varied between 0.0127 m to .0381 m. The behavior of local Nusselt number under the influence of pulsation parameters was studied. The results show enhancement in the local Nusselt number at the entrance region for low Reynolds number. The rate of enhancement decreased as Re increased. However, reduction in the heat transfer coefficient was observed in the fully developed region. Reduction in the mean Nusselt number was observed at all pulsation frequencies and the effect of pulsation is shown to be more significant at high Reynolds numbers. Maximum reduction of about 13% was observed at Re=20,138 and f=6 Hz. It can be concluded that the enhancement in the local heat transfer coefficient is more pronounced in the thermally developing region than in the fully developed region. The effect of pulsation on the mean Nusselt number is insignificant at low values of Re. Also, the effect of amplitude on the mean Nusselt number is insignificant.

MASTER OF SCIENCE DEGREE
KING FAHD UNIVERSITY OF PETROLEUM AND MINERALS
Dhahran, Saudi Arabia
August 1997

ملخص بحث

الاسم : سالم أحمد الديني

العنوان : الكشف التجريبى لتأثير النبضان في خواص الانتقال الحراري داخل أنبوب

الدرجة : ماجستير

التخصص: هندسة ميكانيكية

التاريخ : أغسطس ١٩٩٧ م

تم تجريبياً فحص أثر النبضان علي خواص الانتقال الحراري لهواء مضطرب داخل أنبوب عند حالات مختلفة من ذبذبات النبضان، وأرقام رينولدز، وسعات ذبذبة النبضان. وقد تم تسخين الأنبوب كهربائياً لتوليد فيض حراري منتظم. وقد تفاوتت أرقام رينولدز بين ٥٠٣٢ و ٢٨٩٨٤ في حين أن ذبذبة النبضان تراوحت بين ١ و ٨ هيرتز وفي شكل منحني جيبى تقريباً. بينما تراوحت سعة ذبذبة النبضان الناتج عن جهاز توليد النبضان بين ٥ر٠ بوصة إلي ٥ر١ بوصة. وأظهرت النتائج تحسناً في أرقام نوسلت الموضعية في منطقة التطور الحراري عند أرقام رينولدز المنخفضة، كما أظهرت أن معدل التحسن ينخفض عند زيادة أرقام رينولدز. في المقابل لوحظ انخفاض معدل رقم نوسلت في منطقة التطور الكامل. وأظهرت النتائج أيضاً انخفاضاً لمتوسط رقم نوسلت عند جميع ذبذبات النبضان المدروسة. وتبين النتائج تزايد تأثير ذبذبات النبضان علي رقم نوسلت عند زيادة أرقام رينولدز. ويمكن التلخيص بأن أثر النبضان علي مكافئ انتقال الحرارة يكون ملحوظاً في منطقة التطور الحراري أكثر منه في منطقة التطور الكامل. وأن تأثير ذبذبات وسعات النبضان علي متوسط رقم نوسلت غير ملموس عند أرقام رينولدز المنخفضة.

درجة الماجستير في العلوم

جامعة الملك فهد للبترول والمعادن

الظهران-المملكة العربية السعودية

أغسطس ١٩٩٧ م

Chapter 1

Introduction

1.1 Background

The enhancement and determination of pipe wall convective heat transfer characteristics has likely been one of the most interesting engineering aspects of heat transfer research. This what encourage many investigators to develop different methods to enhance the heat transfer coefficient by which the heat transfer will be enhanced. It has been shown by [1,2] that the rate of heat transfer enhanced considerably in the separated region beyond an abrupt expansion of flow in a circular channel. Significant enhancement on heat transfer has been found also by other investigations [3,4] by the introduction of fins to the heat transfer area of turbulent air flow. The enhancement ratio depends on the Reynolds numbers and fin spacings. Appreciable increase in heat transfer coefficient was recorded when swirl was introduced at the inlet of an abrupt pipe expansion [5]. In addition, increase in heat transfer was recorded [6] by the introduction of wire-coil spring.

Pulsating flow which is defined as flow with periodic fluctuations of the bulk mass flow rate [7], may have the same influence on enhancing the heat transfer coefficients. When pulsations are imposed on a steady flowing fluid it is expected that heat transfer to or from it would be changed. This happens because the pulsation would alter the thickness of the boundary layer and hence the thermal resistance through which heat has to be transferred by laminar diffusion. In the laminar region, this view is also supported by the fact that the velocity profile for pulsating flow is steeper near the wall than for steady flow. It follows from consideration of the Reynolds analogy that the heat transfer should increase under such conditions. A similar process might occur for turbulent flow. As the flow becomes turbulent at high Reynolds numbers, the influence of turbulence becomes significant. Depending on the value of the oscillating frequency and the turbulence intensity either one can be predominant. Hence, it is expected that the combined effect of both turbulence and oscillation on the heat transfer coefficients will depend on the oscillating frequency as well as the turbulence intensity or Reynolds number.

In view of the above, understanding the process of momentum and heat transfer in pulsating flow has become a topic of interest for many engineering applications. The fluid characteristics of pulsating flow inside tubes have been extensively investigated [8,9,10,11] and that many aspects of it are now well understood. However, very little is known about the its heat transfer characteristics . Due to a variety

of control parameters (e.g., frequency, amplitude and Reynolds number), previous work showed conflicting findings for the effect of pulsation on heat transfer. The available experimental data on heat transfer in pulsating flow in a pipe have been inconclusive, and showed conflicting results. Some investigators have reported heat transfer enhancement [12,13], whereas some have reported heat transfer reduction [14]. In some instances, both heat transfer enhancement and reduction were detected in a single experiment [15].

1.2 Engineering Applications

There are several engineering applications in which heat is being transferred to flow that have pulsating motions. This would arise, for example:

- In the inlet and exhaust ducts of reciprocating engines, or in pipelines fed by reciprocating pumps and compressors.
- Flow in systems whose operation is based on the wave action such as the pulse-jet and compressors.
- The screech phenomenon in rocket engines, which is accompanied by high wall temperature, involves flow superimposed oscillations.
- The circulation of blood is a pulsating flow, and the heat interchange between the blood and tissues may, in turn, be influenced by the oscillations.

- Unsteady phenomena in equipment used in power production or process engineering, metallurgy, aviation, chemical and food technology.

1.3 Research Objectives

The main objective of the present work is to investigate the effect of pulsating flow in heat transfer. Particular attention is devoted to the effect of pulsation on average heat transfer coefficient in the thermal entrance and thermally fully developed regions of a turbulent pulsating pipe flow using air as working fluid. To accomplish this objective, an experimental set-up was built. This includes the construction of the air supply unit, the pulsating system and the test sections as well as testing and calibration of the various test rig components and instrumentation.

1.4 Scope of the Present Work

Effect of pulsation on heat transfer in the thermally fully developed region as well as the thermal entrance region of a hydrodynamically fully developed turbulent flow of air was investigated. In this work a total of 90 tests were carried out . Each flow pulsation was preceded by the corresponding steady flow at the same flow Reynolds number. The flow is considered to be incompressible and the fluid properties assumed to be constant along the test section. Flow Reynolds number was varied between 5032 and 28,984 while pulsation frequency ranged from 1 Hz

and 8 Hz. The effect of the amplitude of the induced pulsation was also studied and varied between 0.0127 m to 0.0381 m.

Chapter 2

Literature Review

2.1 Introduction

Many flow configurations may be of interest in pulsating flows. The one of interest to us and which addresses many engineering applications is pulsating internal flows. Pulsating flows in pipes and the attendant heat transfer have been investigated analytically as well as experimentally. In the following, the work done on the hydrodynamic effect of pulsation on velocity and pressure distribution is presented. Then, The effect of flow pulsation on heat transfer in a pipe which has been cited in some of the literature will be described. Both theoretical and experimental work are covered. To date, the available data on heat transfer in pulsating flow have been inconclusive, and they often show conflicting results.

2.2 Studies on Hydrodynamics of Pulsating Flow in a Pipe

In 1971, Gerrard [8] investigated experimentally the effect of pulsation on turbulent flow in a tube. The experiment were made on a pulsating water flow at a mean flow Reynolds number (Re) of 3770 in a cylindrical tube of diameter 0.0381 m. Pulsations were produced by a piston oscillating in simple harmonic motion with a period of 12 s. Turbulence was made visible by means of a sheet of dye produced by electrolysis from a fine wire stretched across the diameter. The sheet of dye was contorted by the turbulent eddies, and cine-photography was used to prove that the velocity of convection is equal to the flow speed except under certain circumstances. The profile of the component of the motion oscillating at the imposed frequency was determined by subtracting the mean flow velocity profile. It was also reported that at any high Reynolds number the structure of turbulence changes during the cycle of pulsation. The turbulent intensity diminishes during acceleration, a phenomenon known as laminarization, and in decelerating flow the turbulent intensity increases. In his experiments the Re lies in the turbulent transition range; consequently the effect of pulsation on the turbulent structure is very noticeable in the appearance of the flow. So that large effects of laminarization were absorbed. In the turbulent phase, the velocity profile was found to possess a central plateau as does the laminar oscillating profile. The level and radial extent of this were little different from the

laminar ones. Also, he observed that near the wall, the turbulent oscillating profile is well represented by the mean velocity power law relationship $u/U\alpha\ (y/a)^{\frac{1}{n}}$. In the laminarized phase, a considerable reduction in turbulent intensity was found at a given Re. The velocity profile for the whole flow (mean plus oscillating) relaxed towards the laminar profile. He concluded that laminarization contributes appreciably to the oscillating component.

In 1976, Ohmi et al. [16] measured the pressure and velocity distribution of pulsating turbulent air and water flows in circular pipes using strain-gauge-type pressure transducer and a hot-wire anemometer, respectively. The Reynolds number varied between 7740 to 95,900 while pulsation frequencies ranged from 0.0432 to 48.0 Hz. The results showed that at low frequencies the time averaged magnitude of the velocity profile is nearly the same as the steady flow velocity profile and the phase angle profile is flat, so that the flow is considered to be in quasi-steady state. The oscillating pressure are also found to decrease, nearly linear along pipe thereby indicating a nearly constant pressure gradient. However, at high frequencies the velocity profile has a peak and becomes flatter while the phase angle increases near the wall, but flat in the central region of the pipe. Approximate solutions were also derived using a four region model and this solution agreed very well with the experimental data.

In 1977, Clamen and Minton [9] used the hydrogen-bubble technique to measure

the velocities of pulsating water flow in a rigid circular pipe. Mean flow with Re between 1275 to 2900 were superimposed on an oscillating flow produced by moving the pipe axially with simple harmonic motion. The velocities in the oscillating boundary layers on the pipe wall were found to be close to those predicted by laminar flow theory, while at the higher Re the velocities near the center of the pipe were lower than those predicted and more uniformly distributed. Also, the intermittency of the periodic bursts of turbulent motion at the higher Reynolds numbers was measured. It was observed that the turbulent intermittency of the flow increased with the mean-flow of Reynolds number and with the frequency and amplitude of the harmonic motion. However, at mean Reynolds numbers below 2000 there were frequencies where an increase in the frequency of the harmonic motion resulted in a small reduction of the turbulent intermittency of the flow. At each mean-flow Reynolds number the turbulent intermittency of the flow was found to be a function of a single parameter: the harmonic flow Reynolds number.

In another investigation carried out by Shemer et al. [10], turbulent and laminar pulsating flows in a straight smooth pipe were compared at identical frequencies and Reynolds numbers. Most measurements were made at mean Reynolds number of 4000, but the influence of Re was checked for $2900 < Re < 7500$. The period of pulsation ranged from 0.5 to 5s, with corresponding change in the non-dimensional frequency parameter $\alpha = R\sqrt{(\frac{\omega}{\nu})}$ (where R, ω and ν are the pipe diameter, the angu-

lar velocity and the kinematic viscosity respectively) from 4.5 to 15. The amplitude of the imposed oscillations did not exceed 35% of the mean in order to avoid flow reversal or relaminarization. Velocities at the exit plane of the pipe and pressure drop along the pipe were measured simultaneously. Velocity measurements were made with arrays of normal hot wire. He observed that the mean properties of the flow are not affected by pulsations in both laminar and turbulent flow regions, when the amplitude is not excessively high. Also, the representation of the oscillating of the flow parameters by amplitude and phase at excitation frequency becomes less accurate for turbulent quantities at higher amplitudes of pulsation. The radial distributions of amplitudes and phases of velocity oscillations are strongly dependent on the flow regime in the pipe. The effect of Reynolds number on the phase distribution in the turbulent flow is substantially more significant. Also, a normalization procedure relating steady and oscillating components in turbulent flow was suggested. A fair agreement was found between the properly normalized time-averaged and time-dependent quantities for the entire range of frequencies considered.

In 1990, Eckmann and Grotbeg [11], used a laser-Doppler velocimeter to analyze volume-cycled oscillatory flow of a Newtonian viscous fluid in a straight circular tube. The axial velocity was measured at radial positions across the diameter of the tube for wide range of amplitude. (A=Stroke distance/tube radius, $2.4 < A < 21.6$) and Womersly parameter ($9 < \alpha < 33$). Transition to turbulence was detected during

the decelerating phase of fluid motion for $500 < R_\delta < 854$, where $R_\delta = \alpha A\sqrt{2}$ is the Reynolds number based on Stokes-Layer thickness. Hot-film anemometer measurements indicated that the core flow remains stable when the boundary layer becomes turbulent for R_δ up to 1310.

In another investigation, Iguchi and Minura [17] investigated the radial propagation of the wall turbulence in pulsatile turbulent flows. Empirical expressions for the propagation time were derived, and models for Reynolds shear stress and eddy viscosity were proposed.

In 1992, Genin et al. [18] investigated the effect of pulsation on hydraulic resistance of turbulent flow of water in a stainless steel tube. The results showed that the coefficient of resistance first of all increases, at frequencies of 2-3Hz it reaches a peak and then as frequency increases further it drops to values close to those of the coefficient of resistance in constant flow rate conditions. The increase in coefficient of resistance was between 10% to 50% for Reynolds number between 1000 to 25000 and pulsation frequencies between 0.5 to 6Hz.

In 1993, Einav and Sokolov [19], measured the velocity profiles and pressure gradient of oscillating pipe flow with a superimposed mean velocity in the transition region. The working fluid was water and the Reynolds number varied between zero to 3000 while the oscillating Reynolds numbers (i.e. $R_{e\omega} = U_\omega D/\nu$) varied between Zero to 4000. The stokes parameter (i.e. $\lambda = d/2\delta$) varied from 7 to 15. The

results showed that depending on the ratio of oscillating Reynolds numbers to the mean Reynolds number (i.e $R_{e\omega}/R_{em}$), phase velocity profiles undergo changes from parabolic like profiles to pseudo turbulent. It was also observed that the transition from laminar to turbulent happens when the mean Reynolds number increases and the oscillating Reynolds number decreases. Also, the flow reversal occurs when the oscillating Reynolds number is greater than the mean Reynolds number. The authors have concluded that as the flow decelerates to a minimum, the eddies die away because the free steam cannot feed them. Also, increasing the frequency parameter at a given Reynolds number squeezes the turbulence out of the flow and the turbulence occurs over a shorter period of the cycle.

In 1995, Carvalho [20] carried out a numerical simulation of behavior of solid inert particles in pulsating flows inside combustors using a computational scheme based on a fourth order Runge-kutta method. The results showed that pulsation decreases the particle residence time in the combustor and increases the rate of particulate emission compared to the steady flow. This becomes significant as pulsation frequency increases and when the particle diameter is close to the diameter for which the particle starts to rise in the ascending gas flow of the combustor.

In view of the above, the following general observations can be made:

- During the cycle of pulsation, pulsation parameters have a noticeable effect on the turbulent structure at high Reynolds numbers[8]. the turbulence intensity

diminishes during acceleration and in decelerating flow it increases. So, the overall effect of pulsation parameters in the turbulence intensity will lead to enhancement or reduction in the heat transfer coefficient. If the turbulence intensity increases enhancement in heat transfer is expected otherwise reduction is expected.

- During pulsation, transition from laminar to turbulent will occur at a lower critical Reynolds number (i.e. $Re_c < 2000$). This will enhance mixing and an increase in heat transfer coefficient is expected.

- Depending on the value of pulsation frequencies, the coefficient of resistance increases or decreases. It follows from Reynolds analogy that this will lead to a change in heat transfer coefficient.

2.3 Heat Transfer of Pulsating Flow in a Pipe

2.3.1 Analytical and Numerical Studies

In 1962, Siegel and Perlmutter [21] obtained an analytical heat transfer solutions for pulsating laminar flow between parallel plates. Two different boundary conditions were considered (i.e. constant surface temperature and constant heat flux). The pulsations were caused by superposing an oscillating pressure gradient on the steady driving pressure of the flow. The heat transfer behavior was obtained along the entire length of the channel; that is, in both the thermal entrance and fully developed

regions. A slug flow (one dimensional) assumption was used to simplify the velocity distribution, but the temperature distributions were two-dimensional. The solution involved three parameters namely; dimensionless frequency, Prandtl number (Pr) and amplitude of pressure oscillation. The results showed a sinusoidal variation of wall temperature and Nusselt number (Nu) along the length of the channel. For high frequency oscillation and pressure pulsation of amplitude near unity, wall heat transfer was not affected. The effect of Prandtl number was mainly on the dimensionless length of oscillation cycle ($x = \pi/M^2 P_r$), (where M is the dimensionless frequency) which was long for small value of Pr and very short for large Pr.

In 1976, Mochlzuki [22] obtained an analytical solution for pulsating Laminar flow in a circular tube. The analysis was made in the fully-developed heat transfer region for a gas of Pr=1.0 and constant heat flux boundary condition. The results showed that when the oscillation frequency is so slow the profiles are essentially quasi-steady. However for higher values of frequencies there will be a time lag between the temperature and velocity profiles as well as between the velocity profile and the pressure gradient resulting in the lag of the wall heat flux. Also, he found that the oscillation amplitude of temperature and wall heat flux decreases as the frequency increases.

Another analytical study was carried out in 1979, by Faghri et al. [23] on laminar fully developed pulsating pipe flow with constant wall heat flux. The velocity field

was modeled as the sum of mean part and a fluctuating part caused by a periodic pressure gradient with zero average over one period. This caused temperature fluctuation and an additional convective term was added in the energy equation which reflects the effect of pulsations in producing higher heat transfer rates. At high pulsating frequencies the Nu was found to be increased. At low frequencies it was found that increase in Nu depends on Prandtl number and another dimensionless pulsating parameter proportional to amplitude.

Another numerical study was carried out in 1989, by krishnan and Sastri [24] on laminar fully developed pulsating pipe flow of fluids with temperature dependent viscosities at constant surface temperature. Pulsation were introduced by superimposing an unsteady pressure gradient over the steady flow value. The differential equations were solved using Crank-Nicholson semi-implicit finite difference formulation with some modification. The results showed that the heat transfer is greatly influenced by pulsation when the fluid is highly viscous. Also they found that the influence of pulsations on heat transfer is more pronounced in the region of development of temperature profile and the heat transfer effects due to pulsation are highly dependent on the non-dimensional distance (i.e. $X = x/(r_0 R_e P_r)$, where r_0 is the radius of the circular pipe). Significant effect of pulsation on the short heat exchange were also reported whereas no effect on the total heat transfer for a very long heat exchanger.

In 1990, Cho and Hyun [25] studied numerically, the heat transfer characteristics of laminar pulsating flow in a pipe with constant wall temperature boundary condition. Complete time dependent boundary layer equations were solved over broad ranges of pulsating frequency parameter and the amplitude of oscillation. The Pr was set at 7.0 to model water. They found out that the influence of oscillation on skin friction is appreciable both in terms of magnitude and phase relation, and that the Nu is either greater or smaller than steady flow value. The Nu trend is amplified as the amplitude increased and when the Prandtl number changed to a lower value below unity. On the other hand, the effect of pulsation was felt in the thin layer near the solid wall.

Kim et al. [26], in 1993, studied numerically the effect of flow pulsation on heat transfer in the thermally developing region of a laminar flow in a channel with uniform wall temperature boundary condition. The unsteady Navier-Stokes equations were solved numerically to simulate a relatively slow through flow at Re= 50 and $P_r = 0.7$. Comprehensive time-dependent flow data were obtained for wide ranges of the pulsation amplitude and the nondimensional pulsation frequency. For large frequencies, the effects of oscillation are confined to a narrow zone adjacent to the walls. The changes in the Nu due to pulsation are pronounced in the entrance region and are minor at far downstream. The effect of frequency on Nu is noticeable when the frequency is small and moderate, but at high frequency Nu is not significantly

affected by the addition of pulsation.

2.3.2 Experimental Investigation

In 1948, Martinelli et al. [27] investigated the heat transfer in a semi-sinusoidal flow of water which is pumped by a reciprocating pump to a 0.0107 m diameter vertical tube with a uniform wall temperature. Reynolds number varied from 2000 to 77,000 and the oscillating frequency ranged from 0.2167 Hz to 4.4167 Hz. In this range of frequency the Nusselt number was not affected. However, in the turbulent flow regime, Nu was slightly higher than the steady flow value for $R_e > 4500$ and was slightly lower for $R_e < 4500$.

West and Taylor [12], in 1952, investigated experimentally the effect of partially damped pulsations from a reciprocating pump on the heat transfer coefficient of water in a 0.05 m diameter, 6.0 m long horizontal tube of a steam heated heat exchanger. The Reynolds number was varied from 30,000 to 85,000. An increase between 60% and 70% in heat transfer coefficient was recorded at a frequency of 1.6 Hz.

In 1954, Haveman and Rao [28] studied the effect of pulsating flow in heat transfer of air at atmospheric pressure, flowing in a horizontal pipe of 0.0254 m, inside diameter and 2.0828 m, effective length. Pulsation was produced by means of a puppet valve operating in the path of the flow. Reynolds number was varied

from 5000 to 3500 and the frequency of pressure pulsation from 5 to 33 Hz. It was found that Nu changed up to about 30% under different conditions of frequency, amplitude, wave form and Re. The change was negative below certain frequency and positive above it. Only a negligible change was found when the amplitude of the pulsation was very low while at higher amplitude Nu change was found to be a function of amplitude, frequency and Re.

In 1961, Lemlich [29] investigated the effect of pulsation on heat transfer coefficient of water in a 0.0127 m. diameter, 0.9144 m. long copper double pipe, steam to water heat exchanger. An electrical-hydraulic pulsator consisting of a solenoid valve triggered by an adjustable pressure switch was employed. The Reynolds number varied from 2000 to 20,000, while frequency of 1.5 Hz was attained. The overall heat transfer coefficient was increased by as much as 80% at Re=2000 depending on the upstream location of the solenoid valve. The closer the valve to the exchanger inlet the better the enhancement.

In 1961, Lemlich and Hwu [30] studied experimentally the effect of acoustic vibration on forced convective heat transfer. Sound at resonant frequencies of 198, 256 and 322 Hz, as well as sound at nonresonant frequencies was imposed on air flowing at Reynolds number of 560 to 5,900 in the double pipe, steam to air heat exchanger. The results showed an increase in the Nusselt number of up to 51% in the Laminar region and up to 27% in the turbulent region. It was observed that the

improvement peaked sharply at resonance and increased with both amplitude and resonant frequency. Also, correlations for the experimental results were obtained.

In 1965, Baird et al. [31] studied the effect of large flow pulsations on heat transfer of cold water passed upwards through a steam-jacketed copper tube of 0.01905 m, internal diameter with a heat transfer area of 0.05546 m^2. Sinusoidal pulsations were produced by means of an air pulser connected to the water line. The pulser consisted of an injection and exhaust valve operated by a balsa-wood float and connected to a glass tube. The Reynolds number varied between 4300 to 16,200, while the frequency of pulsation ranged from 0.8 Hz to 1.7 Hz. The amplitude of pulsation varied from 0.0274 m to 0.335 m. The results showed maximum enhancement of about 41% based on overall heat transfer coefficient for Re less than 8000.

Mamayev et al. [15], in 1976, studied the effect of pulsation frequency on air flowing in a stainless steel vertical tube with internal diameter of 0.008 m and 0.8 m in length using constant heat flux boundary condition. The Reynolds number varied between 540 to 11,000 while the frequency of pulsation ranged from 0.5 Hz to 24.0Hz. The pulsator located downstream of the flow consisted of a magnetic valve driven by a D.C. motor through a rigid pool rod. The results showed that for laminar flow at $f \leq 2$ Hz, the heat transfer rates for pulsed air flow are lower than for unpulsed flow. As the frequency increased from 5 to 24Hzs, the relative heat transfer coefficient (Nu_p/Nu_s) increased, with the highest increment (as much as

44%) observed at f=12 Hz. As f is increased to between 20 Hz and 24 while R_e is held constant the relative heat transfer coefficient drops exponentially and steeply. At f=0.5 to 12 Hz, this ratio tends to unity, while at $f \geq 20$Hz the pulsations have a negative effect on the heat transfer rate.

In 1979, Karamecan and Gainer [13] studied the effect of pulsation frequency on water flowing in heat exchanger. Two heat exchangers, which only differed in length (1.8 and 0.9 m, respectively), were used in the experiments. They both consisted basically of a copper tube, having a nominal inside diameter of 0.02 m., mounted concentrically within an outer shell of 0.057 m, i.d. made of stainless steel, The core carried water heated by the steam flowing counter currently in the annulus. Pulsation in the water stream were generated by reciprocating pump, which consisted of a brass cylinder 0.095 m. in diameter and 0.127 m. in length containing an aluminum piston inside. In order to convert the cyclic output of the transmission into a back-and-forth movement for the piston, a coupling mechanism was devised. Pulsation frequencies ranged up to 300 cycles per minute, and five different displacement amplitudes were used at each flow rate investigated. The Reynolds numbers were in the ranges of 1000 to 50,000. The heat transfer coefficient was found to increase with pulsations, with the highest enhancement observed in the transition flow regime.

In, 1982 krishnan and Sastri [32] carried out on experimental investigation on

the effect of pulsating flows on the heat transfer coefficient of water in a 0.0254 m. diameter, 3.048 m. long copper double pipe, steam to water heat exchanger. The pulsator located just before the inlet of the heat exchanger consisted of a rotating plug valve driven by a variable speed motor through a stepped pulley. the Reynolds number varied between 500 to 2200 while the frequency of pulsation ranged up to 7.0 Hz. The results showed that the effect of the amplitude of pulsation and the dimensionless frequency (i.e. $\omega = fr_0/2U_m$) on heat transfer is negligible. Also, the improvement in heat transfer due to pulsation is more pronounced in the region of the thermal boundary development.

In 1985, Liao and Wang [14] studied the effect of pulsation on heat transfer coefficient of turbulent fully developed flow of water in a stainless steel tube of 1.092 cm in diameter and 1.96 m in length. Flow pulsation was produced by an oscillator consisting of a motor-driven ball valve system. The period of pulsation for one cycle ranged form 2.6 to 13.5 seconds and Re from 3400 to 27,000. It was found that in the range of the experiment, the heat transfer coefficients with pulsation are reduced and the magnitude of reduction mainly depends on amplitudes. however, with flow reversal, there was significant increase in heat transfer coefficient.

In 1989, Al-Haddad and Al-Binaly [33] developed an empirical correlation of heat transfer coefficient for pulsating flow of air through a rigid circular copper pipe of 0.127 m in diameter and 2 m. in length. The copper pipe is fixed for natural

convection air cooling. Pulsation was introduced by a piston cylinder connected to a electric driven motor with variable voltage. The Reynolds number ranged between 1000 and 40,000 while pulsation frequency varied from 5.0 Hz to 60 Hz in sine form. A critical value of 2.1×10^5 for the combined dimensionless number (Re ω' where ω' is the dimensionless frequency) was noticed. Below this value no significant improvement was obtained in Nu. However, above this value Nu increased asymptotically.

Another experimental study was carried out in 1992, by Kang et al. [34] on convection heat transfer from a heated tube to an oscillating flow in a sterling engine with air and helium as working fluids. The dependence of temperature distribution and heat transfer rates on the oscillating frequency, swept volume ratio and mean pressure of a sterling cycle machine was investigated in detail. The experiments were carried out in the range of oscillating frequency 0-16 Hz and swept volume ratio 0.67-1.33 due to the operating limitation of the experimental arrangement. It was found that the heat transfer rate from the tube wall to the flow was increased significantly as the oscillating frequency or swept volume ratio or mean pressure increases. Also, helium was recommended than air for working gas in order to investigate the heat transfer characteristics because it gives more significant dimensionless temperature difference than air at the same condition.

In 1992, Genin et al. [18] studied the effect of pulsation on heat transfer co-

efficient of water flowing in a thin-walled tube made from stainless steel with an internal diameter of 0.029 m which is heated by an electric current passed directly along the wall of the tube. Pulsation was produced by means of a plug -type pulsator. Reynolds number was varied from 2000 to 25,000 and the frequency can be varied from 0.5 to 6 Hz. The results showed that the effect of pulsation on the heat transfer is negligible and it falls within the error limits of the experiment.

In 1993, Tang and Cheng [35] carried out an experiment to study oscillatory heat transfer in a periodically reversing pipe flow. The Reynolds number varied from 7 to 7000 and the frequency from 0.01 to 3Hz. The dimensionless stroke (i.e. $A_w = X_{max}/L$ where X_{max} is the fluid stroke) was varied from 0.06 to 2.21. In this study a multivariate statistical analysis was used to obtain a correlation equation for the cycle-averaged Nusselt number in terms of the Reynolds number, the dynamic Reynolds number (i.e. $R_{e\omega} = \rho\omega D^2/\mu$) where ω is the cycle-averaged velocity and the dimensionless fluid displacement.

In 1993, Isshiki et al. [36] carried out an experimental investigation on the effect of pulsation on heat transfer in fully developed turbulent air flow in a 47.6 mm diameter stainless steel pipe heated with constant wall heat flux. A blower, located downstream was used to suck in air through a bellmouth to the velocity development section that varied between 32 to 116 diameters and through temperature development section of 2.45 m and test section of 0.35 m lengths, respectively.

Flow modulation was generated by rotating 1.0 mm thick circular vane attached to a 5.0 mm diameter axis located perpendicularly in the pipe and downstream after the test section. Turbulent quantities were measured using hot and cold wire technique at time-averaged Reynolds number of about 7450 while pulsation frequencies are in the ratio of 0.32, 0.61, 1.7 and 3.3 to the turbulent bursting frequency (9.73 Hz). The result showed no change in the time averaged characteristics of the flow and thermal fields near the wall. Nusselt number was found to vary periodically at lower pulsating frequencies than the bursting frequency while it is unchanged at higher frequencies. The summary of previous experimental work on heat transfer in pulsating flows and the trend of findings is shown in Table 2.1.

2.4 Models of Pulsating Turbulent Flows

In view of the above, the experimental data available on how pulses in the flow rate affect heat transfer are contradictory. So, the hydrodynamics and thermal behavior of pulsating flows have attracted the use of certain models of turbulence for pulsating flow in making sense out of these contradictions. Two of these models are discussed here: quasi-steady flow model and viscous sublayer renewal model.

2.4.1 Quasi-Steady Flow Model

Quasi-Steady state model has been suggested by many investigators as a first approximation to pulsating flow. In the approach based on the model of quasi-steady

Table 2.1 Summary of previous experimental work on heat transfer in pulsating flows

Date	**Investigators**	**Working Fluid / Nature of flow**	**Summary of Investigation**	**Results / Remarks**
1943	Martinelli et al.	Steam heated **water** (Vert. Heat exch.)	**$2000 \le Re \le 77000$** **$0.217 \le f \le 4.417$Hz** Pulsator: recr.pump semi sinus pulsation	No significant change in Nu
1952	West and Taylor	Steam heated **water** (Heat exch)	**$30000 \le Re \le 85000$** **$f = 1.67$ Hz** **$1.0 \le A_r \le 1.56$** Pulsator: rec.pump	**Increase** of **60 - 70 %** in h.t.c at f as A_r increases.
1954	Haveman and Rao	Steam heated **air**, fully developed turbulent flow.	**$5000 \le Re \le 35000$** **$5 \le f \le 33$Hz** Pulsator: puppet valve operating in path of the flow	Nu changed up to 30% **increase** for f above certain value & **decrease** below it.
1961	Lemlich R.	Steam heated **water** (Heat exch)	**$2000 \le Re \le 20000$** **$0 \le f \le 1.5$Hz** Pulsator:Solenoid valve.	**Increase** of **80%** in Nu at Re= 2000 when pulstor upstream
1961	Lemlich R.	Steam heated **air** (Heat exch)	**$560 \le Re \le 5900$** **$180 \le f \le 340$ Hz** Electro magnetc driver actuated thru audio ampl.by varia sinus audi signal gen	**Increase** of 51% in Nu in laminar & up to 27% in the turbulent region
1966	Baird et al.	Steam heated **water** (Heat exch)	**$4300 \le Re \le 16200$** **$0.7 \le f \le 1.7$ Hz** **$0.027 \le A \le 0.335$m** sine pulse gen by air plser oper by b.w.fl	**Increase** of 41% in Nu at Re < 8000 at high **A** leading to flow reversal
1976	Mamayev. et al	**Air** fully dev. flow in a tube	**$540 \le Re \le 11000$** **$0.5 \le f \le 24$ Hz** Pulsator: magnetic valve (loc. downst) driven by a D.C motor	**Decrease** in htc at f < 2Hz and **increase** at f >5Hz (laminar) **Increase** all thru and up to 40% at f=12Hz in the turbulent regime

Date	Investigators	Working Fluid / Nat- ure of flow	Summary of Investigation	Results / Remarks
1979	Karamercan et al.	Steam heated **water** (Heat exch.)	**1000 $\leq$ Re $\leq$ 50000** **0 $\leq f \leq$ 5 Hz** Pulsator: rec.pump 5 displ.amplitude large to cause fl. rev	Max **increase** in htc up to factor of 5.84 at **.26Hz** Re=7800, less incr at highr Re
1982	Krishnan and Sastri	Steam heated **water** (Heat exch.)	**500 $\leq$ Re $\leq$ 2200** **0 $\leq f \leq$ 7 Hz** Pulsator:plug valve (loc. upstream) driven by a D.C motor	The effect of the amplitude of pulsation and dimensionless frequency on htc is **negligible. Improvment** in htc is more pronounced in the entrance region
1988	Liao and Wang	**Water** Electrically heated tube Turb. Flow	**3400 $\leq$ Re $\leq$ 27000** **0.074 $\leq f \leq$ 0.385Hz** Pulsator: motor driven ball valve	**Decrease** in htc Relative htc dep mainly on ampl. and not freq.
1989	Al-Haddad and Al-Binally	Furnace heated **air**, subjected to conv.coolng	**1000 $\leq$ Re $\leq$ 40000** **5 $\leq f \leq$ 60Hz** Pulsator: piston-cyl connected to a var. voltage elect.motor	**Increase** in Nu above a critical dimensionless no. $Re(2\pi . fr^2) / \nu$ & no significant improv below it
1992	Genin et al.	**Water** Electrically heated tube	**10000 $\leq$ Re $\leq$ 25000** **0.2 $\leq f \leq$ 6 Hz** Pulsator:Plug type	No significant effect on Nu
1993	Isshiki et al.	**Air** Electrically heated tube fully devel. flow.	**Re=7450** f in the ratio of 0.32,0.61,1.7 & 3.3 to the turb bursting f_b of **9.73Hz**	Nu unchanged at $f \cdot f_b$ and varied periodica lly at $f \cdot f_b$

flow, it is assumed that pulsating frequencies are low enough such that usual steady-state correlations hold at every instant. This means that the velocity and temperature profiles can be replotted and at any point in time correspond to the value of the Reynolds number at that moment. The illustration of this model as carried out by Lemlich [29] is given in the following:

For a forced convective heat exchanger in which the axial flow of a fluid with constant physical properties is periodically decreased or interrupted but not reversed, the average velocity V_m over a cycle period of 1/f as obtained from mass conservation is given by

$$V_m = f \int_0^{1/f} V \, d\tau \tag{2.1}$$

Within reasonable limits of the mass flow rate the heat transfer coefficient for the flow with pulsation and without pulsation can be approximated respectively as

$$h = k \, V^n \tag{2.2}$$

$$h' = k \, V_m^n \tag{2.3}$$

Where n is constant.

Now, if the change in temperature difference Δ T is small throughout the cycle, then by the heat balance over a cycle period

$$Q = \frac{h_m \, A \, \Delta T}{f} = A \, \Delta T \int_0^{1/f} h \, d\tau \tag{2.4}$$

knowing that the time averaged heat transfer coefficient for pulsation is given by:

$$h_m = f \int_0^{1/f} h \, d\tau \tag{2.5}$$

and A is the heat transfer area. Dividing Eqn. (2.4) by Eqn. (2.3), and then substituting Eqns. (2.1) and (2.2) yields

$$\frac{h_m}{h'} = \frac{f^{1-n} \int_0^{1/f} V^n \, d\tau}{\left(\int_0^{1/f} V d\tau\right)^n} \tag{2.6}$$

Let

$$\theta = 2\pi f \tau \tag{2.7}$$

thus

$$d\theta = 2\pi f \, d\tau$$

Substituting Eqn. (2.7) in Eqn. (2.6) and altering limits, the improvement ratio due to pulsation is given by [31]

$$R = \frac{h_m}{h'} = \frac{(2\pi)^{n-1} \int_0^{2\pi} V^n \, d\theta}{\left(\int_0^{2\pi} V \, d\theta\right)^n} \tag{2.8}$$

for any wave form of pulsation Eqn. (2.8) is independent of frequency. Also, for n less than unity, which is almost always the case, Eqn. (2.8) will predict a decrease in coefficient with pulsation. When n is greater than unity, however, which sometimes occurs in the transitional flow region, Eqn. (2.8) will show an increase in heat transfer coefficient. For n equal to unity there is no change. Even though in this model relative heat transfer coefficient is independent of pulsation frequency, the frequency level above which a system is no longer quasi-steady and the prediction fails has not been reliably established for the general case according to [29]. For the case of Sinusoidal pulsations of amplitude A and frequency ω:

$$V = V_s + \frac{d}{dt}(A \sin \omega t) = V_s (1 + k \cos \omega t) \tag{2.9}$$

where V_s is the steady component of the velocity and $k = \frac{\omega A}{V_s}$ is known as relative velocity oscillation amplitude. When Eqn. (2.9) is substituted in Eqn. (2.8) we obtain

$$\frac{h_m}{h'} = \frac{1}{2\pi} \int_0^{2\pi} (1 + k \cos \omega t)^n \, d\theta \tag{2.10}$$

It is clear from Eqn. (2.10) that the improvement ratio for Sinusoidal pulsation does not depend on the pulsation frequency of the flow rate and is only a function of relative amplitude k. In the case where k> 1, reverse flow occurs in the duct and

this results in increase in relative heat transfer coefficient, while for k< 1, there is no flow reversal and Eqn. (2.9) predicts a reduction in the heat transfer coefficient but this reduction is very small [18].

2.4.2 Turbulent Bursting Model

The bursting process is composed of a sequence of quasi-cyclic events that occur near the wall of the turbulent flow. Although the exact description of the phenomenon as well as its cause is still in question, it's generally agreed that the bur sting process plays a dominant role in energy production and in transports of heat, mass and momentum in a turbulent boundary layer [14]. According to the viscous sublayer as renewal model reported by [18], the viscous sublayer is unstable, its grows and collapses in a periodic manner in the statistical sense of the process. The thickness of the viscous sublayer increases to a certain critical value. Then the layer of retarded fluid very close to the wall looses stability, breakdown and discharges mass into the core of the flow simultaneously, and a new sublayer is formed or 'renewed'. This turbulent bursting frequencies were studied by Mizushina et al. [37]. They measured not only the mean bursting period but also the histogram of the intervals between bursts. They found that in steady flow bursting occurs over a "preferred range" of frequencies centered around a mean bursting frequency. They also found that the upper and lower ends of the histogram, as well as the mean burst period depend on

Reynolds number ranged from $10^3 - 10^5$.

From their measurements Ramaprine and Tu [38] obtained approximate relations for the mean; lower and upper bound of bursting frequency which are expressed respectively in the following:

$$\frac{\omega D}{U^*} \approx 1.58\ R_e^{1/8} \tag{2.11}$$

$$\frac{\omega_{bl} D}{U^*} \approx 166\ R_e^{-0.54} \tag{2.12}$$

$$\frac{\omega_{bu} D}{U^*} \approx 31\ R_e^{0.125} \left[10^{-(3.32-0.667 \log R_e)}\right] \tag{2.13}$$

where

D = pipe diameter

$\omega = 2\pi f_b$, is the circular bursting frequency, and

$U^* = (\frac{\tau_0}{\rho})^{1/2}$ is the friction velocity

Effect of Pulsation on Turbulent Bursting Frequencies

Besides the fact that pulsation varies the mass flow rate about its mean value the basic turbulent exchange process may be altered with the flow pulsation. It has been reported by [14,18,38] that such phenomenon is related to the bursting in the

turbulent boundary layer. Mizushina et al. [37] found that if the pulsation frequency is close to the turbulent bursting frequency, then certain resonance interaction may occur which may show up as stimulation or suppression of corresponding frequencies in the turbulent energy spectrum and as changes in the characteristics of turbulent transfer. Consequently, this has its effect on the enhancement or reduction of heat transfer coefficient. However, when the pulsation frequency lies outside the preferred range, flow pulsation does not affect the burst histogram and the mean bursting frequency, independent of the pulsation frequency, is equal to that of steady flow at the same Reynolds number.

As mentioned before whether the turbulent structure is affected by unsteadiness or not depends on whether the pulsation frequency interacts with the turbulent bursting frequency. In order to study this interaction we need to relate the pulsating frequency to the turbulent bursting frequencies by writing the pulsation frequency in a dimensionless form (i.e. $\frac{\omega D}{U^*}$) in order to compare the dimensionless pulsating frequency with the relations of the bursting frequency given in equations (2.11), (2.12) and (2.13) at different Reynolds numbers.

In doing this, U^* is assumed to be approximated by its average value which is calculated from the coefficient of resistance λ, defined by Blasius formula [39] given as:

$$\lambda = 0.3164\, R_e^{-0.25} \tag{2.14}$$

The friction velocity can be expressed as

$$U^* = (\frac{\tau_0}{\rho})^{1/2} = \left(1/8\, \lambda\, U^2\right)^{1/2} \tag{2.15}$$

Substituting Eqn. (2.14) into Egn.(2.15) we get

$$U^* = \frac{0.1988718\bar{U}}{Re^{0.125}} \tag{2.16}$$

Hence we obtain

$$\frac{\omega D}{U^*} = \frac{2\pi f D Re^{0.125}}{0.1988718\bar{U}} \tag{2.17}$$

where $\bar{U}$ is the average velocity and f is the pulsation frequency The term $\frac{\omega D}{U^*}$ is the turbulent Stokes number which is a measure of the relative distance from the wall up to which the unsteady effects will penetrate [38].

Ramaprian and Tu [38] classified pulsating flow into several regimes as shown in Fig. 2.1 based on the approximate relations for the mean, upper and lower bursting frequency equations (2.11), (2.12) and (2.13) they obtained from Mizushina et al. measurements.

Regime I which lies below the lower bound of the bursting frequency line is called the 'lower frequency zone' and the mean bursting frequency is independent of pulsation frequency. In this region the turbulent structure is not affected since

$\frac{\omega D}{U^*}$ is still less than $\frac{\omega_b D}{U^*}$. The heat transfer coefficient is expected to be reduced with pulsation and the flow departs from quasi-steady behavior but the quasi-steady turbulence model can still be used to predict the flow. But where $\frac{\omega D}{U^*}$ is very small (i.e. $\leq 10^{-1}$), the turbulent flow behaves like steady flow and also the heat transfer coefficient is expected to decrease but the difference between them is very small (no more than 5 %) as reported by [18] and behave in a manner of quasi-steady state model.

Regimes II and III cover the preferred range of the bursting frequency. Regime II which is called 'intermediate frequency regime' and the mean bursting frequency is subdued as a result of resonance occurring at the pulsation frequency. Accordingly, the heat transfer behavior shall be affected. In Regime III, the imposed pulsation will interact strongly with the turbulent bursting process at the wall. The effect in the turbulent structure is, therefore, strong. This regime is called 'high frequency regime'. In this regime the heat transfer coefficient is expected to increase because the pulsation frequency is higher than the mean bursting frequency.

Regime IV is called the 'rapid pulsation regime'. The interaction between the imposed pulsation and the turbulent structure will be very strong. However, the effect of pulsation on turbulence structure as well as heat transfer has not adequate studies in this regime [14,18,38].

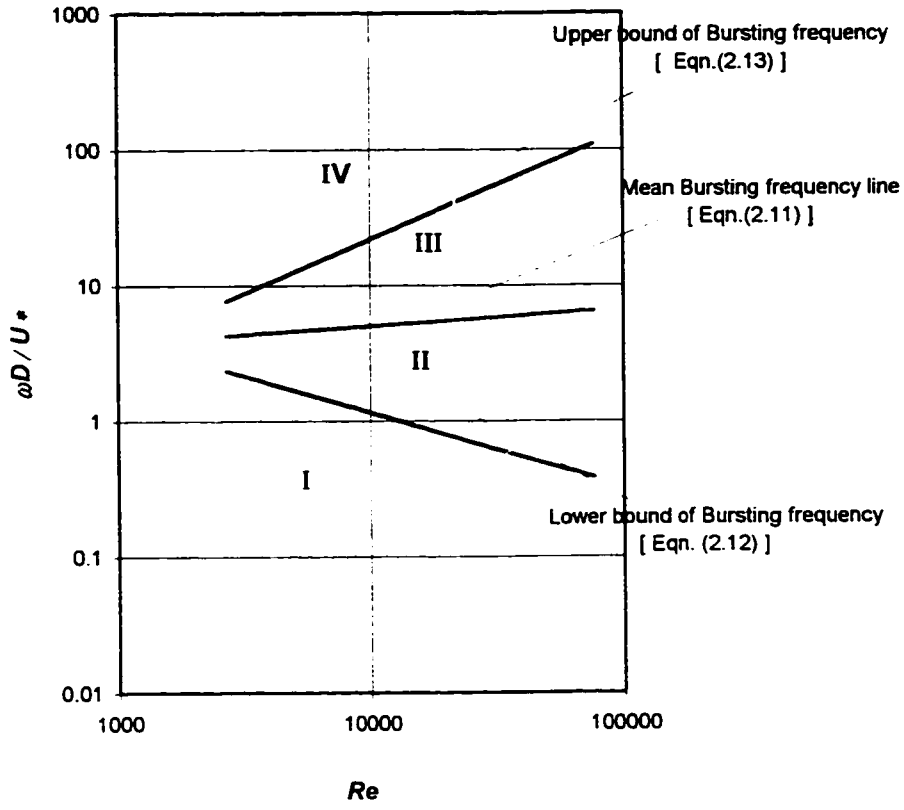

Fig.2.1 Classification of unsteady(periodic) turbulent flows

Chapter 3

Experimental Set-up

This chapter presents the detailed description of the experimental set-up as well as instrumentation.

3.1 Test Rig

The test rig which is shown in Fig. 3.1 is an open-loop unit in which air as working fluid is to be pumped by an air blower near atmospheric pressure and is discharged to the atmosphere through the test section after being heated. The rig consists of the air supply unit, the test section, and the pulsating system. These are described in the following subsections.

3.1.1 Air Supply Unit

This unit consists of the air blower, piping system, orifice meter, settling chamber and the velocity development section. The air blower, made of cast iron runs at a constant speed of 3000 rpm. It has a 0.15 m (6 inch) diameter outlet port which is

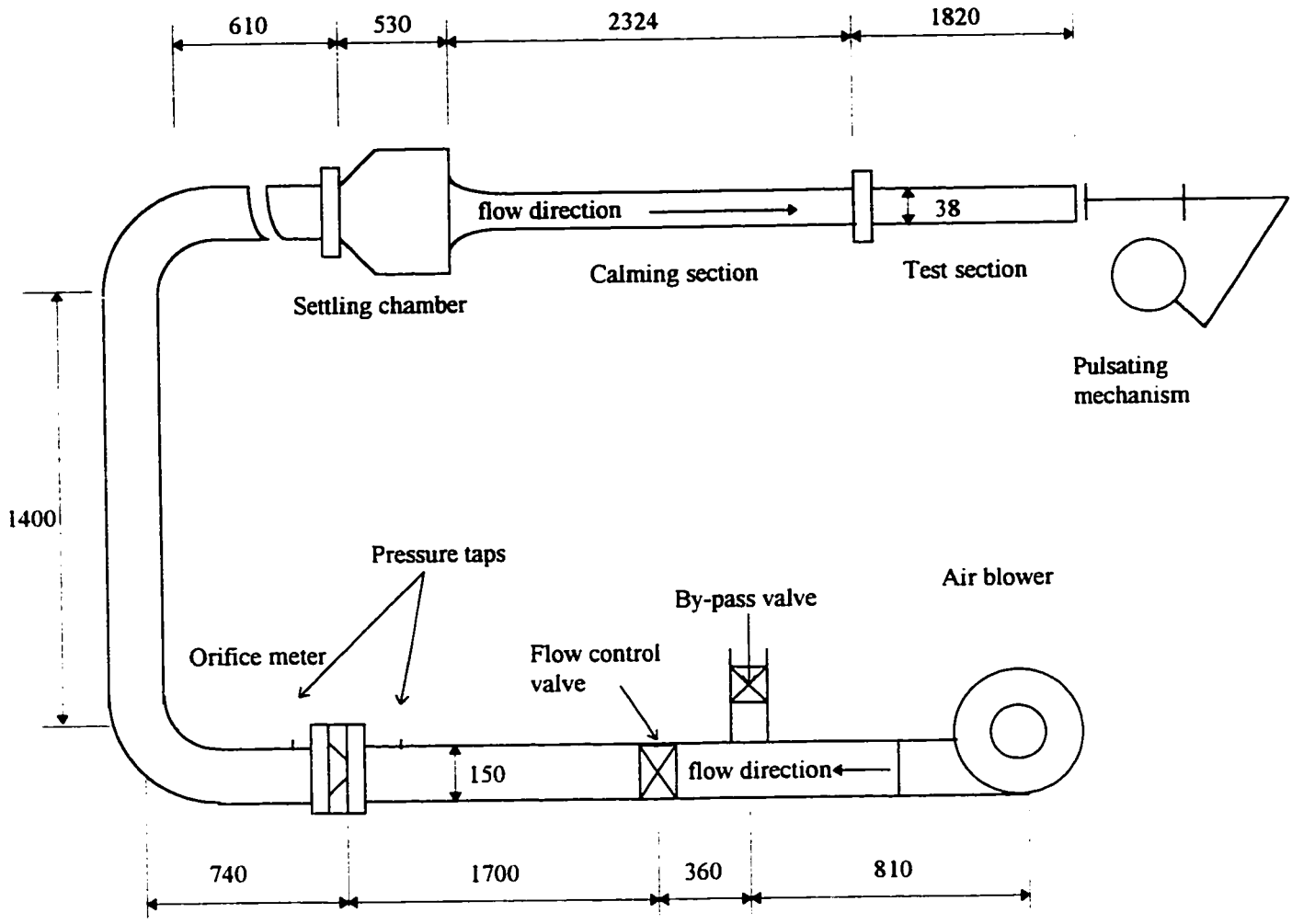

(Dimensions are in mm)

Fig. 3.1 Test Set-up

connected to 1 m. long PVC pipe of the same nominal diameter. The PVC pipe consists of a main and bypass valves in order to control and to maintain a constant mass flow rate. For the low flow rate this 1 m PVC pipe is connected to another PVC piping system of 0.076 m (3 inch) nominal diameter through a convergent nozzle. However, for the high flow rate this PVC pipe is connected to another PVC piping system of the same nominal diameter through coupling. The flow rate was measured through pressure drop across a calibrated sharp edge orifice installed between two flanges.

For the low flow rate, the orifice meter has a 0.3 diameter ratio (i.e. B = 0.3) and the two flanges are located at approximately 1 diameter(i.e. L/D=1) from the nozzle and the length of the PVC pipe after these two flanges is about 10 diameters (i.e. L/D=10) as recommended by Stearns et al. [40]. The pressure taps which represent a vena contract tap connection are located 0.085 m and 0.075 m upstream and downstream from the orifice ,respectively, as recommended in [40]. But for the high flow an orifice meter of 0.5 diameter ratio (i.e. B = 0.5) was used and the two flanges were located at approximately 2.87 m. from the blower. The pressure taps which also, represent a vena contracts tap connection are located at 0.16 m and 0.11 m upstream and downstream from the orifice respectively as recommended in [40]. The air is admitted in a 0.3 m diameter and 0.53 m average length settling chamber made of mold steel where flow instabilities are damped before velocity development

takes place in the calming section. The calming section is a copper pipe with 0.0381 m in diameter preceding the test section and the length of it is kept approximately according to [41] as long as 61 times the tube diameter (i.e. L/D = 61) to ensure that a hydrodynamically fully developed flow exists at the entrance of the heated test section.

3.1.2 Test Section

The test section shown in Fig 3.2 is a copper pipe of 1.78 m length (L) and 0.0381 m internal diameter (D). It is connected to the calming section through two flanges which are insulated from each other to avoid axial end-conduction from the test section to the calming section. Heat is supplied to the pipe wall through four amox fiber, insulated heating tapes each of length 2.438m (8ft) and 0.025 m width. The tapes are of equal wound length of approximately 0.445 m along the pipe. The effective length of the test section (L_e) which is 1.335 m. and equivalent to 33 pipe diameters corresponds to the first three heating tapes. An extra heating tape was used to minimize the end effect. To minimize heat transfer to surrounding the test section together with the wound heating tapes are insulated by fiber glass insulation material of approximately 0.0381 m and 0.48 m internal and external diameters, respectively. The pipe wall temperatures are directly measured by 24 plastic-covered K-type thermocouples (positioned as shown in the figure) whose

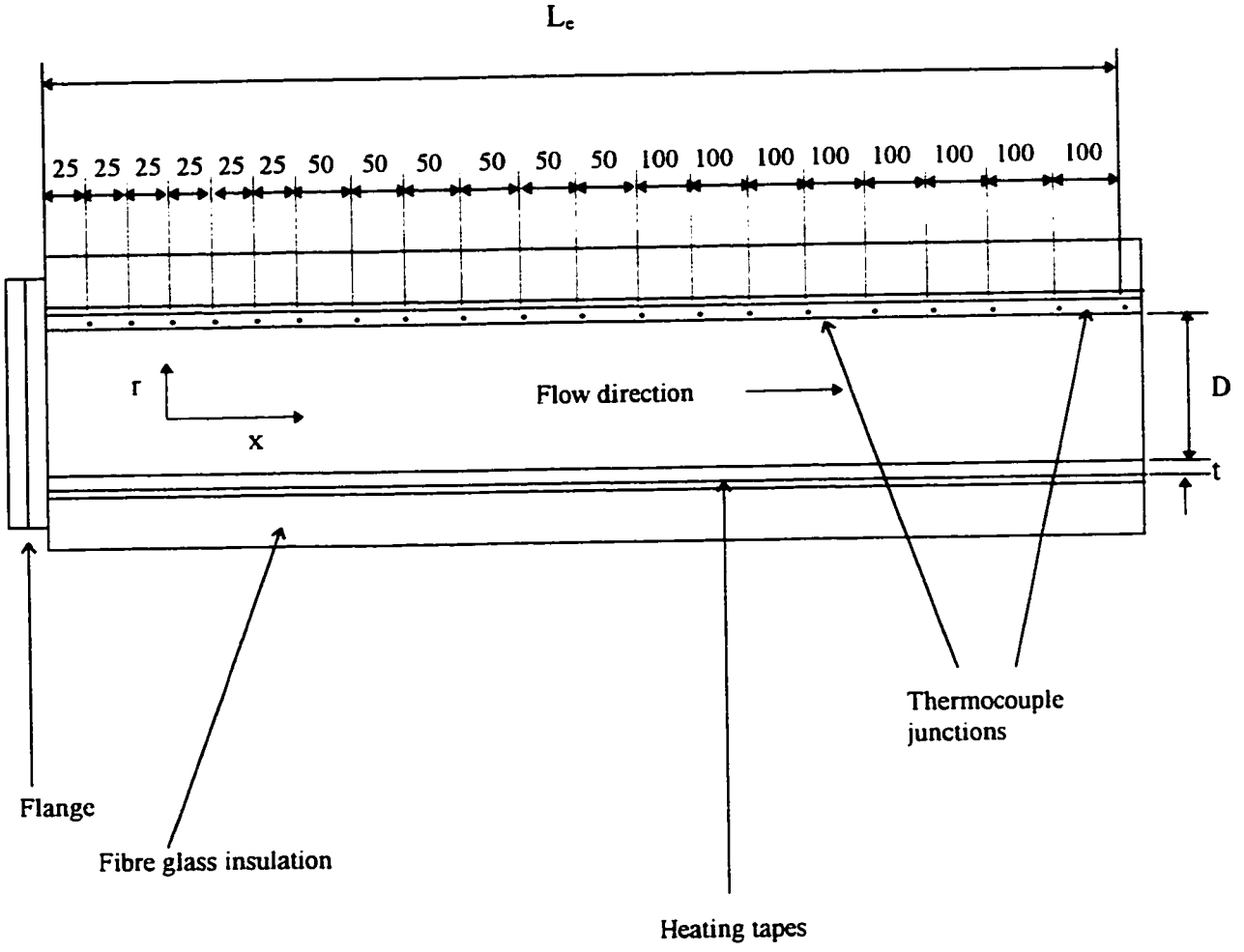

(Dimensions are in mm.)

Fig. 3.2 Test section

junctions are embedded in holes each of diameter 0.002m and depth 0.0015m drilled on to the pipe surface. The air inlet temperature is also determined from K-type thermocouple enclosed in a ceramic tube which is inserted in a hole drilled through the flanges at the inlet.

3.1.3 Pulsating Mechanism

The pulsating mechanism shown in Fig 3.3 is a four bar slider crank mechanism ,driven by a variable voltage D.C. motor. The slider is connected to a flexible disc in form of a piston which moves back and forth in order to create the pulsation. The displacement amplitude is equivalent to the strok of the piston which can be adjusted by altering the pivot point along link 3 which is connected to the slider. The effect of three different amplitude was studied in this experiment. The pulsation frequency corresponds to the rotational speed of the motor. In this experiment the pulsating mechanism is located downstream at the exit of the pipe.

Kinematic Analysis of The Pulsating Mechanism

As it is shown in Fig 3.4 , when the motor rotates, the displacement , x between the crank and link 2 causes an angular displacement of link 3 about the pivot which in turn results in a reciprocating motion movement of the slider L_s whose motion is constrained in the horizontal direction. Hence, from the diagram; we have:

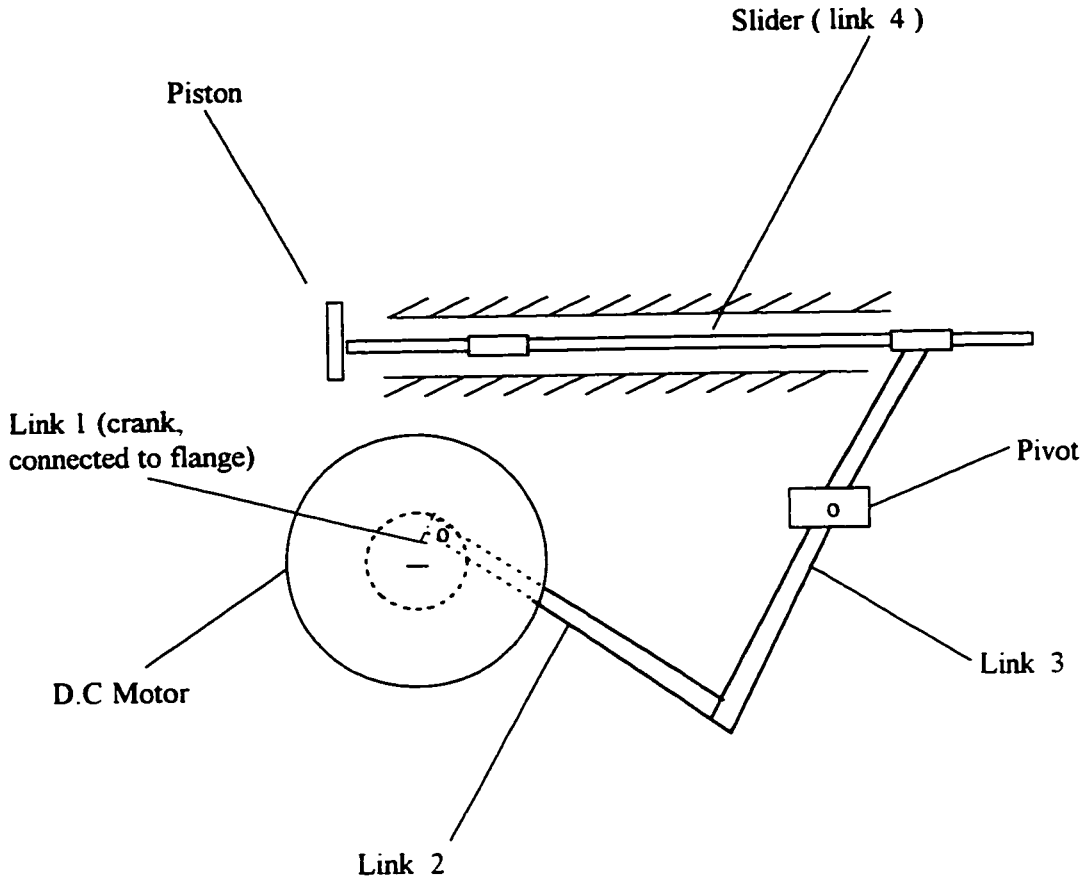

Fig. 3.3 Schematic diagram of the pulsating mechanism

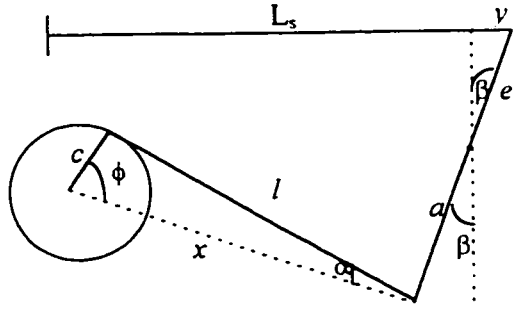

Fig. 3.4 Kinematic analysis of the pulsating mechanism

$$x = a\cos\phi + b\cos\alpha \tag{3.1}$$

using sine formula, we have:

$$\sin\alpha = \frac{a}{b}\sin\phi \tag{3.2}$$

and we know that

$$\cos^2\alpha = 1 - \sin^2\alpha \tag{3.3}$$

so, this will lead to

$$\cos\alpha = \left[1 - \left(\frac{a}{b}\right)^2 \sin^2\phi\right]^{1/2} \tag{3.4}$$

substituting Eqn. (3.4) into Eqn. (3.1) we get:

$$x = a\cos\phi + b\left[1 - \left(\frac{a}{b}\right)^2 \sin^2\phi\right]^{1/2} \tag{3.5}$$

differentiating the above equation with respect to ϕ we have:

$$dx = -a\sin\phi\left\{1 + \frac{a}{b}\cos\phi\left[1 - \left(\frac{a}{b}\right)^2 \sin^2\phi\right]^{-1/2}\right\} d\phi \tag{3.6}$$

for small angle $d\beta$, we can write :

$$dx = c d\beta$$

thus

$$d\beta = \frac{dx}{c} \tag{3.7}$$

The differential displacement of the slider can be approximated by :

$$dy = e\, d\beta \tag{3.8}$$

using Eqn. (3.7) with Eqn. (3.8) we get:

$$dy = \frac{e}{c} dx \tag{3.9}$$

substituting dx from Eqn. (3.6) we get:

$$dy = -\frac{ae}{c} \sin\phi \left\{ 1 + \frac{a}{b} \cos\phi \left[1 + \left(\frac{a}{b}\right)^2 \sin^2\phi \right]^{-1/2} \right\} d\phi \tag{3.10}$$

Integrating Eqn. (3.9) between $\phi = 0$ to any arbitrary ϕ, we get the displacement of the slider induced pulsation.

$$y = \frac{e}{c} \left\{ a\cos\phi + b \left[1 - \left(\frac{a}{b}\right)^2 \sin^2\phi \right]^{1/2} \right\} - \frac{e}{c}(a+b) \tag{3.11}$$

Replacing ϕ by ωt, where ω is the angular velocity of the motor which corresponds to the circular frequency of pulsation, Eqn. (3.10) can be written as:

$$y = \frac{e}{c}\left\{a\cos(\omega t) + b\left[1 - \left(\frac{a}{b}\right)^2 \sin^2(\omega t)\right]^{1/2}\right\} - \frac{e}{c}(a+b) \qquad (3.12)$$

Differentiation of Eqn. (3.12) with respect to time yields to the velocity of the piston which induces pulsation to the flow

$$\frac{dy}{dt} = V_p = -\frac{ea}{c}\sin(\omega t)\left\{1 + \frac{a}{b}\cos(\omega t)\left[1 - \left(\frac{a}{b}\right)^2 \sin^2(\omega t)\right]^{-1/2}\right\}\omega \qquad (3.13)$$

Direct measurement of the links of the mechanism at an amplitude of (1 inch) are

$a = 0.026\ m.$, $b = 0.205\ m.$, $c = 0.143\ m.$ and $e = 0.063\ m.$

Substituting the above values into Eqn. (3.13) , the velocity of the induced pulsation as a function of time for different frequencies can be obtained as shown in Fig 3.5. A comparison between the piston velocity and a pure sinusoidal wave are also presented in Fig 3.6 in order to show the almost sinusoidal trend of the induced pulsation.

3.2 Instrumentation

The following instruments were used in the experiment, in order to obtain an accurate results:

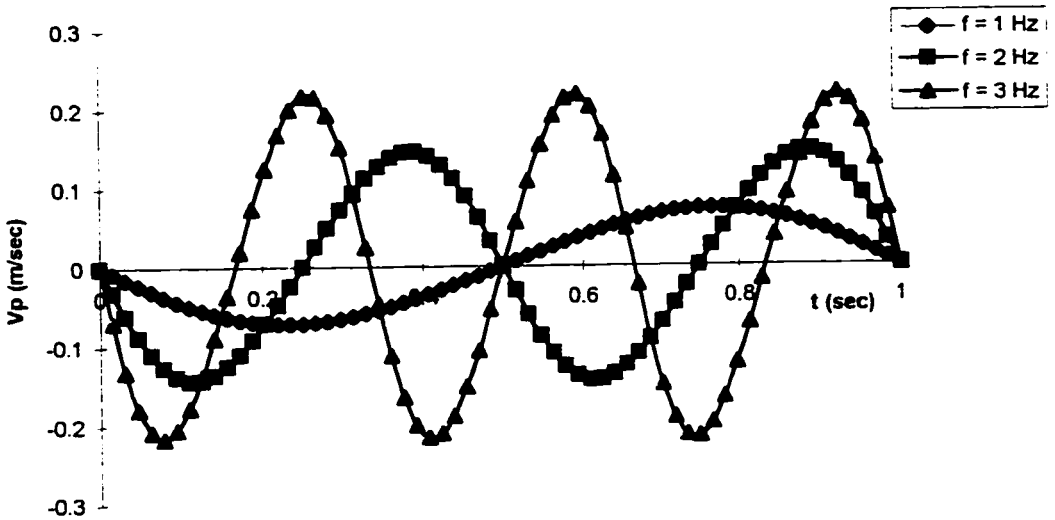

Fig.3.5 Nearly sinusoidal velocity of the oscillation inducing piston as a function of time at different frequencies

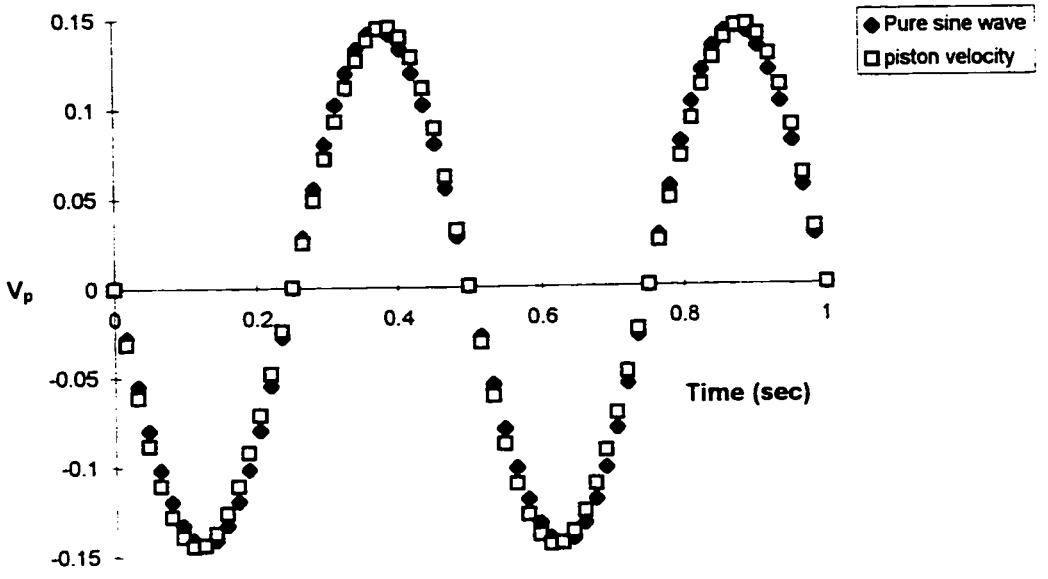

Fig. 3.6 Comparison between oscillating piston velocity and a pure sinusoidal wave-form

Manometers

Betz manometer (model 5585 series, manufactured by T.E.M. Engineering Limited, with a new name of Elven Precision Limited) was used to determine the pressure drop across the orifice. The manometer has an accuracy in reading of 0.2 mm of H_2O.

Heaters and Power Meters

Heating power was supplied using four variable voltage transformers which are of 220 volts input, made by Lab Sciences. They were employed in providing uniform heat flux to the wall of the test section. The power supplied was measured using Valhalla Scientific, model 2100 digital power analyzer.

Thermometers

The surface temperatures and the inlet temperatures were measured using type K thermocouples connected to a thermocouples selectors switch. The thermocouples selector switch was connected to type K Omega model 871 digital thermometer of 0.1°C resolution and 0.25% accuracy.

Tachometer

The speed of the D.C. motor which is equivalent to the frequency of pulsation was measured using Cole-Parmer model 8200-50 digital tachometer with photo electric probe.

Chapter 4

Experimental Procedure and Data Reduction

4.1 Introduction

This chapter presents the test procedure and the measurements of the various parameters. All necessary calculations needed to achieve the desired values of heat transfer and Nusselt numbers for both steady and pulsed flows are also described. Finally, uncertainty analysis for measured and calculated parameters are carried out in order to examine the accuracy of the results.

4.2 Test Procedure

Before starting the test runs , the flow line is properly aligned and the whole system is checked against any air leakage. The main and by-pass valves are adjusted until the desired mass flow rate is achieved which corresponds to the desired Reynolds number inside the test section. The room temperature is recorded and conditioned

against any arbitrary variation. The power was adjusted to have a constant heat flux. It was observed, during the experiment, that a high power is needed for the high flow rate in order to have appreciable rise in the surface temperature to get the expected surface temperature profile for constant heat flux boundary condition. However, a relatively lower electrical power is needed for the low flow rate.

Depending on the flow rate and power settings, certain length of time was required to achieve steady state conditions for flow without pulsation and corresponding pulsed flow. This was observed to be longer for low flow rates and shorter for higher flow rates. Data were collected when the pipe surface temperature showed no variation or variation less than 0.1°C per hour. Then the data were fed into a Fortran Computer program (Sample programs and output are shown in the appendix) through which the values of Reynolds numbers, local and average heat transfer coefficients and Nusselt numbers for both steady and pulsed flows were calculated.

4.3 Data Collection

In this section the measured parameters will be discussed and how each parameter was measured. These parameters include the air mass flow rate, power supplied and heat loss, surface and inlet temperatures and the pulsation frequency.

4.3.1 Mass Flow Rates

The mass flow rate is determined from the pressure drop across the orifice meter using the well known relation :

$$\dot{m} = C_d \rho A_0 \left[2g \left(\frac{\rho_1}{\rho} - 1 \right) \Delta h \right]^{1/2} \tag{4.1}$$

The discharge coefficient (C_d) for different Reynolds numbers were calculated based on empirical relation described by Stearns et al. [40] which takes into account all necessary design parameters for orifice meter. Two different orifice meters with diameter ratio of 0.3 and 0.5 were designed based on the standard suggested by [40] to satisfy the design condition needed in order to use the empirical relation. For 0.3 and 0.5 diameter ratio orifice meters (with Vena Contracta pressure tap connections), the relation for the discharge coefficients (C_d) are determined by [40]:

$$C_{d(0.3)} = 0.6042 \left(1 + \frac{243.4209}{Re} \right) \tag{4.2}$$

$$C_{d(0.5)} = 0.6247 \left(1 + \frac{539.8402}{Re} \right) \tag{4.3}$$

In order to ensure accurate determination of the mass flow rates through the calculated discharge coefficients for the orifice-plate meters, the orifice-plate meters were calibrated using a calibrated rotameter. The rotameter readings were in excellent

agreement with the calculated flow rate value obtained using Eqn. (4.1) as shown in Fig. 4.1 and Fig. 4.2. In data reduction, the value of the mass flow rate used is the one measured from the calibrated rotameter.

4.3.2 Heat Input

To measure the heat input to the test section through the heating tap segments, the digital wattmeter which measure input currents, voltages and power simultaneously was used. The voltage coming from the main through a voltage stabilizer was adjusted through four variable voltage transformers to achieve uniform input power at the pipe wall.

4.3.3 Temperatures Measurements

The pipe surface temperature as well as fluid inlet temperature were measured directly using the k-type thermocouples which is connected to the thermocouples switch and readout from a digital thermometer.

4.3.4 Heat Loss

Heat loss was assumed to be in the radial direction through the insulation only. To determine the heat loss, the outer surface temperatures of the insulation were measured at the corresponding points where the pipe surface temperature were measured. Using the Fourier low of radial heat conduction, the heat flux through

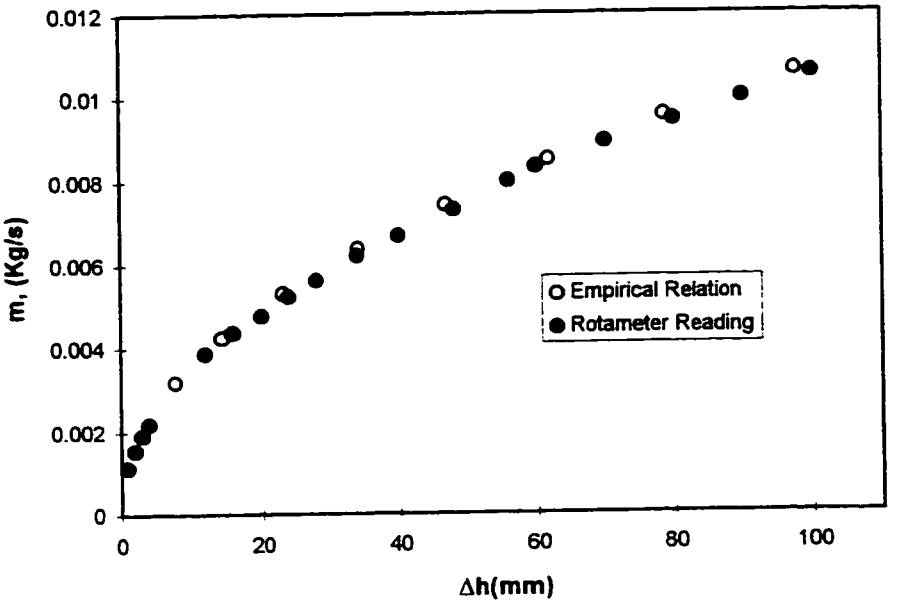

Fig. 4.1 Orifice meter calibration curve for B=0.3

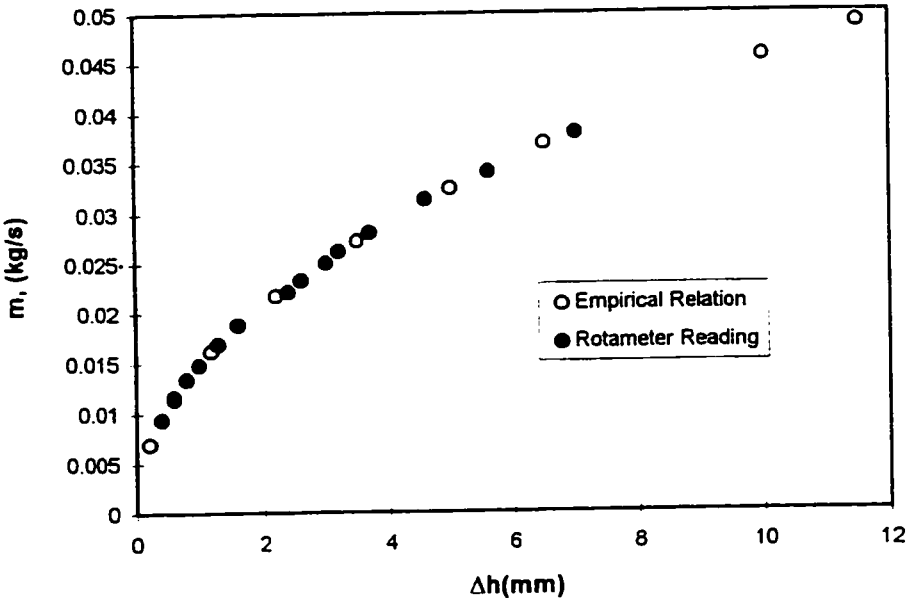

Fig. 4.2 Orifice meter calibration curve for B=0.5

the insulation at the center of each heater segment can be determined and given as:

$$q''_{loss} = \frac{-k\left[T_{0s}(x) - T_{is}(x)\right]}{R_i \ \ln(\frac{R_o}{R_i})} \tag{4.4}$$

The heat loss from each segment using the above equation with inner radius of 0.0572 m and outer radius of 0.147 m was found to be constant within difference of 1.6%. The total heat loss from the heaters was, therefore, found to be 4.4% of the total heat input.

4.3.5 Pulsation Frequency

The rotational speed of the D.C. motor whose output shaft is connected to a flange that drives the crank of the pulsating mechanism is determined by employing a digital tachometer with a photo electric probe. This probe emits light into the flange of the motor which is taped at one side with a reflector. As the flange rotates.each reflection is counted by the probe. The number of reflections per minute is a measure of the speed of the motor. This rotational speed of the motor correspond to the frequency of pulsation.

4.4 Data Reduction

The data obtained by measurements were reduced to obtain the flow Reynolds numbers, bulk temperature, heat transfer coefficient and Nusselt numbers as follows.

4.4.1 Reynolds Number

The flow Reynolds number in the test section is calculated by:

$$Re = \frac{4\dot{m}}{\pi\ D\ \mu} \tag{4.5}$$

4.4.2 Fluid Local Bulk Mean Temperature

The local bulk mean temperatures of the fluid was determined using energy balance as follows:

$$T_{j,o} = \frac{q_j}{\dot{m}C_p} + T_{j,i} \tag{4.6}$$

where

q_j =Heat transferred to the fluid at j^{th} segment

$T_{j,i}$ =Fluid inlet temperature to the jth segment

$T_{j,o}$ =Fluid outlet temperature at thej^{th} segment

From the measured inlet temperature the local bulk mean temperatures, at the corresponding points along the test section where the pipe wall temperature are measured, were calculated by linear interpolation of the mean temperatures at the end of the heater segments.

4.4.3 The Heat Flux

The heat flux is given by:

$$q'' = \frac{Q_{trans}}{\pi\ D\ L} \tag{4.7}$$

where $Q_{trans} = Q_{input} - Q_{loss}$

4.4.4 The Heat Transfer Coefficient

The local and average heat transfer coefficients are determined respectively by:

$$h(x) = \frac{q''}{T_s(x) - T_m(x)} \tag{4.8}$$

$$h_{mean} = \frac{1}{L}\int_0^L h(x)\ dx \tag{4.9}$$

The above integration of Eqn. (4.9) is carried out numerically using trapezoidal rule.

4.4.5 Nusselt Number

Using Eqns. (4.8) and (4.9), the local Nusselt number Nu(x) and the mean Nusselt numbers Nu_{mean} are determined using

$$Nu(x) = \frac{h(x)\ D}{k} \tag{4.10}$$

$$Nu_{mean} = \frac{h_{mean}\ D}{k} \tag{4.11}$$

4.5 Uncertainty Analysis

Uncertainty analysis of various measured parameters was carried out in order to estimate the accuracy of the experimental results. This analysis is based on the method of Kline and McClintock as presented in [42]. The method is based on the specification of the uncertainties in the various primary experimental measurements. This is obtained from the accuracy of the instrument as specified by the manufacturer. This can be also obtained through calibration of an instrument with standard of very high precision. Also, the specification of uncertainties can be assigned by the experimenter based on the total laboratory experience. In the following, the method which has been used to , estimate the uncertainties in the calculated results on the basis of the uncertainties in the primary measurements is described. For a given result R as a function of the independent variables $x_1, x_2, x_3, \ldots\ldots\ldots\ldots, x_n$. Then,

$$R = R(x_1, x_2, x_3, \ldots\ldots\ldots\ldots x_n)$$

Let w_R be the uncertainty in the result and $w_1, w_2, \ldots\ldots\ldots, w_n$ be the uncertainties in the independent variables. The uncertainty in the result is given by

$$w_R = \left[\left(\frac{\partial R}{\partial x_1} w_1\right)^2 + \left(\frac{\partial R}{\partial x_2} w_2\right)^2 + \left(\frac{\partial R}{\partial x_n} w_n\right)^2\right]^{1/2} \tag{4.12}$$

4.5.1 Uncertainties in The Mass Flow Rate

As mentioned above, the mass flow rate was calculated from Eqn. (4.1) which indicates that the primary quantities measured for calculating the flow rate are the diameters for the orifices meter from which the area of the orifices met er can be calculated and the manometer reading Δh. The orifice meter is machined to very high precision and as a result, uncertainty in diameter is considered negligible. The uncertainty in reading the liquid level of the projection manometer used in obtaining the pressure drop across the orifice meter has been estimated to be 0.05 mm for the high flow rate (i.e., B = 0.5) and varying between 0.05 mm to 1 mm depends on the manometer readings for the low flow rate (i.e., B = 0.3). Also, comparing the calculated discharge coefficient for the same diameter ratio, Reynolds number and pressure tap connection with ASME data on fluid meter report given by stearns et al. [40]. Uncertainty in c_d is estimated to be about 0.87% for the high flow rate and 0.88 % for the low flow rate. The uncertainty in the mass flow rate is therefore, calculated as follows:

$$\dot{m} = C_d \, \rho \, A_0 \left[2g \left(\frac{\rho 1}{\rho} - 1 \right) \Delta h \right]^{1/2} \tag{4.13}$$

Differentiating Eqn. (4.13), we get

$$\frac{\partial w_{\dot{m}}}{\partial w_{C_d}} = \rho\, A_0 \left[2g\left(\frac{\rho_1}{\rho} - 1\right)\Delta h\right]^{1/2} = \frac{\dot{m}}{C_d} \tag{4.14}$$

$$\frac{\partial w_{\dot{m}}}{\partial w_{\Delta h}} = C_d\, \rho\, A_0 \left[2g\left(\frac{\rho_1}{\rho} - 1\right)\Delta h\right]^{1/2} \frac{1}{2\sqrt{\Delta h}} = \frac{\dot{m}}{2\Delta h} \tag{4.15}$$

$$w_{\dot{m}} = \left[\left(\frac{\dot{m}}{C_d} w_{C_d}\right)^2 + \left(\frac{\dot{m}}{2\Delta h} w_{\Delta h}\right)^2\right]^{1/2} \tag{4.16}$$

Where $w_{\dot{m}}, w_{C_d}$ and $w_{\Delta h}$ are the uncertainties in the mass flow rate, discharge coefficient and manometer reading respectively. Dividing both sides of Eqn. (4.16) by $\dot{m}$, we get

$$\frac{w_{\dot{m}}}{\dot{m}} = \left[\left(\frac{w_{C_d}}{C_d}\right)^2 + \left(\frac{w_{\Delta h}}{2\Delta h}\right)^2\right]^{1/2} \tag{4.17}$$

The Uncertainty in The Mass Flow Rate for B = 0.3

For the minimum manometer reading (corresponding to Re = 5032) we have

$$\Delta h = 7.0\ mm$$

$$w_{\Delta h} = 0.05\ mm$$

$$\frac{w_{C_d}}{C_d} = 0.88\ \%$$

Substituting these into Eqn. (4.17) the relative uncertainty in the mass flow rate is given as:

$$\frac{w_{\dot{m}}}{\dot{m}} = \left[(0.0088)^2 + (0.0036)^2\right]^{1/2} \tag{4.18}$$

$$= 9.4 \times 10^{(-3)}$$

$$= 0.94\ \%$$

Similarly for the maximum manometer reading (corresponding to Re = 14,460)

$$\Delta h = 61.0\ mm$$

$$w_{\Delta h} = 1.0\ mm$$

$$\frac{w_{C_d}}{C_d} = 0.0088$$

$$\frac{w_{\dot{m}}}{\dot{m}} = \left[(0.0088)^2 + (0.0082)^2\right]^{1/2} \tag{4.19}$$

$$= 0.012$$

$$= 1.2\%$$

The Uncertainty in The Mass Flow Rate For B = 0.5

For the minimum manometer reading (corresponding to Re = 20,138)

$$\Delta h = 0.6\ mm$$

$$w_{\Delta h} = 0.05\ mm$$

$$\frac{w_{C_d}}{C_d} = 0.0087$$

The relative uncertainties in the mass flow rate in this case is given as

$$\frac{w_{\dot{m}}}{\dot{m}} = \left[(0.0087)^2 + (0.042)^2\right]^{1/2} \tag{4.20}$$

$$= .042$$

$$= 4.2\ \%$$

Similarly for the maximum manometer reading (corresponding to Re=28,984)

$$\Delta h = 1.2\ mm$$

$$w_{\Delta h} = 0.05\ mm$$

$$\frac{w_{C_d}}{C_d} = 0.0087$$

The relative uncertainty in the mass flow rate in this case is given as

$$\frac{w_{\dot{m}}}{\dot{m}} = \left[(0.0087)^2 + (0.021)^2\right]^{1/2} \tag{4.21}$$

$$= .022$$

$$= 2.2\%$$

4.5.2 Uncertainty in Heat input Q

The heat input can be calculated using

$$Q = I \,.\, V \tag{4.22}$$

By differentiating the relation we obtain

$$\frac{\partial Q}{\partial V} = I \tag{4.23}$$

$$\frac{\partial Q}{\partial I} = V \tag{4.24}$$

Hence, the uncertainty in the heat input becomes:

$$w_Q = \left[\left(\frac{\partial Q}{\partial V} w_V\right)^2 + \left(\frac{\partial Q}{\partial I} w_I\right)^2\right]^{1/2} \tag{4.25}$$

$$w_Q = \left[(I\ w_V)^2 + (V\ w_I)^2\right]^{1/2} \tag{4.26}$$

Dividing both sides of Eqn. (4.26) by Eqn. (4.22) the relative uncertainty in the heat input becomes

$$\frac{w_Q}{Q} = \left[\left(\frac{w_V}{V}\right)^2 + \left(\frac{w_I}{I}\right)^2\right]^{1/2} \tag{4.27}$$

The relative uncertainty in the measured voltages and currents were estimated to be 1%. Hence Eqn. (4.27) becomes

$$\frac{w_Q}{Q} = \left[(0.01)^2 + (0.01)^2\right]^{1/2} \tag{4.28}$$

$$= 1.42\ \%$$

4.5.3 Uncertainty in the Mean Bulk Temperature

The mean bulk temperature is expressed as

$$T_m = \frac{Q}{\dot{m}C_p} + T_{in} \tag{4.29}$$

Differentiating Eqn. (4.29) we get:

$$\frac{\partial T_m}{\partial \dot{m}} = \frac{-Q}{\dot{m}^2 C_p} \tag{4.30}$$

$$\frac{\partial T_m}{\partial T_{in}} = 1 \tag{4.31}$$

$$\frac{\partial T_m}{\partial Q} = \frac{1}{\dot{m}C_p} \tag{4.32}$$

Hence, the uncertainty in the bulk mean temperature

$$w_{T_m} = \left[\left(\frac{\partial T_m}{\partial Q} w_Q\right)^2 + \left(\frac{\partial T_m}{\partial \dot{m}} w_{\dot{m}}\right)^2 + \left(\frac{\partial T_m}{\partial T_{in}} w_{T_{in}}\right)^2\right]^{1/2} \tag{4.33}$$

$$w_{T_m} = \left[\left(\frac{w_Q}{\dot{m}C_p}\right)^2 + \left(\frac{-Q}{\dot{m}^2 C_p} w_{\dot{m}}\right)^2 + (w_{T_{in}})^2\right]^{1/2} \tag{4.34}$$

$$w_{T_m} = \left[\left(\frac{w_Q}{\dot{m}C_p}\right)^2 + \left(\frac{-Q}{\dot{m}^2 C_p} w_{\dot{m}}\right)^2 + (w_{T_{in}})^2\right]^{1/2} \tag{4.35}$$

After rearranging, the uncertainty in the bulk mean temperature can be expressed as:

$$w_{T_m} = \frac{Q}{\dot{m}C_p}\left[\left(\frac{w_Q}{Q}\right)^2 + \left(\frac{w_{\dot{m}}}{\dot{m}}\right)^2 + \left(\frac{\dot{m}C_p}{Q} w_{T_{in}}\right)\right]^{1/2} \tag{4.36}$$

Now, the relative uncertainty of the inlet temperature is taken as the accuracy of the digital thermometer which is specified as 0.25% of reading.

The uncertainty in the Mean Bulk Temperature For B = 0.3

For the minimum manometer reading (corresponding to Re = 5032) we have

$$\dot{m} = 2.878 \times 10^{(-3)}\ kg/s$$

$$Q = 100.338\,W$$

$$C_p = 1007\ J/kg^oC$$

For $T_{in} = 23.8^oC$, the uncertainty in the inlet temperature becomes $w_{T_{in}}$=0.0595°C Substituting above into Eqn. (4.36) the uncertainty in the mean bulk temperature becomes

$$w_{T_m} = 0.59^oC$$

Similarly for the maximum manometer reading (corresponding to Re = 14,460) we have

$$\dot{m} = 8.27877 \times 10^{(-3)}\ kg/s$$

$$Q = 280.95\,W$$

$$C_p = 1007\ J/kg^oC$$

For $T_{in} = 23.2^oC$, the uncertainty in the inlet temperature becomes $w_{T_{in}}$=0.058°C Substituting above into Eqn.(4.36) the uncertainty in the mean bulk temperature becomes

$$w_{T_m} = 0.63^oC$$

The uncertainty in the mean bulk temperature for B = 0.5

For the minimum manometer reading (corresponding to Re = 20,138)

$$\dot{m} = 1.1596 \times 10^{(-2)}\ kg/s$$

$$Q\ = 344.016\ W$$

$$C_p\ = 1007\ J/kg^oC$$

For $T_{in} = 29.8^oC$, the uncertainty in the inlet temperature becomes $w_{T_{in}}$=0.0745^oC

Substituting above into Eqn.(4.36) the uncertainty in the mean bulk temperature becomes

$$w_{T_m} = 1.32^oC$$

Similarly for the maximum flow rate (Re=28,984) with 2.2% relative uncertainty in the mass flow rate,

$$w_{T_m} = 0.66^oC$$

4.5.4 Uncertainties in Heat Transfer Coefficient and Nusselt Number

From Eqns. (4.7) and (4.8) the heat transfer coefficient h is expressed by:

$$h = \frac{Q_{trans}}{\pi\ D\ L\ (T_s - T_m)} \tag{4.37}$$

Differentiating the above equation, we get:

$$\frac{\partial h}{\partial Q} = \frac{1}{\pi\ D\ L\ (T_s - T_m)} = \frac{1}{\pi\ D\ L\ \Delta T} \tag{4.38}$$

$$\frac{\partial h}{\partial T_s} = \frac{-Q}{\pi\ D\ L\ (T_s - T_m)^2} = \frac{-Q}{\pi\ D\ L\ (\Delta T)^2} \tag{4.39}$$

$$\frac{\partial h}{\partial T_m} = \frac{Q}{\pi\ D\ L\ (T_s - T_m)^2} = \frac{Q}{\pi\ D\ L\ (\Delta T)^2} \tag{4.40}$$

So, the uncertainty in the heat transfer coefficient becomes:

$$w_h = \left[\left(\frac{\partial h}{\partial Q} w_Q\right)^2 + \left(\frac{\partial h}{\partial T_s} w_{T_s}\right)^2 + \left(\frac{\partial h}{\partial T_m} w_{T_m}\right)^2\right]^{1/2} \tag{4.41}$$

Substituting the above differential and dividing both side by Eqn. (4.37) the relative uncertainty in the heat transfer coefficient becomes:

$$\frac{w_h}{h} = \left[\left(\frac{w_Q}{Q}\right)^2 + \left(\frac{w_{T_s}}{\Delta T}\right)^2 + \left(\frac{w_{T_m}}{\Delta T}\right)^2\right]^{1/2} \tag{4.42}$$

The Nusselt number is defined as :

$$Nu = \frac{hD}{k} \tag{4.43}$$

Differentiating Eqn. (4.43), we get

$$\frac{\partial Nu}{\partial h} = \frac{D}{k} \tag{4.44}$$

$$\frac{\partial Nu}{\partial k} = \frac{-hk}{k^2} \tag{4.45}$$

$$\frac{\partial Nu}{\partial D} = \frac{h}{k} \tag{4.46}$$

Therefore, the uncertainty in the Nusselt number becomes

$$w_{Nu} = \left[\left(\frac{\partial Nu}{\partial D} w_D\right)^2 + \left(\frac{\partial Nu}{\partial k} w_k\right)^2 + \left(\frac{\partial Nu}{\partial h} w_h\right)^2\right]^{1/2} \tag{4.47}$$

Substituting the above differential and dividing both side by Eqn. (4.43) the relative uncertainty in the Nusselt number becomes:

$$\frac{w_{Nu}}{Nu} = \left[\left(\frac{w_D}{D}\right)^2 + \left(\frac{w_k}{k}\right)^2 + \left(\frac{w_h}{h}\right)^2\right]^{1/2} \tag{4.48}$$

The scatter in the measured surface temperature is about ± 1.3°C. The wall-to - bulk average temperature difference encountered in the present experiment centered around $\Delta T = 42^oC$. The relative uncertainties in the thermal conductivity was estimated to be ± 4.2 % at low Re and ± 3.4 % at high Re. Also, the relative uncertainty in the pipe diameter was estimated to be ± 0.2 %. Hence, substituting this value into Eqns. (4.42) and (4.48), the relative uncertainties in the heat transfer

coefficient or the Nusselt number for the low and high flow rates are calculated as follows:

For the manometer reading (corresponding to Re = 5032 and Re=14,460)

$$\frac{w_h}{h} = 3.7\%$$

$$\frac{w_{Nu}}{Nu} = 5.6\%$$

For the manometer reading (corresponding to Re = 20,138)

$$\frac{w_h}{h} = 4.6\%$$

$$\frac{w_{Nu}}{Nu} = 5.7\%$$

For the manometer reading (corresponding to Re = 28,984)

$$\frac{w_h}{h} = 3.74\%$$

$$\frac{w_{Nu}}{Nu} = 5.0\%$$

Therefore, the average relative uncertainty in heat transfer coefficient and Nusselt number is about 4.2% and 5.4% respectively. The uncertainties in the measurements are summarized as shown in table 4.1.

Table 4.1 Uncertainties of Measurements

Parameter	**Absolute Uncertainty**	**Relative Uncertainty**
Mass flow rate		± 0.94 % to ± 4.2 %
Reynolds number		± 0.94 % to ±4.2 %
Heat supplied		± 1.41 %
Bulk mean temperature	$\pm 0.6\,^{o}C$ to $\pm$ 1.32 ^{o}C	
Surface temperature	± 1.3 ^{o}C	
Heat transfer coefficient		≈ ± 4.2 %
Nusselt number		≈ ± 5.4 %

Chapter 5

Results and Discussion

5.1 Validation

The present experiments include a total of 90 tests for different cases of Reynolds number, frequency and amplitude. Each pulsation test was preceded by steady flow test at the same Reynolds number. Comparisons between the present experimental data with the data reported in the literature for the steady flow (i.e., without pulsation) have been done in order to validate the present experimental data. The comparison includes the axial variation of the surface temperature along the test section, the values of the Nusselt number in the thermally fully developed region as well as the thermally developing section.

The axial variation of the surface temperature distribution measured in the present work for the Reynolds number varied between 5032 to 28,984 (samples shown in Fig. 5.1) agrees very well with the published patterns [41,44] for forced convection heat transfer in pipes heated with uniform heat flux. Also the values of Nusselt

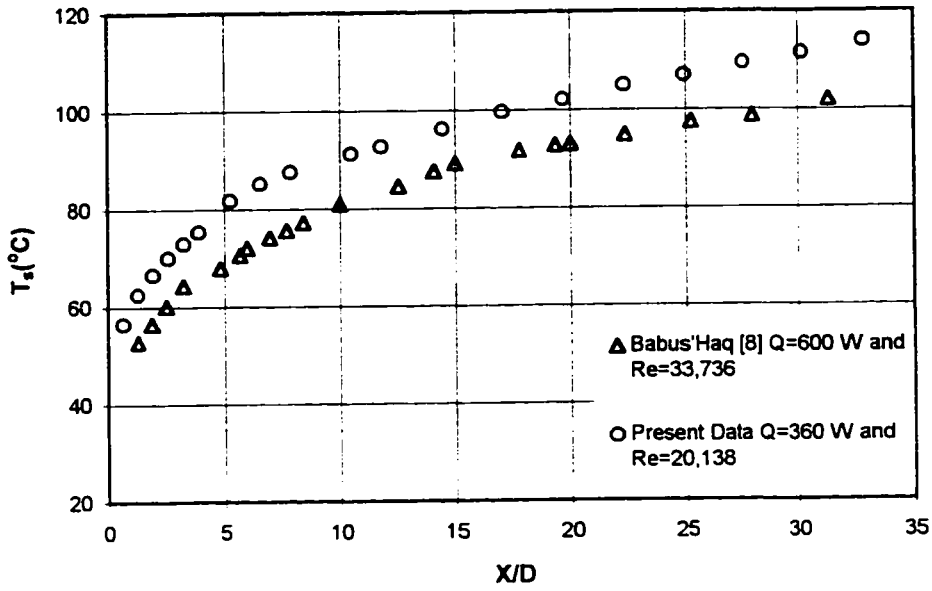

Fig. 5.1 Steady flow surface temperature distribution

number in the thermally fully developed region were compared with the following correlation for $Re < 10^5$ and (Pr 0.5 to 1.0) as reported in [43]

$$N_u = .022 Re^{0.8} P_r^{0.5} \tag{5.1}$$

As shown in Fig. 5.2, these values were found to be in very excellent agreement. Also, the results show that the fully developed region starts around 10 to 15 diameters downstream from the inlet of the test section as shown in Fig. 5.3. This result agrees with the result reported in [43]. In Fig. 5.4 the local Nusselt number for a sample of the present data and others data [41,44] was divided by the corresponding fully developed mean Nusselt number calculated from Eqn.(5.1). The data in the fully developed region collapsed at a relative Nusselt number of one. This indicates a good agreement between the data available and the correlation (Eqn. (5.1)).

5.2 Description of The Experimental Results

The effect of pulsation frequency and amplitude on heat transfer for the local Nusselt number as well as the relative mean Nusselt number is discussed in the following subsections.

5.2.1 The Effect of Pulsation Frequency on Local Nusselt Numbers

Since the present work is devoted to study the effect of pulsation in the thermal entrance region as well as the thermally fully developed region, it becomes pertinent

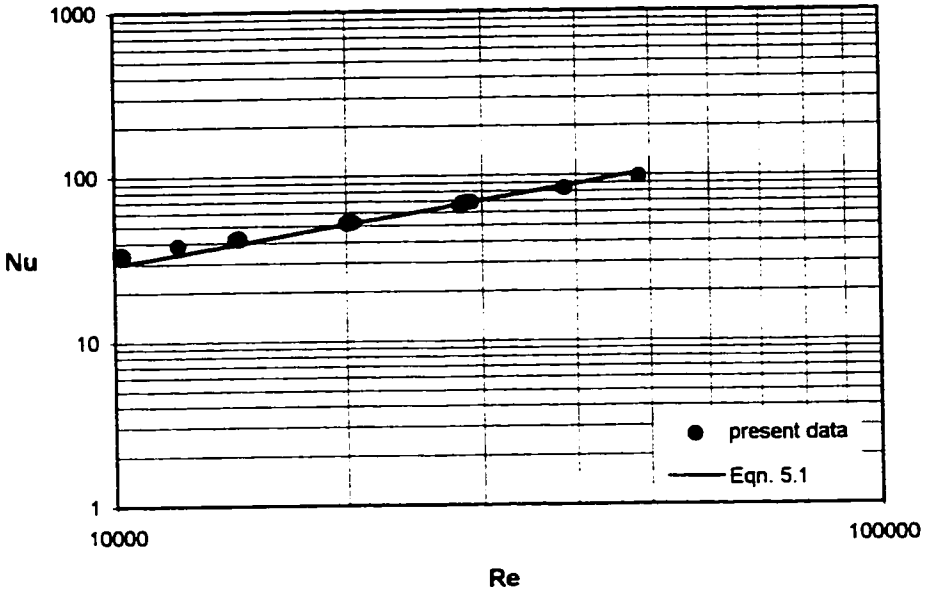

Fig.5.2 Comparison of measured fully developed Nusselt numbers and correlated data of Eqn. 5.1

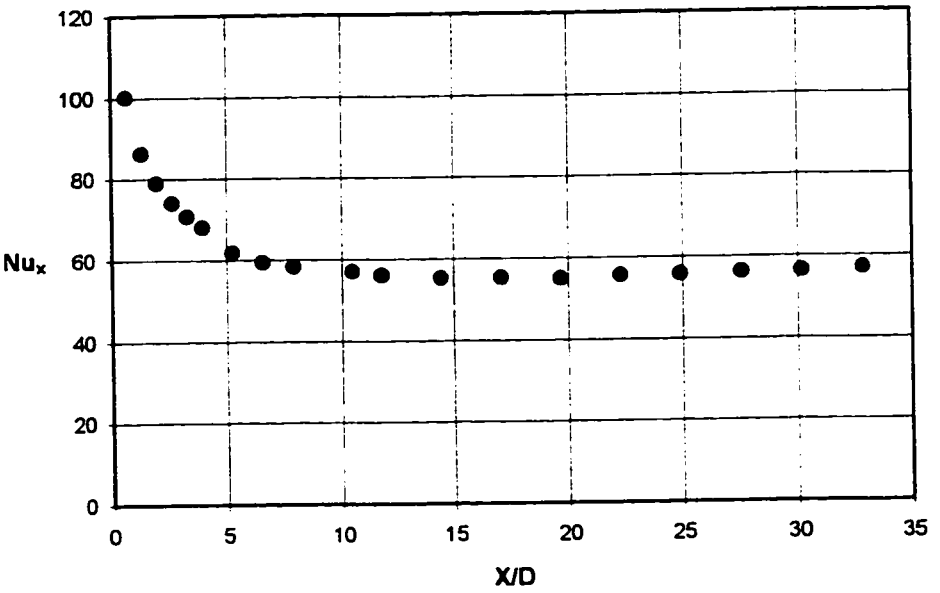

Fig.5.3 Local Nusselt number for steady flow at Re=20,138

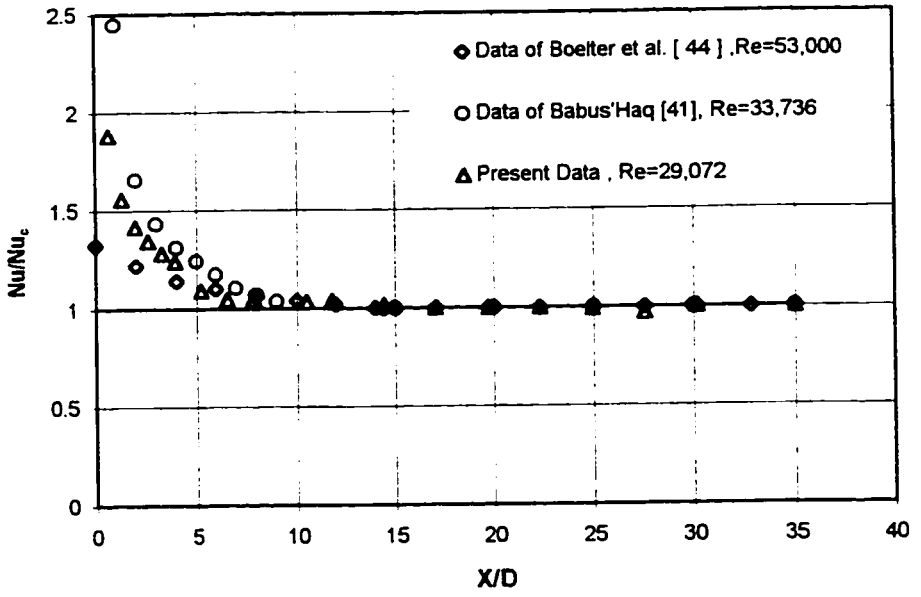

Fig. 5.4 Relative local Nusselt number for steady flow

to examine the behavior of the local Nusselt number along the test section, under the influence of pulsation parameters. The local Nusselt number variation along the pipe for different flow frequencies at different flow Reynolds numbers for the three different amplitudes are shown in Figs. 5.5 to 5.34. It is observed that the local Nusselt numbers exhibit pattern similar to that of steady flow. This may be due to the observed similar pattern of surface temperature for the two cases. As can be seen from Figs. 5.5 and 5.6 for Re = 5032 and $A = 0.5''$ a local heat transfer enhancement is observed close to the inlet for pulsation frequency ranged from 2 Hz to 4 Hz. This enhancement extends down to a length of about 6.5 pipe diameters (X/D=6.5) for pulsation frequency of 3 Hz and 4 Hz and to a length of about 4 pipe diameters (X/D=4) for f=2 Hz. In this frequency range, the maximum increase in the heat transfer coefficient is confined very close to the inlet between 1 and 2 pipe diameters length with maximum value of about 4% near the inlet at f = 4 Hz. On the other hand relative reduction in heat transfer coefficient is observed in the entrance region for the other pulsation frequency, with maximum reduction of about 3% at f=8 Hz. Reduction in the heat transfer coefficient in the fully developed region is also observed at all pulsation frequencies. Maximum and minimum reduction of about 8% at f=6 Hz and 3% at f=1 Hz respectively are obtained.

At the same Reynolds number but for($A = 1.0''$) as shown in Figs. 5.6 and 5.7, a similar trend compared to the previous case ($A = 0.5''$) is observed. In this case ,

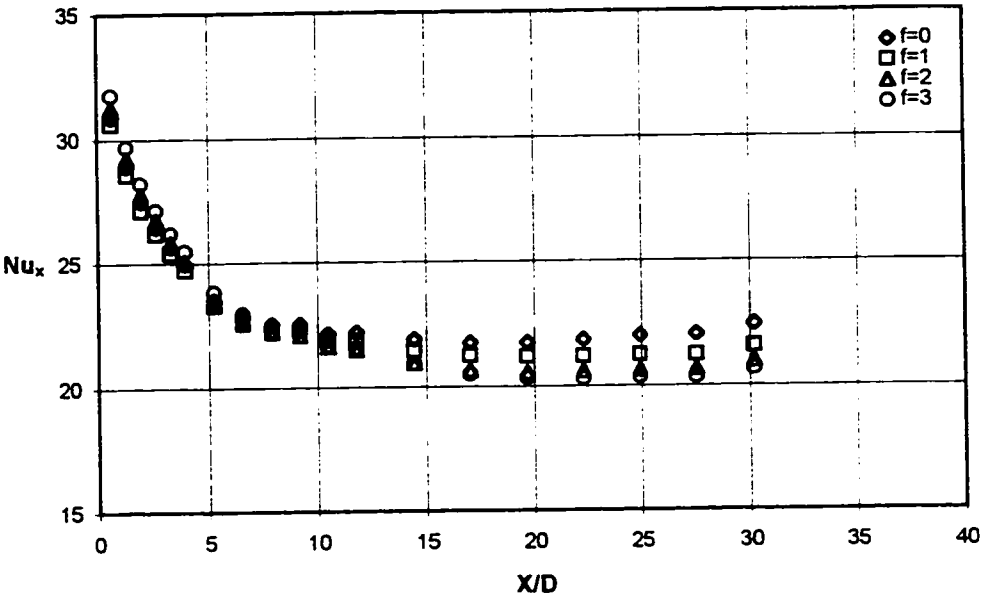

Fig.5.5 Effect of pulsation frequency on local Nusselt numbers at Re=5032 and A=0.5"

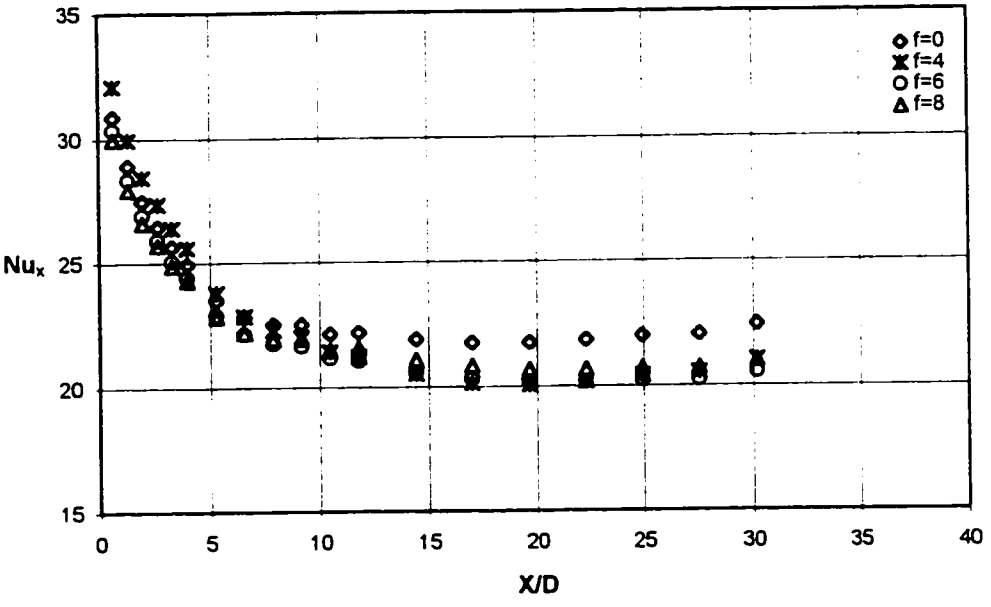

Fig.5.6 Effect of pulsation frequency on local Nusselt numbers at Re=5032 and A=0.5"

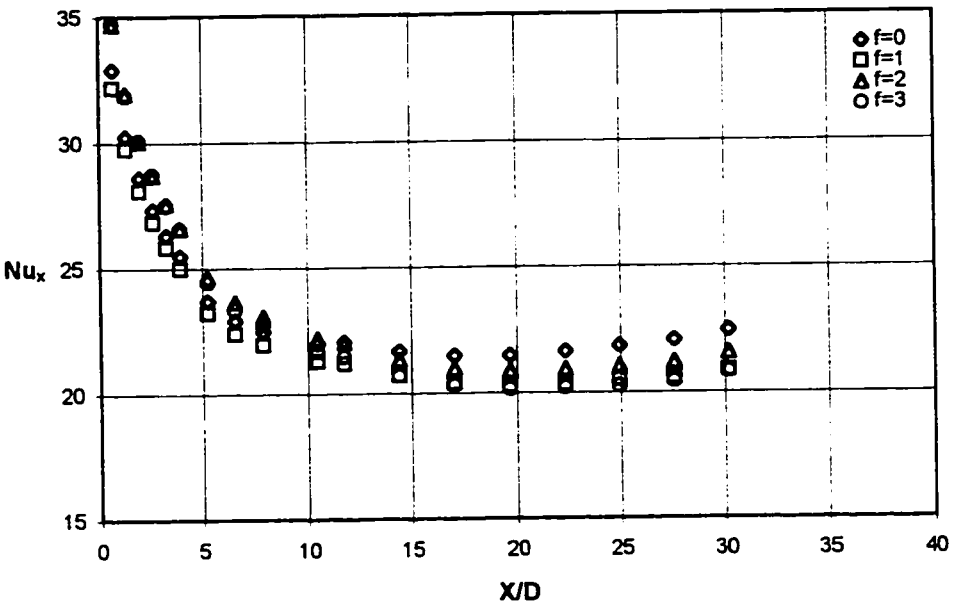

Fig.5.7 Effect of pulsation frequency on local Nusselt numbers at Re=5032 and A=1.0"

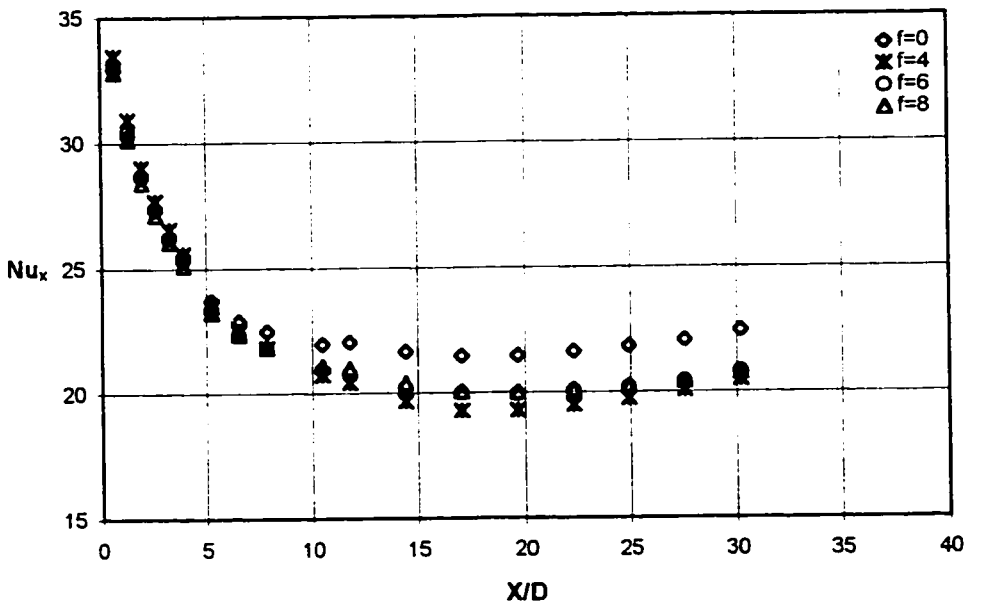

Fig.5.8 Effect of pulsation frequency on local Nusselt numbers at Re=5032 and A=1.0"

the frequency band where the local enhancement in the heat transfer coefficient in the entrance region did occur is from 2 Hz to 6 Hz. Another observation is that the enhancement in the heat transfer coefficient very close to the inlet is increased with 4% at f=2 Hz and with 2% at f=3 Hz compared to the previous case. However, the enhancement at f=4 Hz is reduced with about 2.5% compared to the previous case, while, the maximum reduction in the Nusselt number in the entrance region is observed at f=1 Hz. In this particular amplitude, the reduction in the fully developed region is more compared to the previous case . Maximum and minimum reduction of about 10% at f=4 Hz and 4% at f=2 Hz respectively are observed.

When the pulsation amplitude increased to 1.5″ ($A = 1.5''$) as shown in Figs. 5.9 and 5.10 the local enhancement in the heat transfer coefficient is observed very close to the inlet and extends up to X/D=8 for all pulsation frequency. This enhancement is more compared to the previous case ($A = 1.0''$). Here, maximum enhancement of about 6% very close to the inlet is observed at f=4 Hz. The maximum reduction in heat transfer coefficient in the fully developed region is of about 5% at all pulsation frequencies which is less than the maximum reduction in the previous case.

For Re = 10,235 and $A = 0.5''$ As shown in Figs. 5.11 and 5.12, local reduction in heat transfer coefficient is observed along the test section for all pulsation frequencies. The reduction of the Nusselt number values in the entrance region is less than the reduction in the fully developed region. Maximum reduction of about 2%

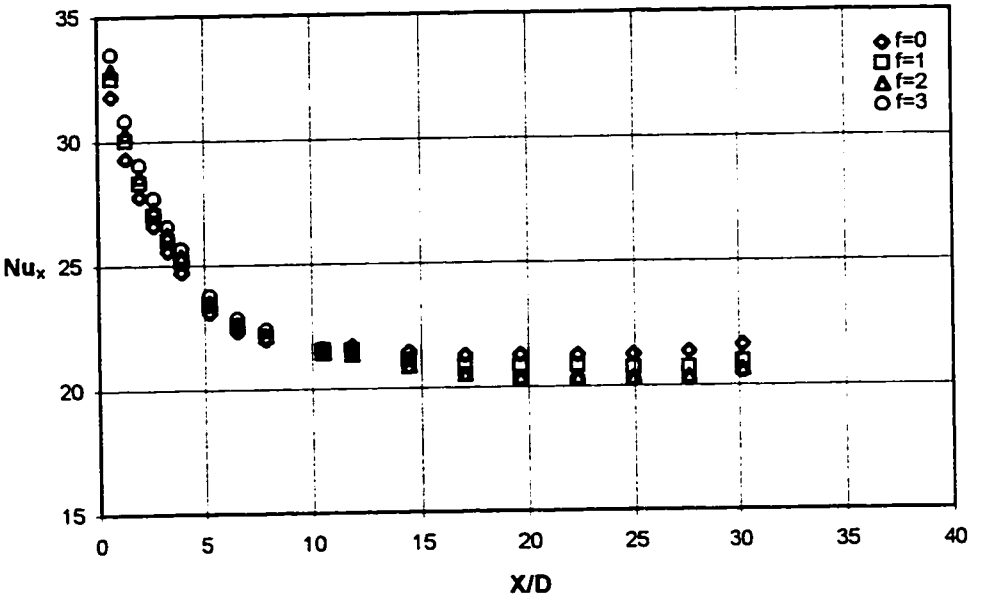

Fig.5.9 Effect of pulsation frequency on local Nusselt numbers at Re=5032 and A=1.5"

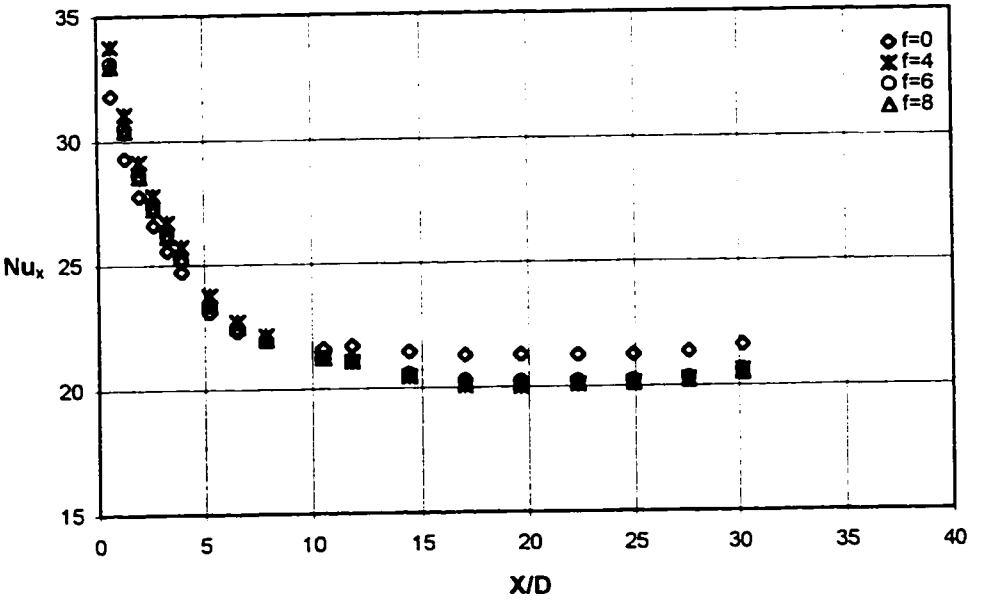

Fig.5.10 Effect of pulsation frequency on local Nusselt numbers at Re=5032 and A=1.5"

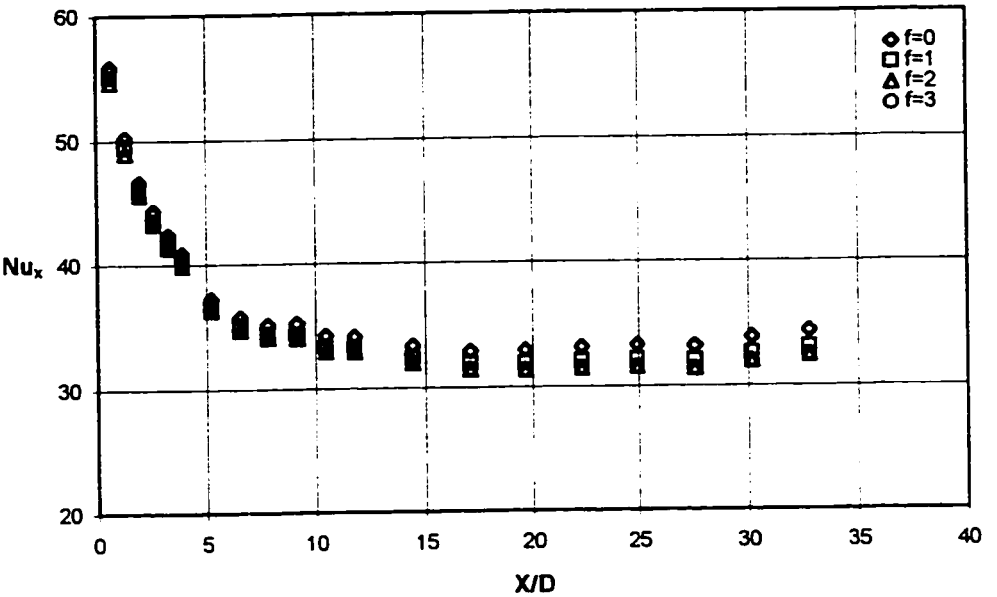

Fig.5.11 Effect of pulsation frequency on local Nusselt numbers at Re=10,235and A=0.5"

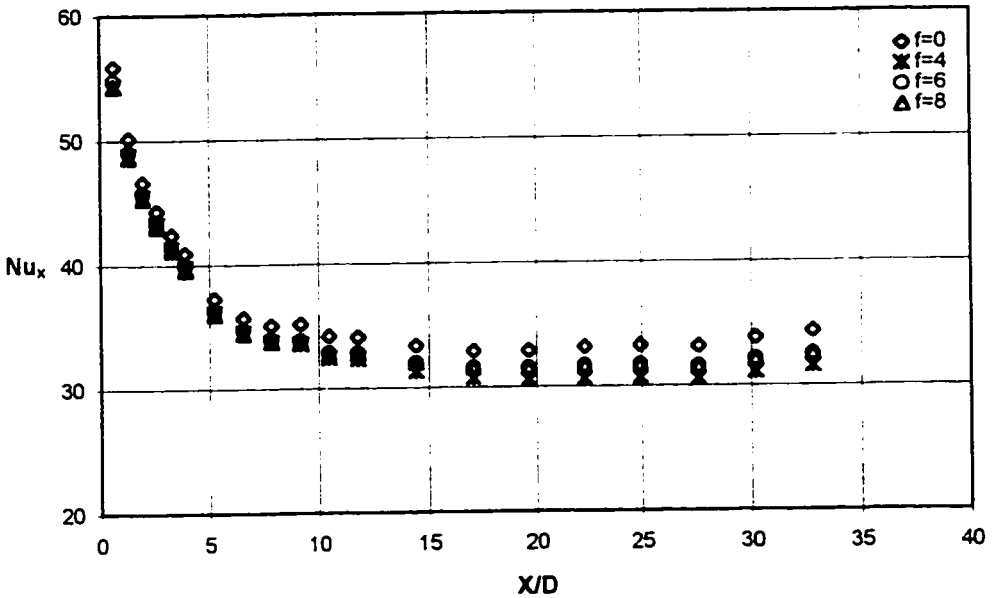

Fig.5.12 Effect of pulsation frequency on local Nusselt numbers at Re=10,235 and A=0.5"

to 3% is observed very close to the inlet at all pulsation frequencies except at f=1 Hz where the reduction is of about 1%. However, in the fully developed region maximum reduction of about 8% in heat transfer coefficient is observed at f = 4 Hz and of about 4% to 5% at the other pulsation frequencies. A similar trend is observed for $A = 1.0''$ as shown in Figs. 5.13 and 5.14, except at pulsation frequencies of 1 Hz , 2 Hz and 3 Hz. At these frequencies the reduction in local heat transfer coefficient very close to the inlet increased to about 4%. In this case, the reduction in the heat transfer coefficient in the entrance region at f = 4 Hz is of about 2% less than that when $A = 0.5''$. However, the reduction in the fully developed region is more than the previous case with about 2% to 4% at all pulsation frequencies.

For the same Reynolds number but at $A = 1.5''$ as shown in Figs. 5.15 and 5.16, the results showed similar trend to that at $A = 0.5''$ except at pulsation frequency ranged from 2 Hz to 4 Hz. In this frequency range a slight enhancement of about 0.7% is observed very close to the inlet and extends down to a length of about 6.5 pipe diameters. In this case , the reduction in the fully developed region at f=4 Hz is of about 2% less than that when $A = 0.5''$.

As shown in Figs. 5.17 and 5.18 for Re = 14,460 and $A = 0.5''$, a local reduction in the heat transfer coefficient is observed along the test section, this reduction is about 2% to 4% in the entrance region at all pulsation frequencies. However, in the

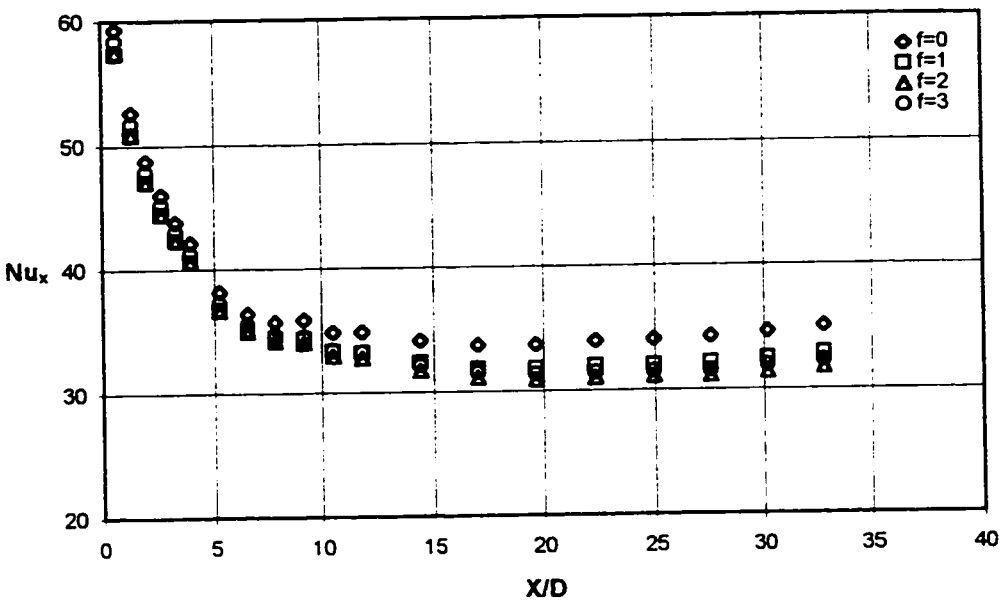

Fig.5.13 Effect of pulsation frequency on local Nusselt numbers at Re=10,235 and A=1.0"

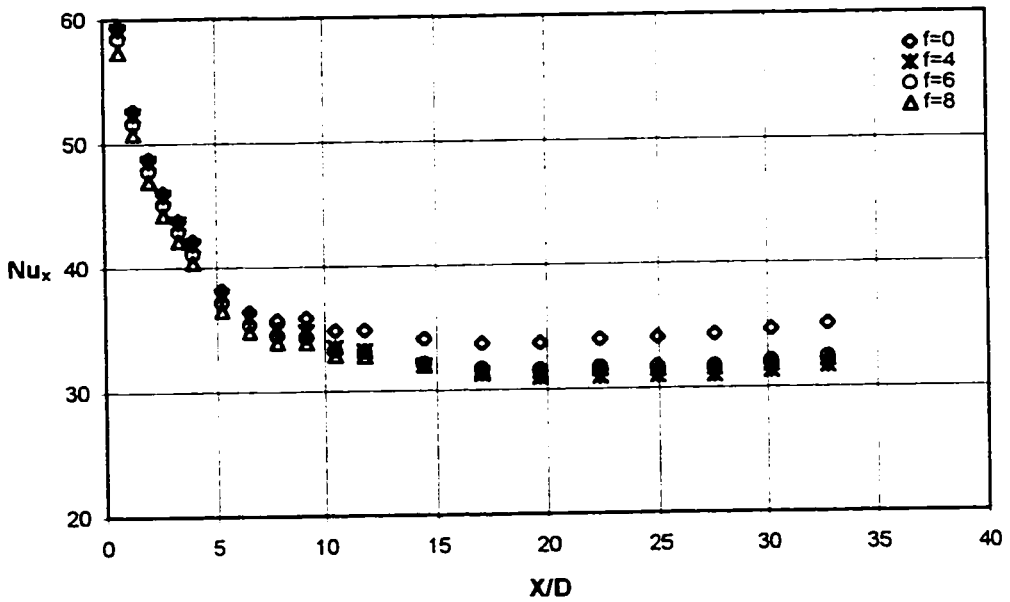

Fig.5.14 Effect of pulsation frequency on local Nusselt numbers at Re=10,235 and A=1.0"

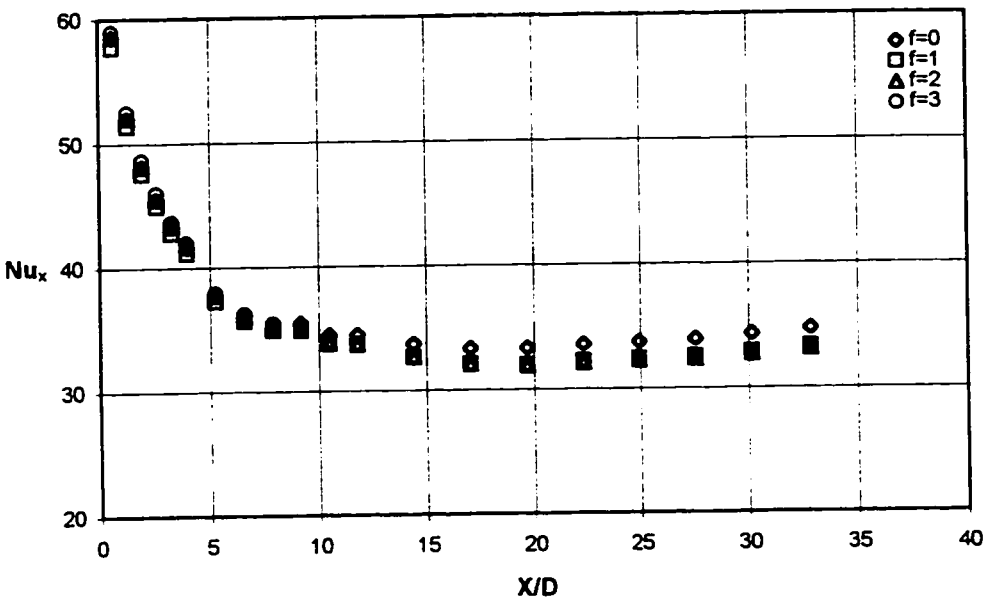

Fig.5.15 Effect of pulsation frequency on local Nusselt numbers at Re=10,235 and A=1.5"

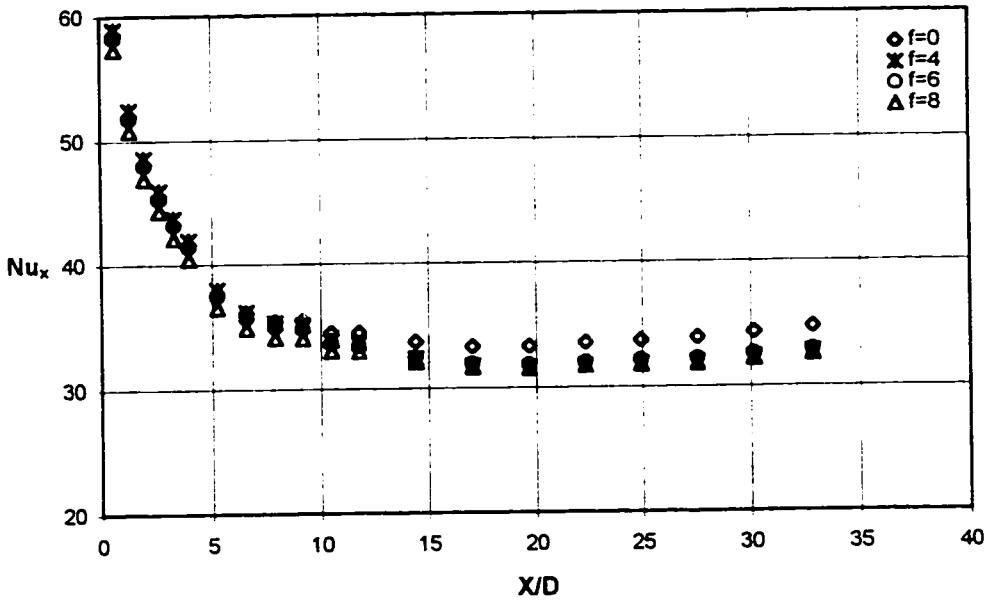

Fig.5.16 Effect of pulsation frequency on local Nusselt numbers at Re=10,235 and A=1.5"

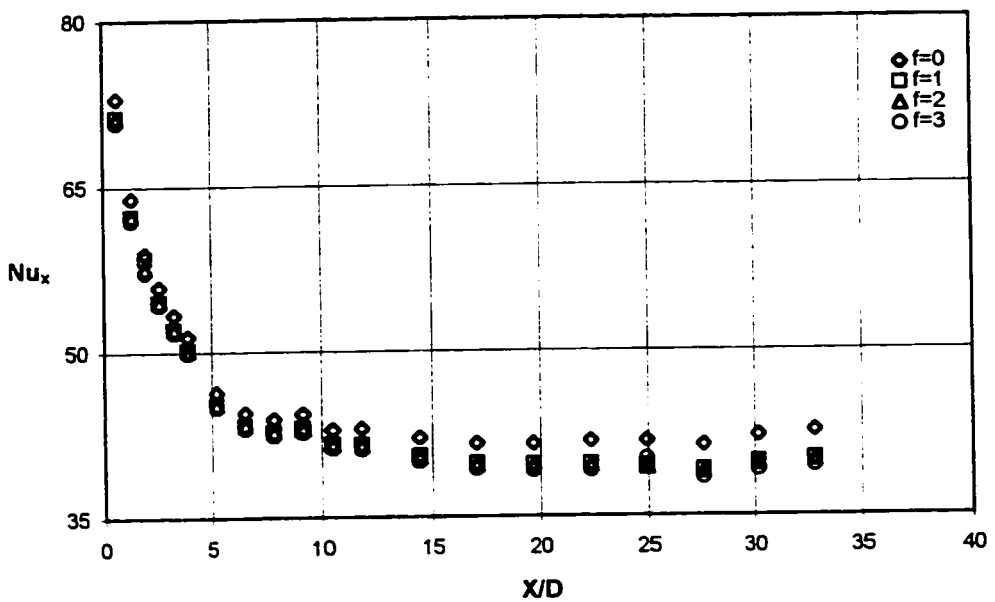

Fig.5.17 Effect of pulsation frequency on local Nusselt numbers at Re=14,460 and A=0.5"

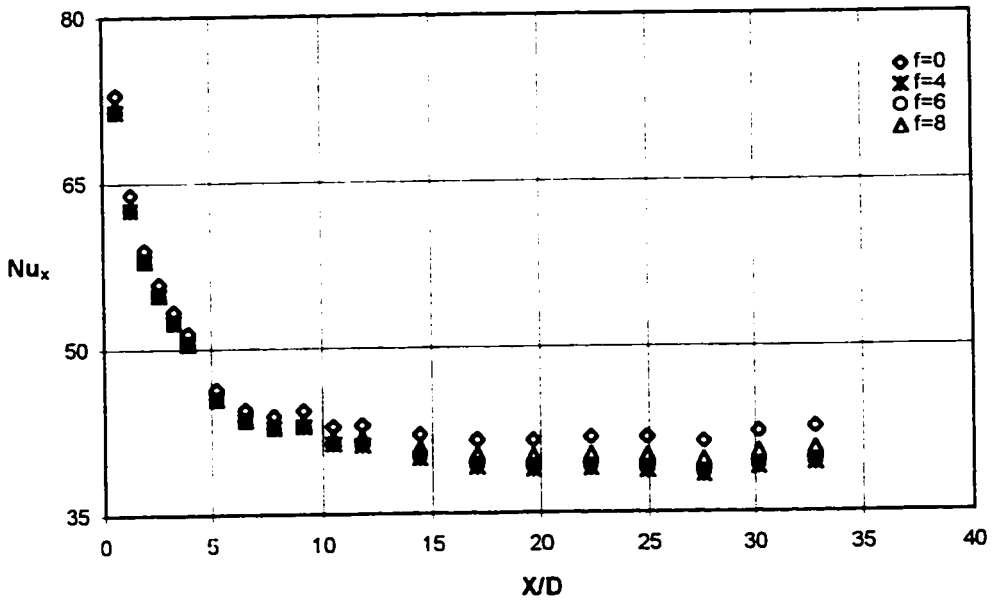

Fig.5.18 Effect of pulsation frequency on local Nusselt numbers at Re=14,460 and A=0.5"

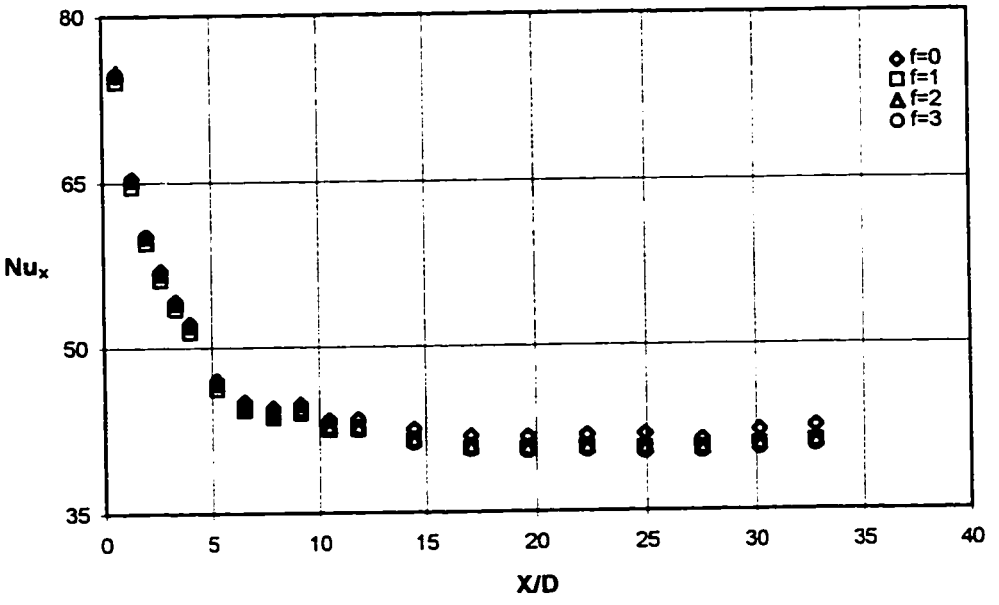

Fig.5.19 Effect of pulsation frequency on local Nusselt numbers at Re=14,460 and A=1.0"

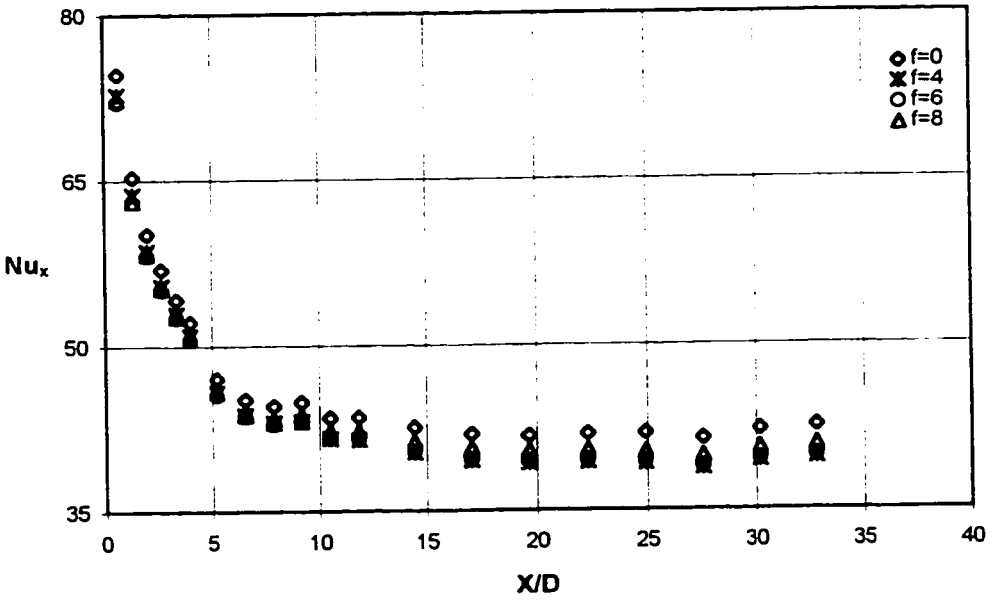

Fig.5.20 Effect of pulsation frequency on local Nusselt numbers at Re=14,460 and A=1.0"

fully developed region the maximum reduction in heat transfer coefficient is about 7% at pulsation frequencies of 4 Hz and 6 Hz and about 4% to 6% at other pulsation frequencies.

A similar trend is observed at $A = 1.0''$ as shown in Figs. 5.19 and 5.20, except at pulsation frequencies of 2 Hz and 3 Hz. At these particular frequencies a negligible effect of pulsation frequencies in the heat transfer coefficient in the entrance region is observed (i.e., less than 1%). However, in the fully developed region, the reduction in the heat transfer coefficient of at pulsation frequency ranged from 1 Hz to 3 Hz, is less compared to the previous case.

At $A = 1.5''$ as shown in Figs. 5.21 and 5.22 , a negligible effect of pulsation frequency on local heat transfer coefficient at f = 1 Hz along the test section is observed. Also, at f = 4 Hz and f = 6 Hz, a negligible effect of pulsation frequency is observed in the entrance region while less reduction compared to the previous cases ($A = 0.5''$ and $A = 1.5''$) is observed in the fully developed region . On the other hand, almost a similar trend to that at $A = 1.0''$ is observed at the other pulsation frequencies.

At Reynolds number of 20,138 for the three different amplitudes as shown in Figs. 5.23 to 5.28, a similar trend of local reduction in heat transfer coefficient along the test section is observed. Also, This reduction is more in the fully developed region compared to the entrance region. The results for pulsation amplitudes of 1.0″ and

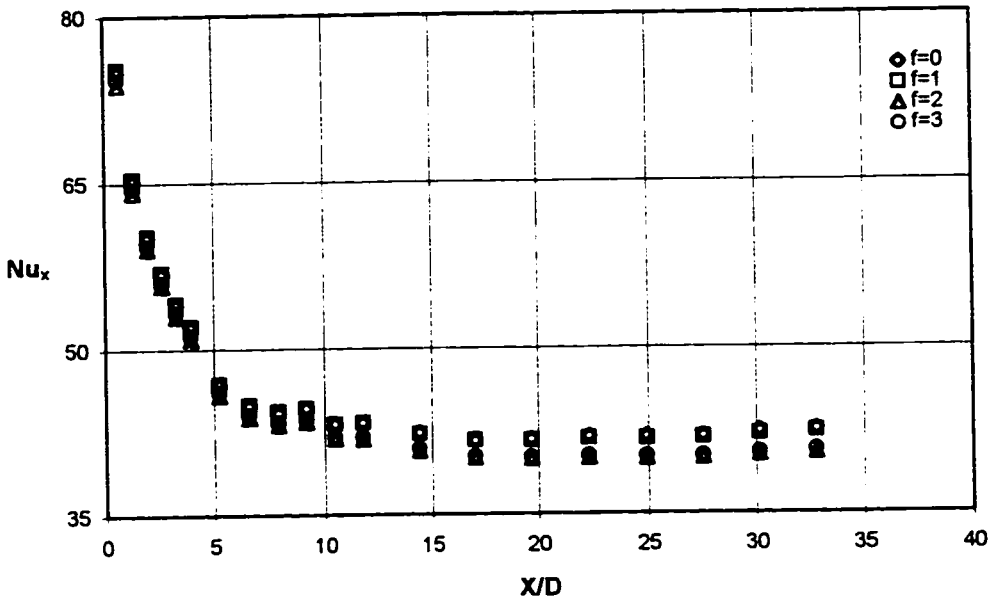

Fig.5.21 Effect of pulsation frequency on local Nusselt numbers at Re=14,460 and A=1.5"

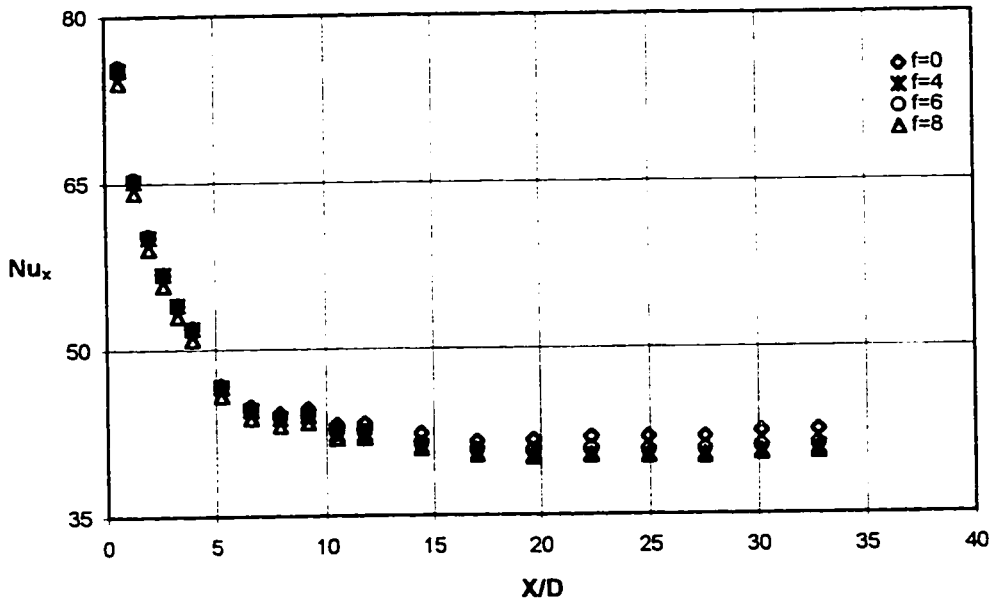

Fig.5.22 Effect of pulsation frequency on local Nusselt numbers at Re=14,460 and A=1.5"

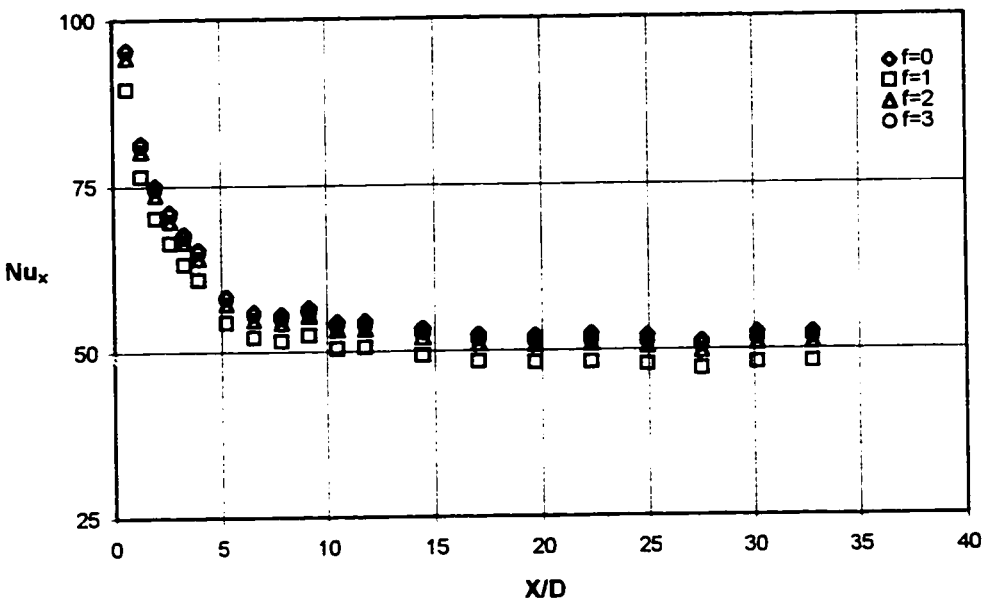

Fig.5.23 Effect of pulsation frequency on local Nusselt numbers at Re=20,138 and A=0.5"

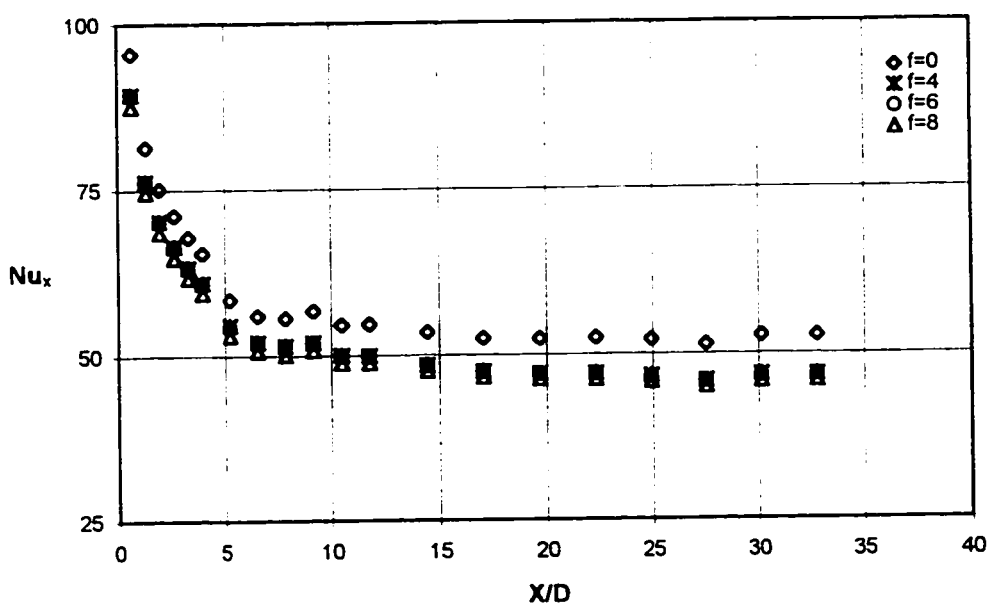

Fig.5.24 Effect of pulsation frequency on local Nusselt numbers at Re=20,138 and A=0.5"

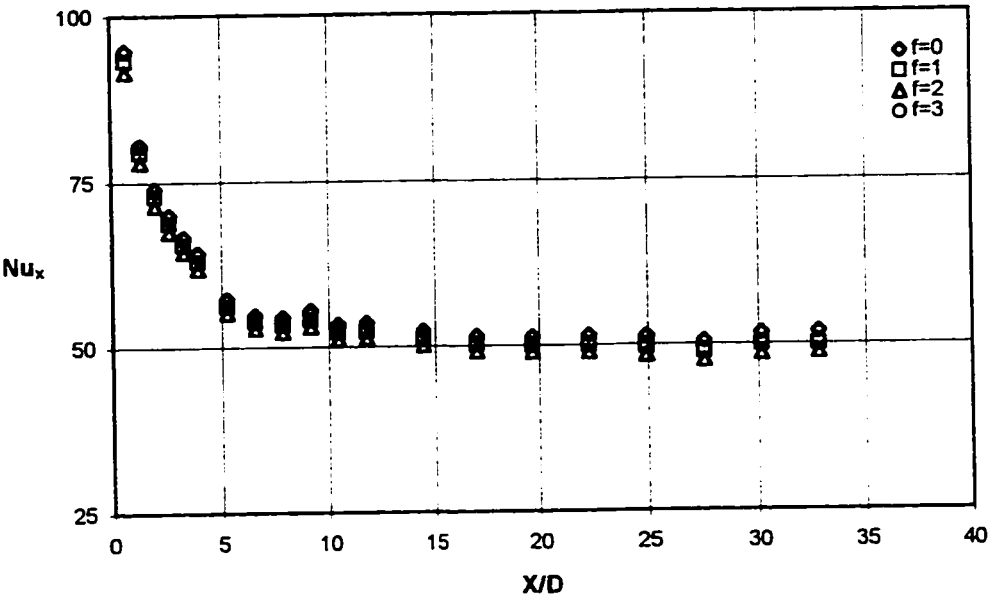

Fig.5.25 Effect of pulsation frequency on local Nusselt numbers at Re=20,138 and A=1.0"

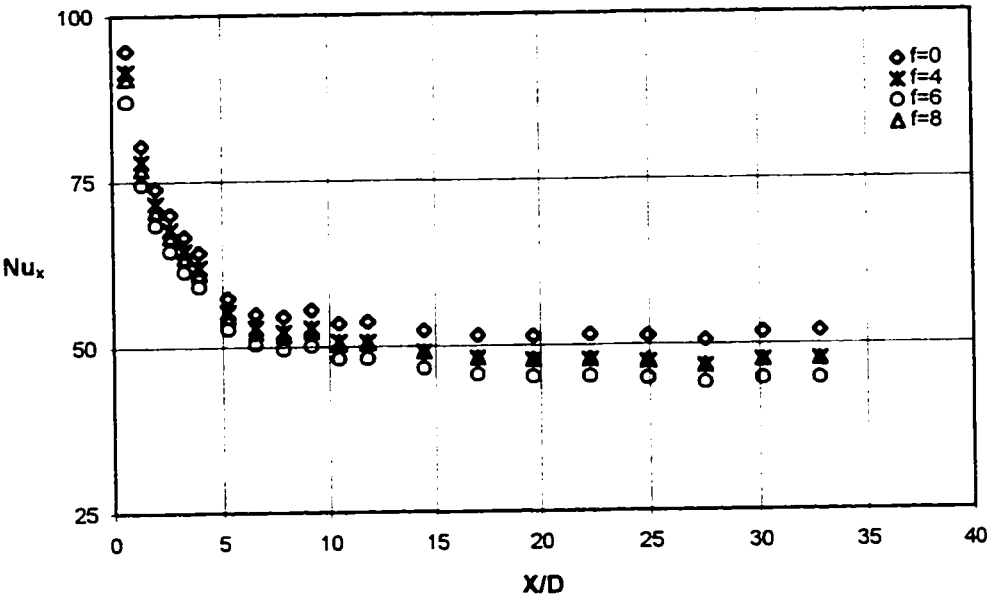

Fig.5.26 Effect of pulsation frequency on local Nusselt numbers at Re=20,138 and A=1.0"

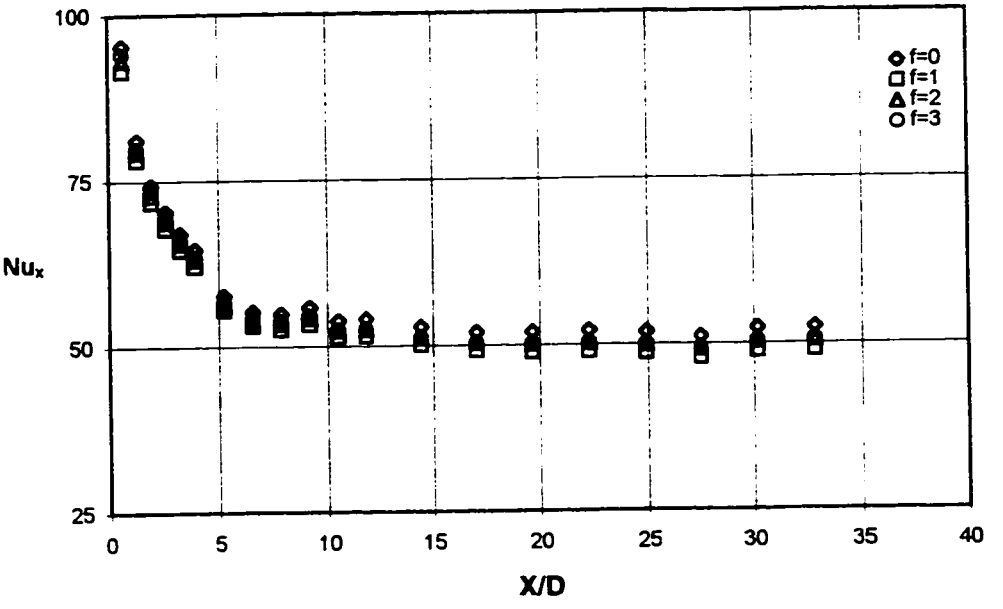

Fig.5.27 Effect of pulsation frequency on local Nusselt numbers at Re=20,138 and A=1.5"

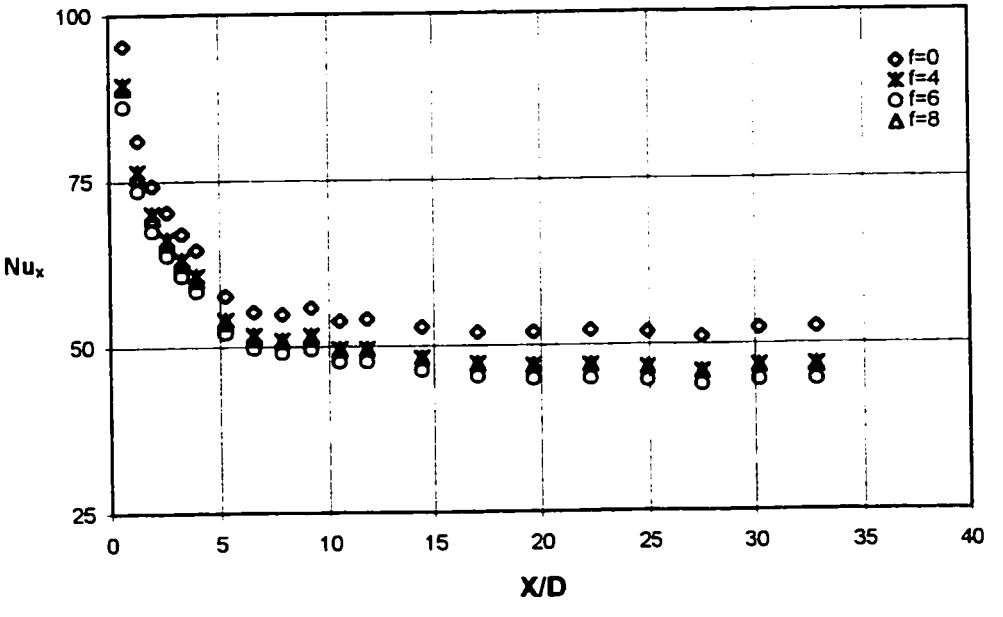

Fig.5.28 Effect of pulsation frequency on local Nusselt numbers at Re=20,138 and A=1.5"

1.5″ showed almost the same effect on the heat transfer coefficient at all pulsation frequencies with maximum difference of about 3%. In this case , a maximum reduction of about 10% in the entrance region and 14% in the fully developed region is observed at pulsation parameters of 6 Hz and 1.5″. The general trend of the results showed that, when the pulsation amplitude increased the reduction in the heat transfer coefficient decreased or remained the same with difference of about 2%. This is true in most cases except at f=6 Hz.

For Re =28,984 and A = 0.5″ as shown in Figs. 5.29 and 5.30 a similar trend to the previous case (Re=20,138) except at f=8 Hz where a local enhancement of about 2% in the entrance region is observed. Here, the reduction in the heat transfer coefficient along the test section is less compared to the previous case (Re=20,138). However, the results for Re=28,200 and pulsation amplitudes of A = 1.0″ and A = 1.5″ as shown in Figs. 5.31 to 5.34 are almost similar for all pulsation frequencies with maximum difference of about ±2%. In this case, maximum reduction of about 8% in the entrance region and 12% in the fully developed region is observed at pulsation parameters of 6 Hz and 1.0″. It is important to note that there is difference of about 3% in the Reynolds number between the case of pulsation amplitude of 0.5″ and the other cases . This difference is due to the unexpected change in the room temperature which cause a difference in the fluid properties used to calculate the Reynolds number.

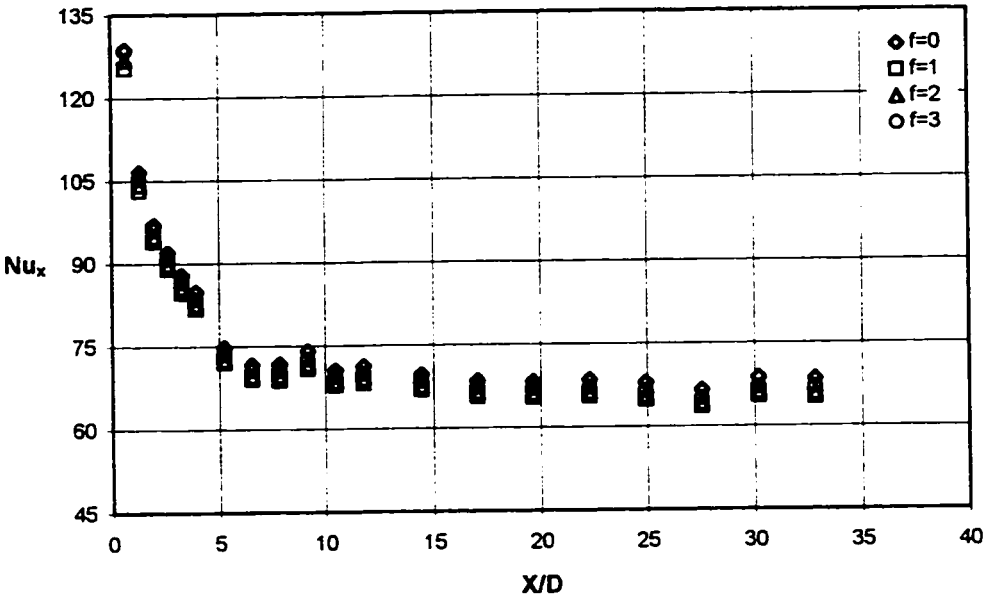

Fig.5.29 Effect of pulsation frequency on local Nusselt numbers at Re=28,984 and A=0.5"

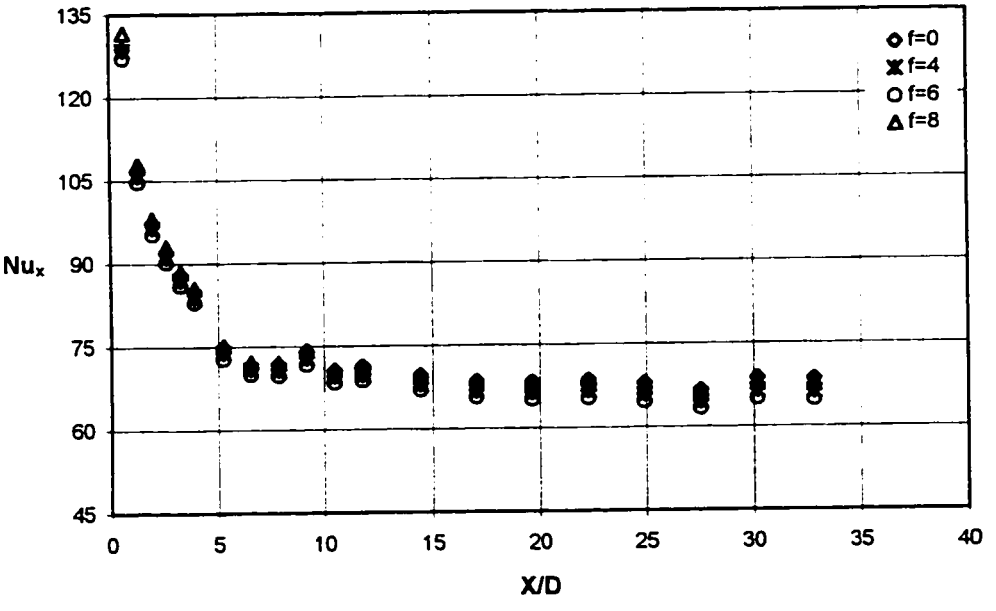

Fig.5.30 Effect of pulsation frequency on local Nusselt numbers at Re=28,984 and A=0.5"

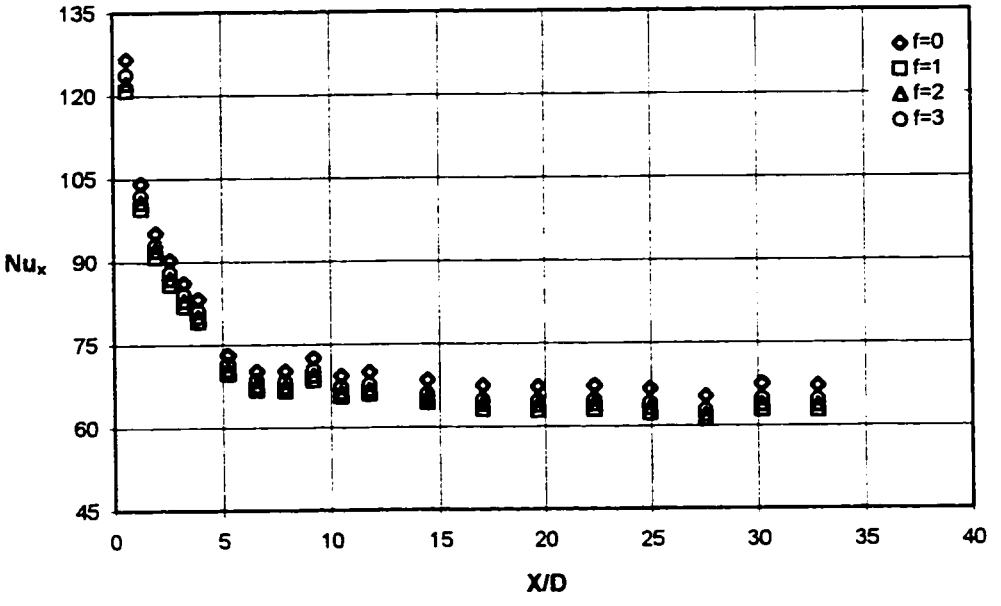

Fig.5.31 Effect of pulsation frequency on local Nusselt numbers at Re=28,200 and A=1.0"

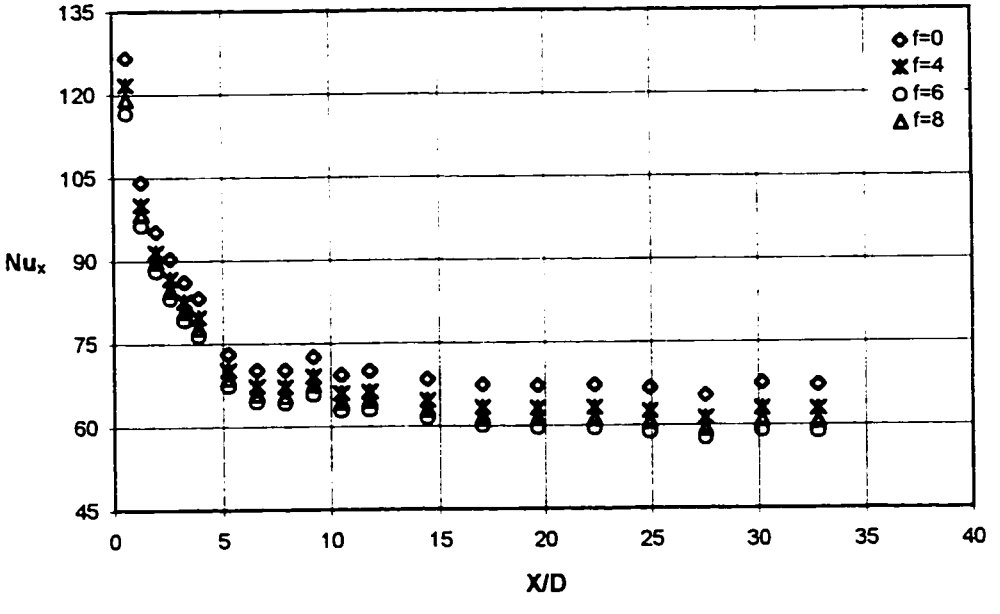

Fig.5.32 Effect of pulsation frequency on local Nusselt numbers at Re=28,200 and A=1.0"

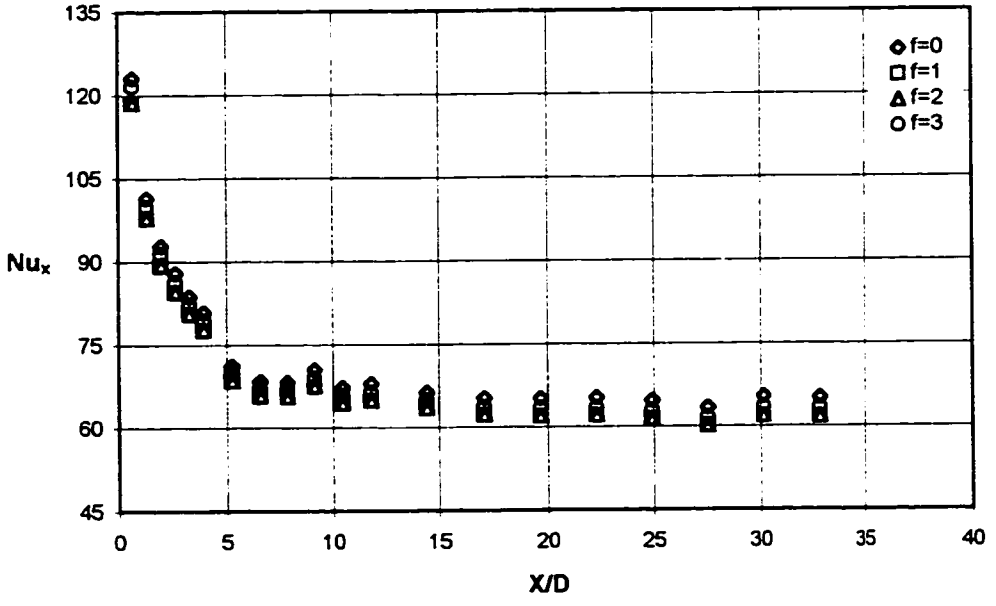

Fig.5.33 Effect of pulsation frequency on local Nusselt numbers at Re=28,200 and A=1.5"

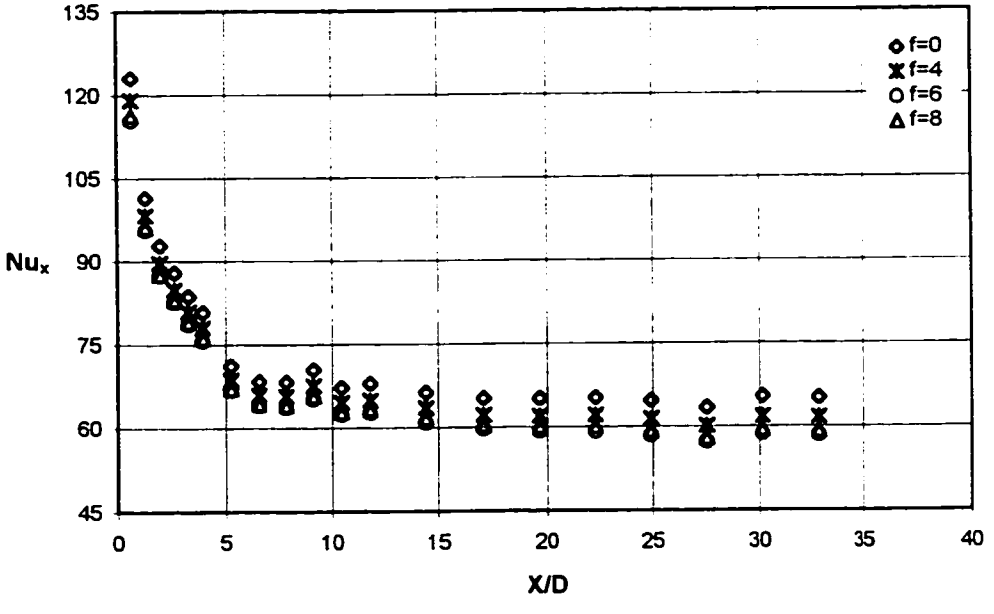

Fig.5.34 Effect of pulsation frequency on local Nusselt numbers at Re=28,200 and A=1.5"

5.2.2 The effect of Amplitude on the local Nusselt Numbers

In this subsection the behavior of the local Nusselt number along the test section, under the influence of pulsation amplitudes is discussed. Here, the local Nusselt number for pulsed flow at different Reynolds numbers and pulsation frequencies for the three different amplitudes are shown in Figs. 5.35 to 5.64.

At low Reynolds number of lower than or equal 14,460, Figs. 5.35 to 5.52, indicate that the effect of pulsation amplitude in the local Nusselt number is more significant in the entrance region. Here, the influence of pulsation amplitude of 1.0″ and 1.5″ on the local Nusselt number are almost the same except at some pulsation frequencies (i.e., f= 2 and 3 Hz at Re=5302, f=2 Hz at Re=10,328 and f=4.6 Hz at Re=14,460) where the difference is limited to around ±3%. In the same region , lower value of the local Nusselt number for pulsed flow is observed at pulsation amplitude of 0.5″ compared to the other pulsation amplitudes. Maximum difference of about 10% in the value of Nu between this particular amplitude ($A = 0.5''$) and the other pulsation amplitudes. This maximum difference decreased as the Reynolds number increased until it reached 5.5% at Re=14,460. However, in the fully developed region, the influence of pulsation amplitudes is within ±3% at Reynolds numbers of 5032 and 10,328, and ±4% at Re=14,460 for all pulsation frequencies.

At Re=20,138 as shown in Figs. 5.53 to 5.58, the effect of pulsation amplitudes

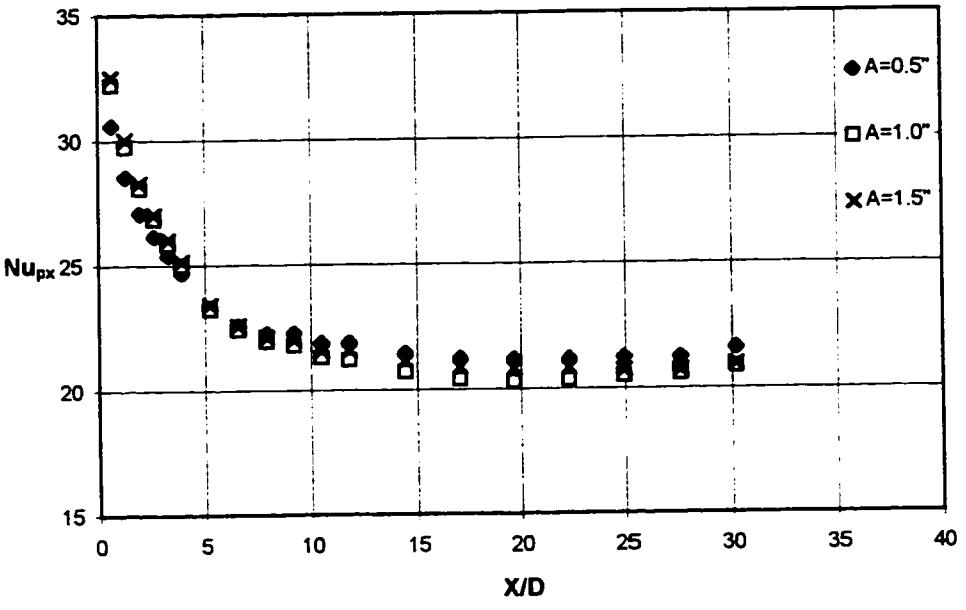

Fig.5.35 Effect of pulsation amplitude on local Nusselt numbers at Re=5032 and f=1.0 Hz

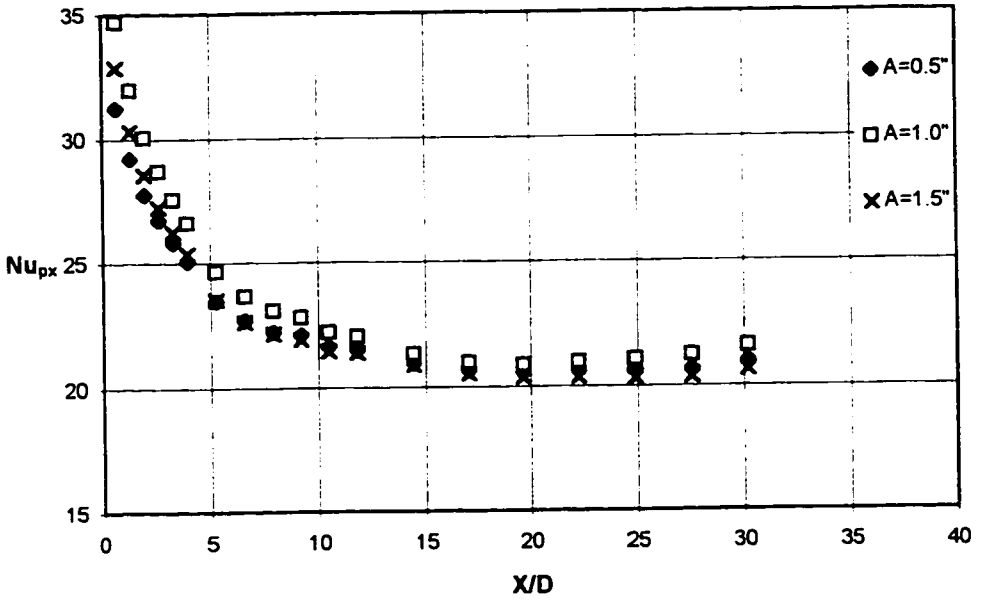

Fig.5.36 Effect of pulsation amplitude on local Nusselt numbers at Re=5032 and f=2.0 Hz

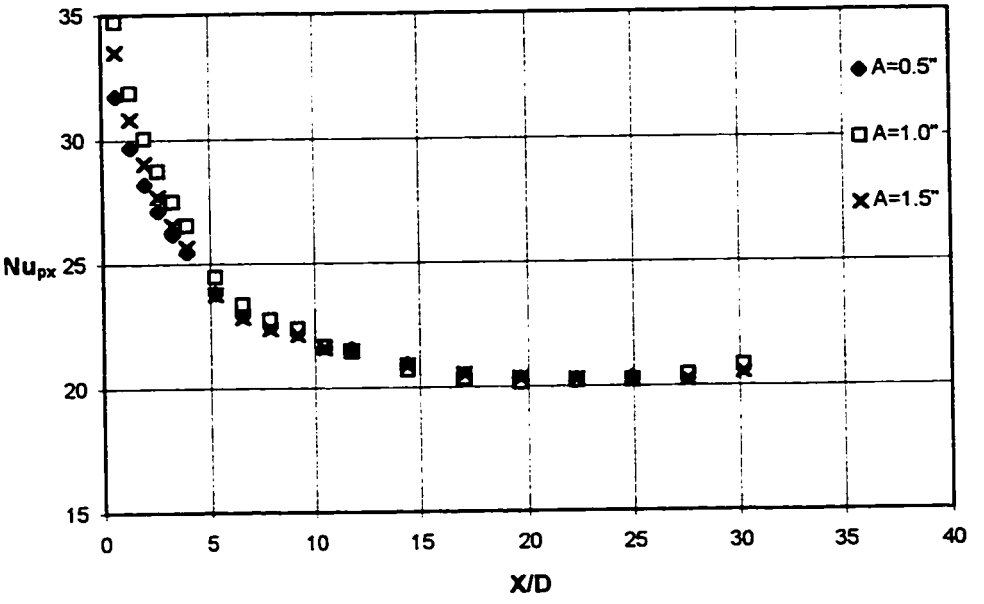

Fig.5.37 Effect of pulsation amplitude on local Nusselt numbers at Re=5032 and f=3.0 Hz

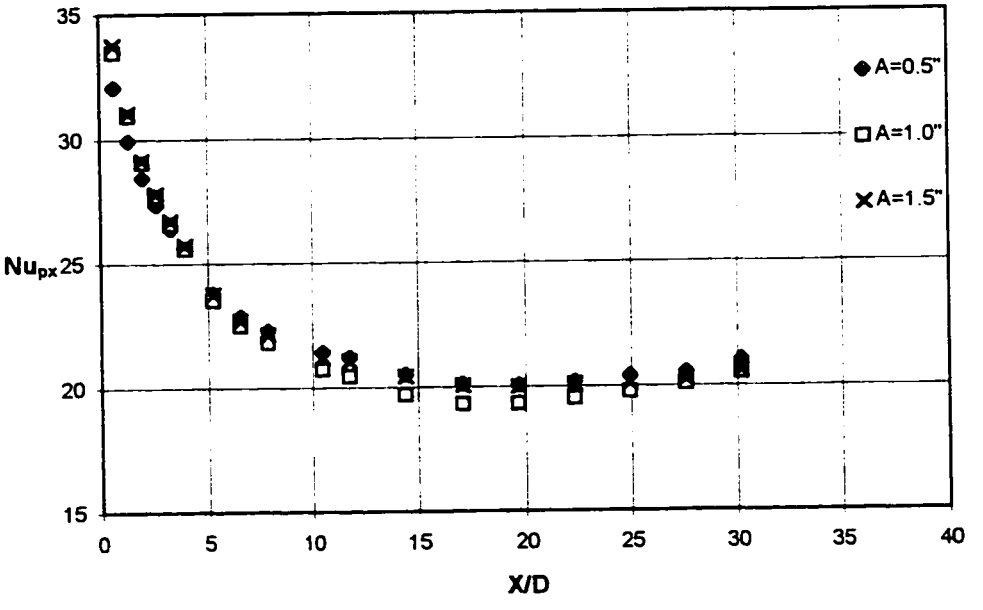

Fig.5.38 Effect of pulsation amplitude on local Nusselt numbers at Re=5032 and f=4.0 Hz

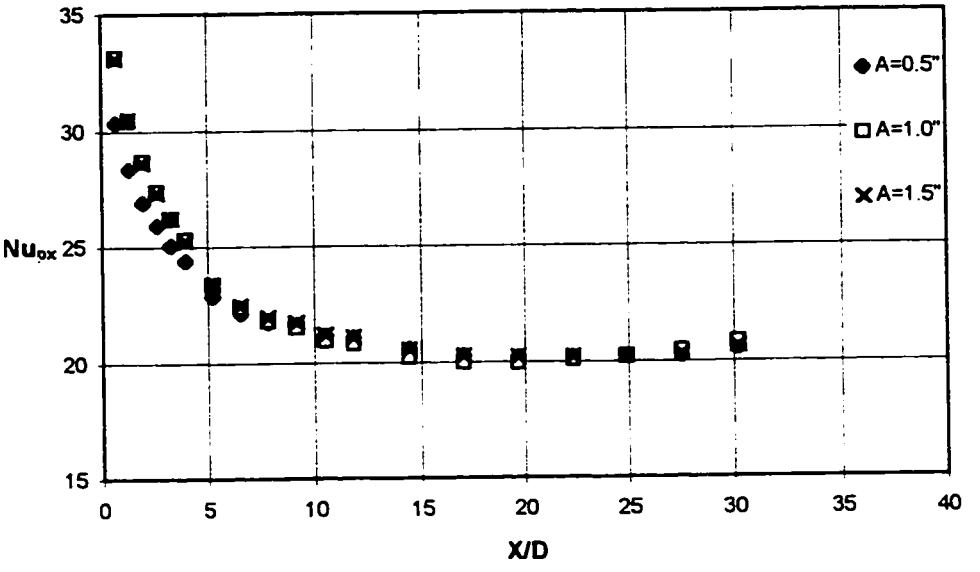

Fig.5.39 Effect of pulsation amplitude on local Nusselt numbers at Re=5032 and f=6.0 Hz

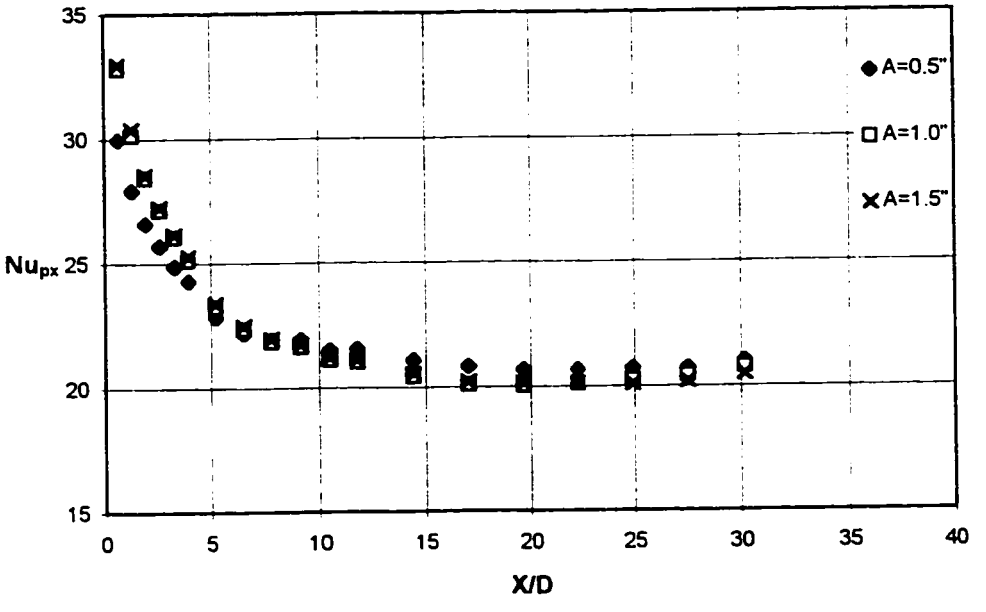

Fig.5.40 Effect of pulsation amplitude on local Nusselt numbers at Re=5032 and f=8.0 Hz

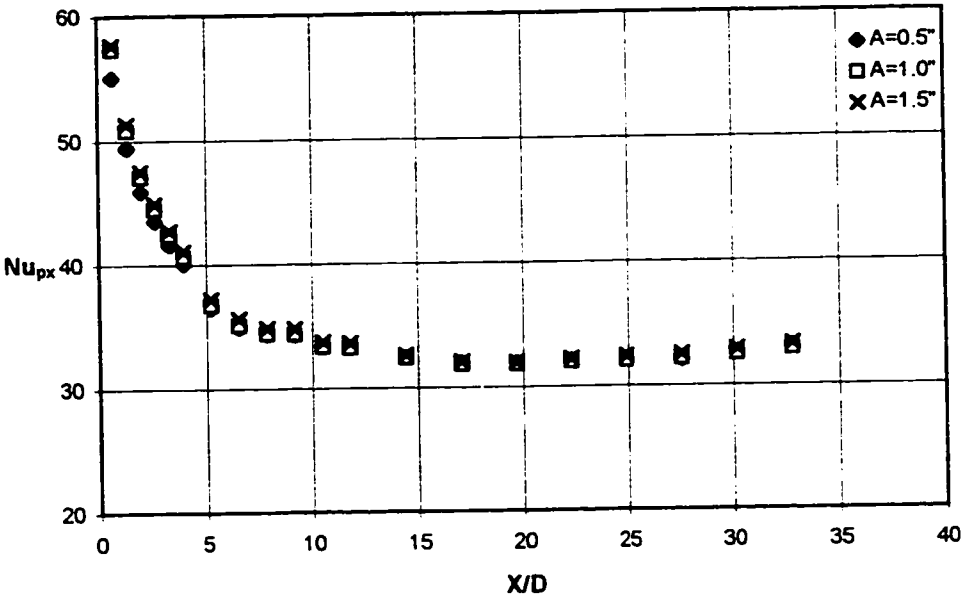

Fig.5.41 Effect of pulsation amplitude on local Nusselt numbers at Re=10,235 and f=1.0 Hz

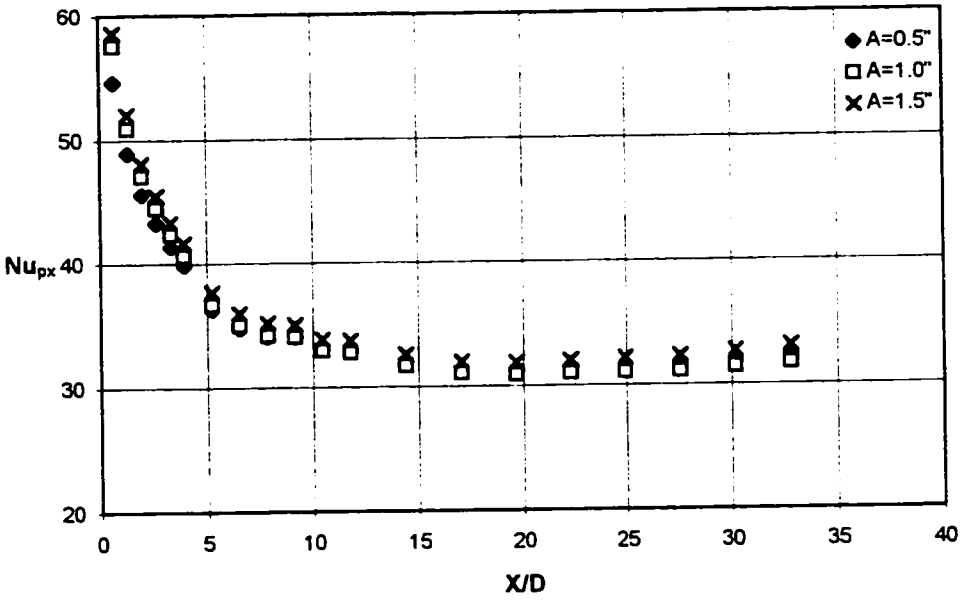

Fig.5.42 Effect of pulsation amplitude on local Nusselt numbers at Re=10,235 and f=2.0 Hz

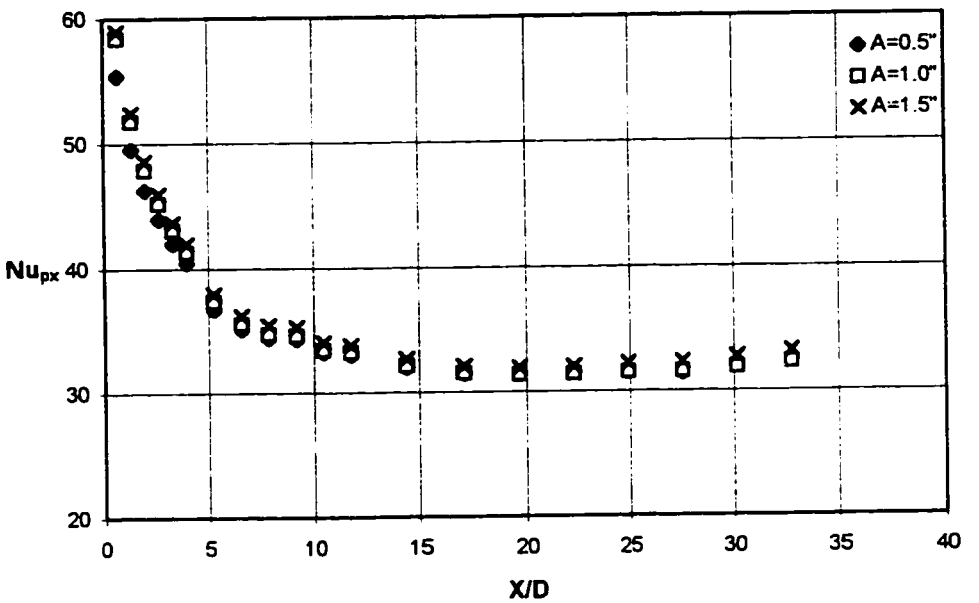

Fig.5.43 Effect of pulsation amplitude on local Nusselt numbers at Re=10,235 and f=3.0 Hz

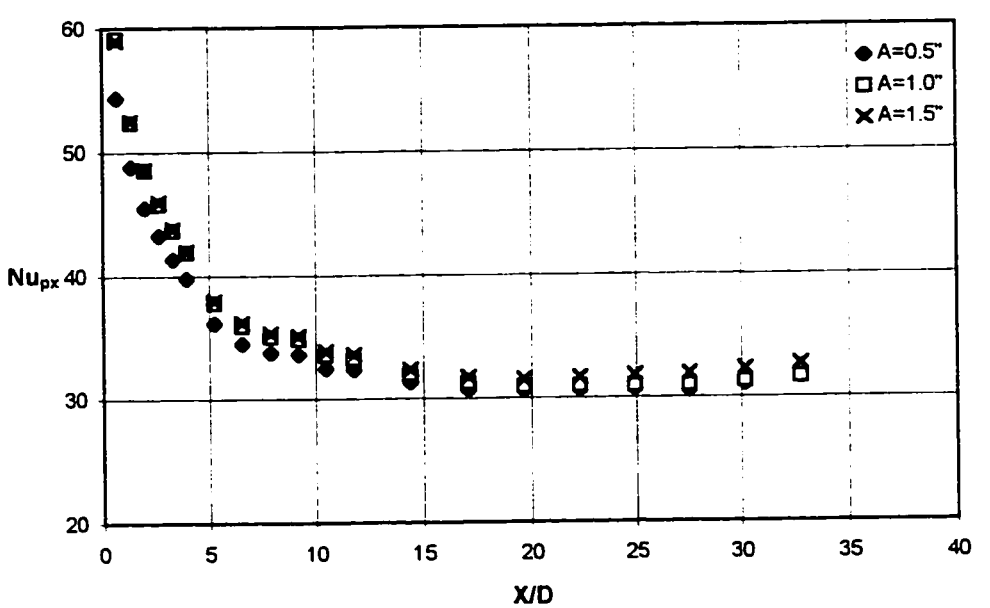

Fig.5.44 Effect of pulsation amplitude on local Nusselt numbers at Re=10,235 and f=4.0 Hz

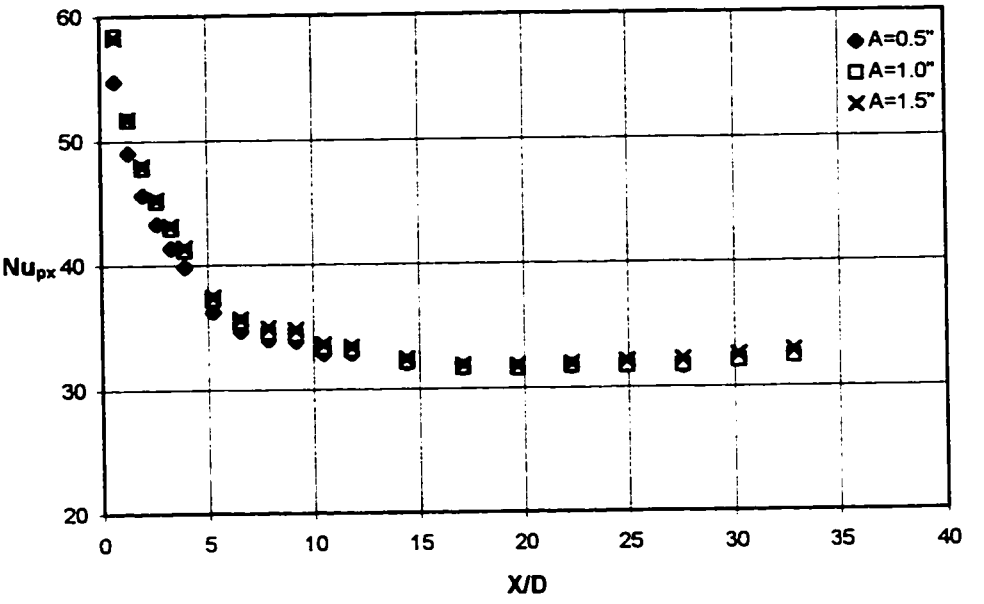

Fig.5.45 Effect of pulsation amplitude on local Nusselt numbers at Re=10,235 and f=6.0 Hz

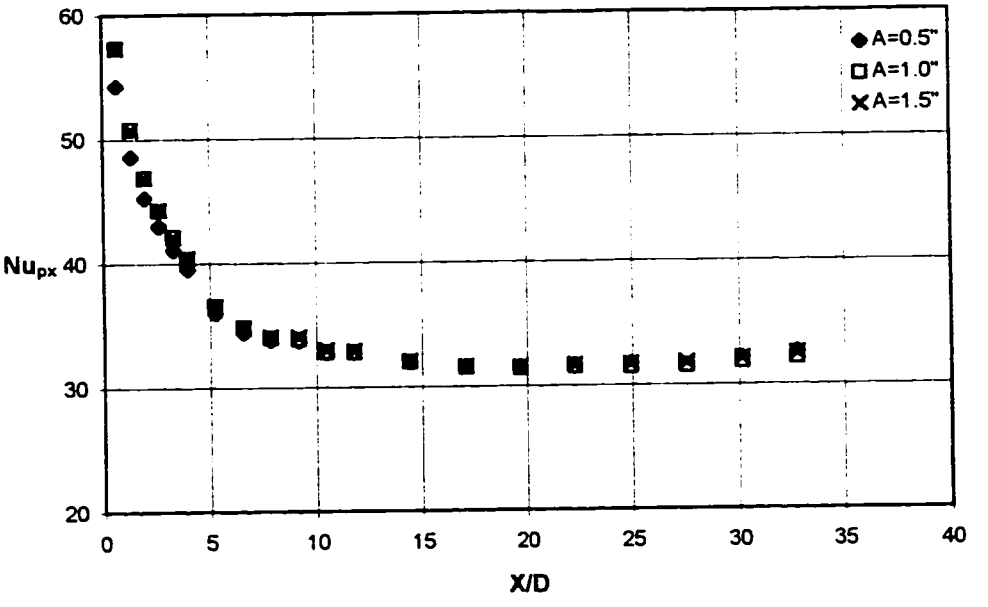

Fig.5.46 Effect of pulsation amplitude on local Nusselt numbers at Re=10,235 and f=8.0 Hz

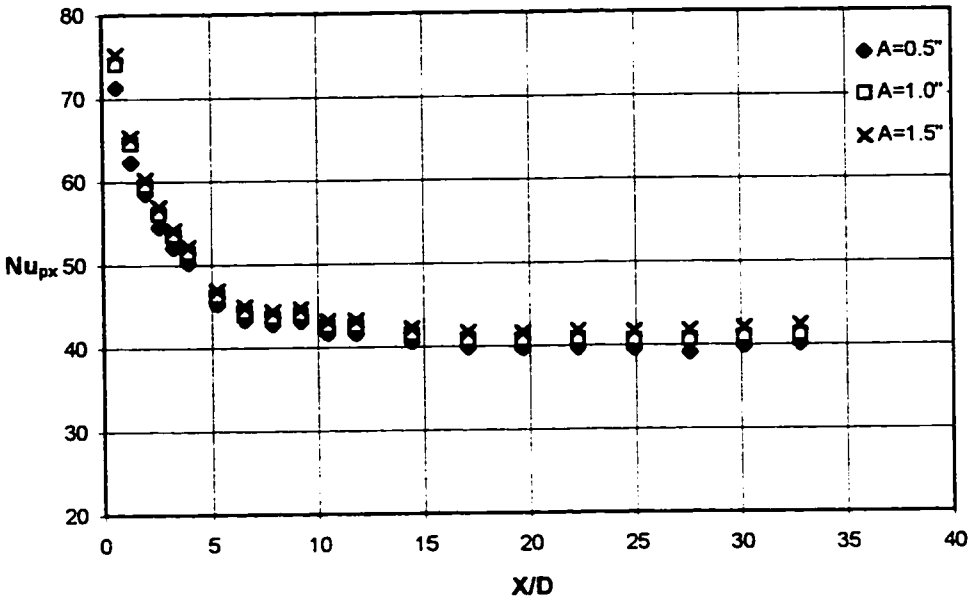

Fig.5.47 Effect of pulsation amplitude on local Nusselt numbers at Re=14,460 and f=1.0 Hz

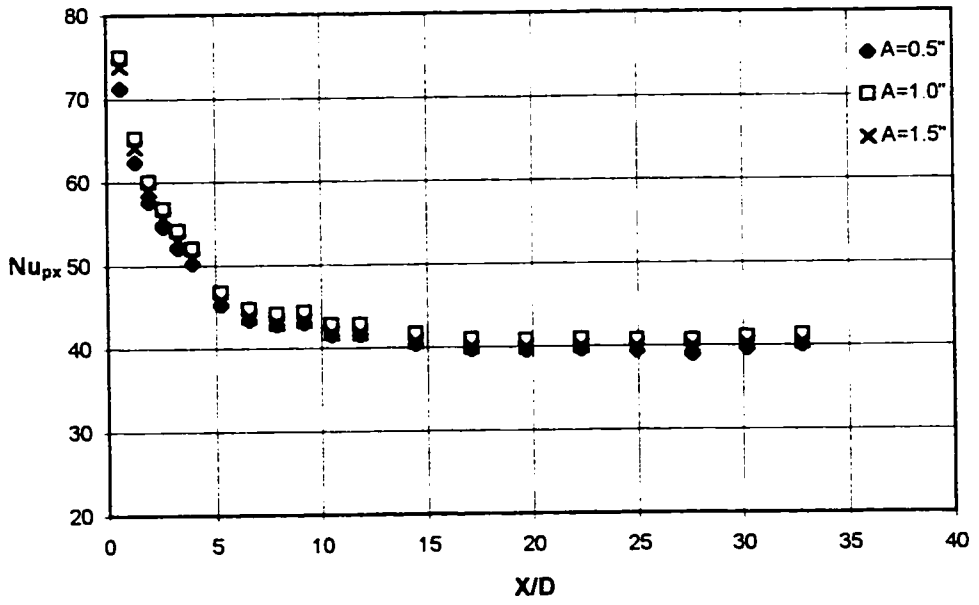

Fig.5.48 Effect of pulsation amplitude on local Nusselt numbers at Re=14,460 and f=2.0 Hz

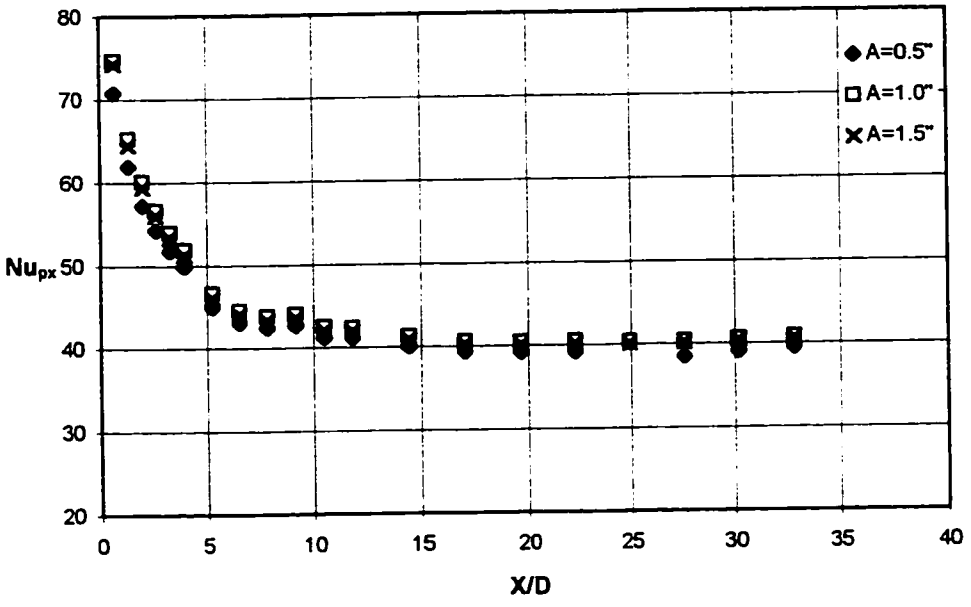

Fig.5.49 Effect of pulsation amplitude on local Nusselt numbers at Re=14,460 and f=3.0 Hz

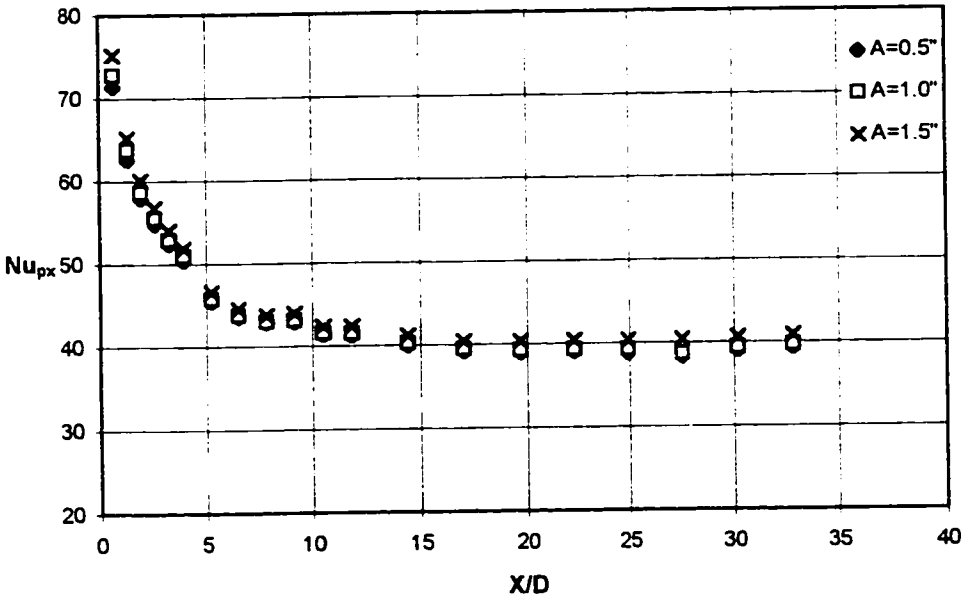

Fig.5.50 Effect of pulsation amplitude on local Nusselt numbers at Re=14,460 and f=4.0 Hz

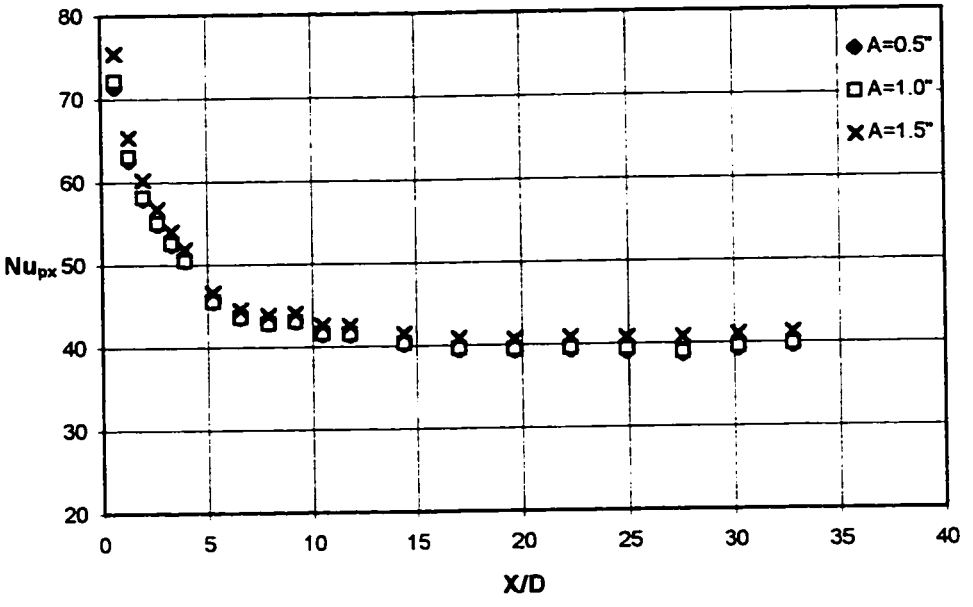

Fig.5.51 Effect of pulsation amplitude on local Nusselt numbers at Re=14,460 and f=6.0 Hz

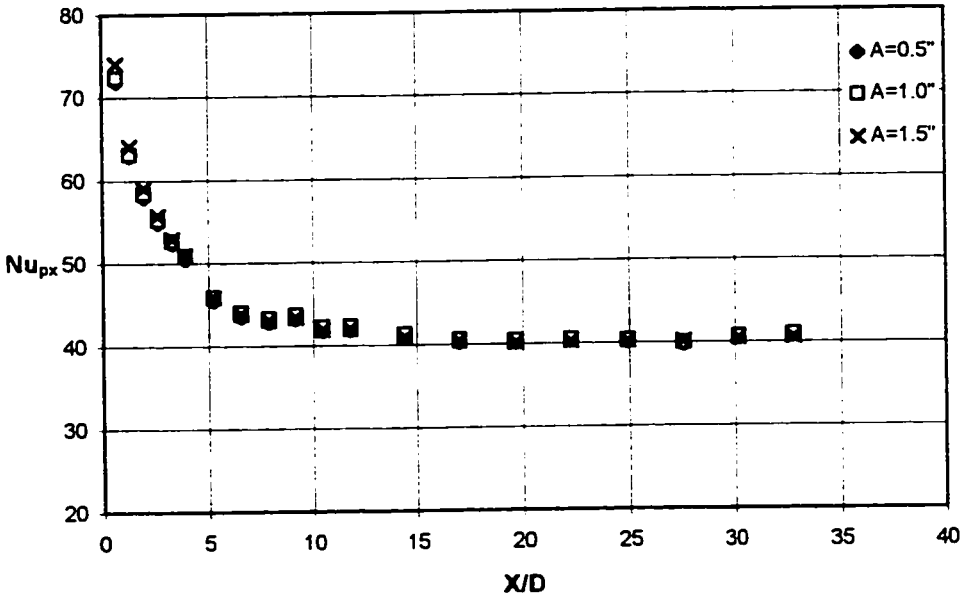

Fig.5.52 Effect of pulsation amplitude on local Nusselt numbers at Re=14,460 and f=8.0 Hz

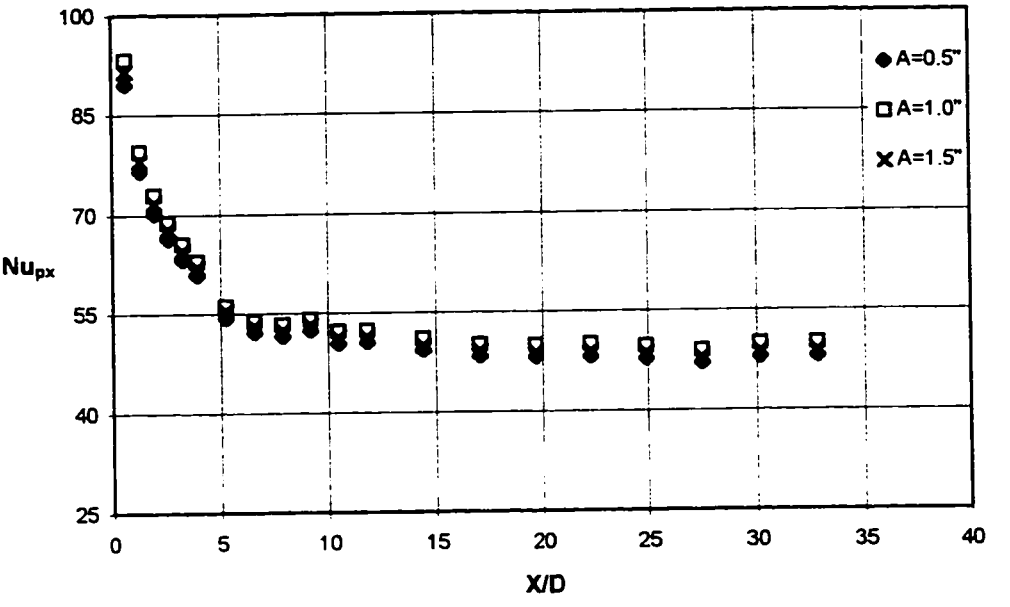

Fig.5.53 Effect of pulsation amplitude on local Nusselt numbers at Re=20,138 and f=1.0 Hz

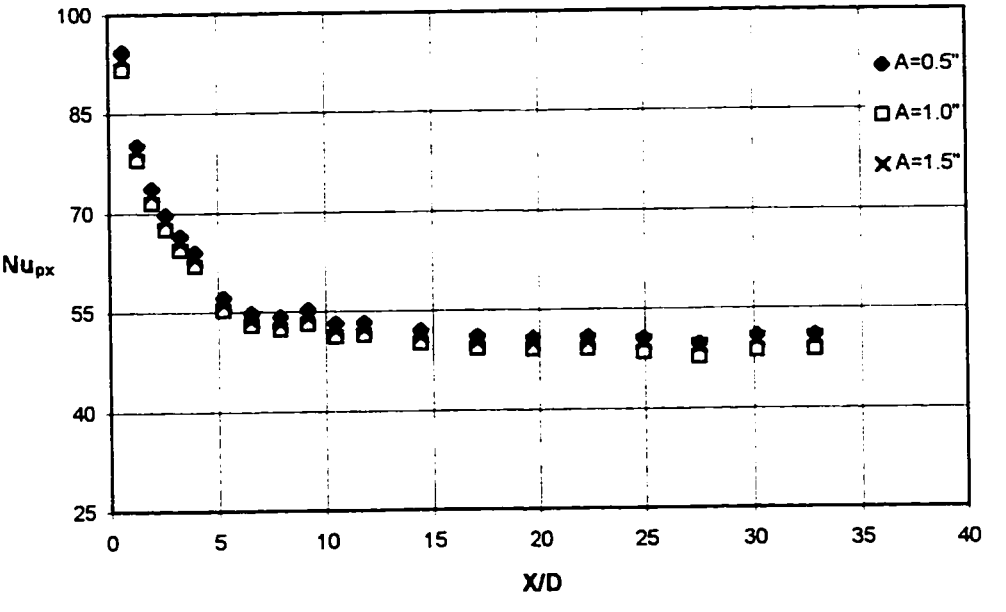

Fig.5.54 Effect of pulsation amplitude on local Nusselt numbers at Re=20,138 and f=2.0 Hz

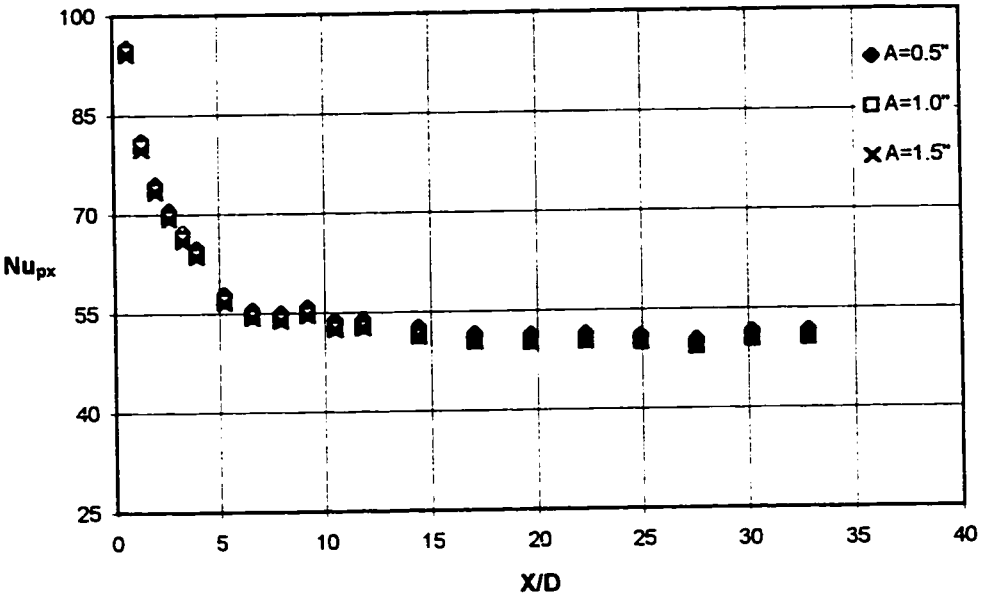

Fig.5.55 Effect of pulsation amplitude on local Nusselt numbers at Re=20,138 and f=3.0 Hz

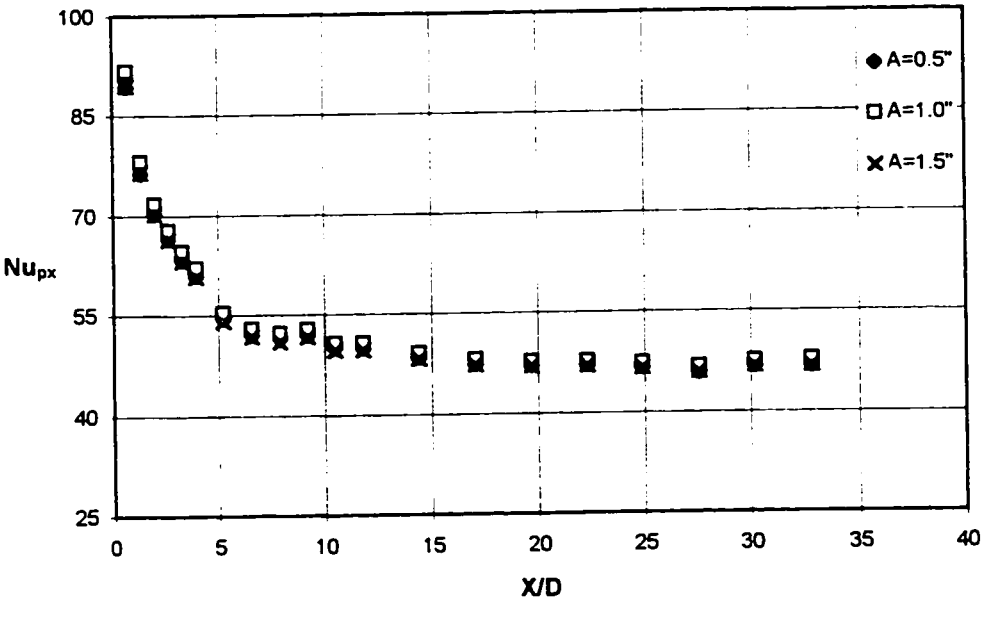

Fig.5.56 Effect of pulsation amplitude on local Nusselt numbers at Re=20,138 and f=4.0 Hz

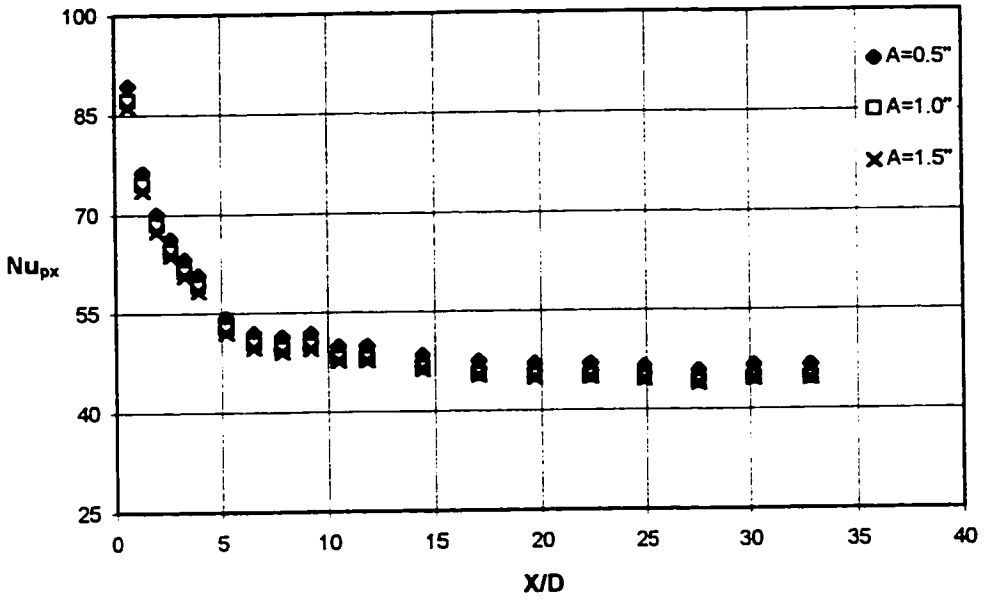

Fig.5.57 Effect of pulsation amplitude on local Nusselt numbers at Re=20,138 and f=6.0 Hz

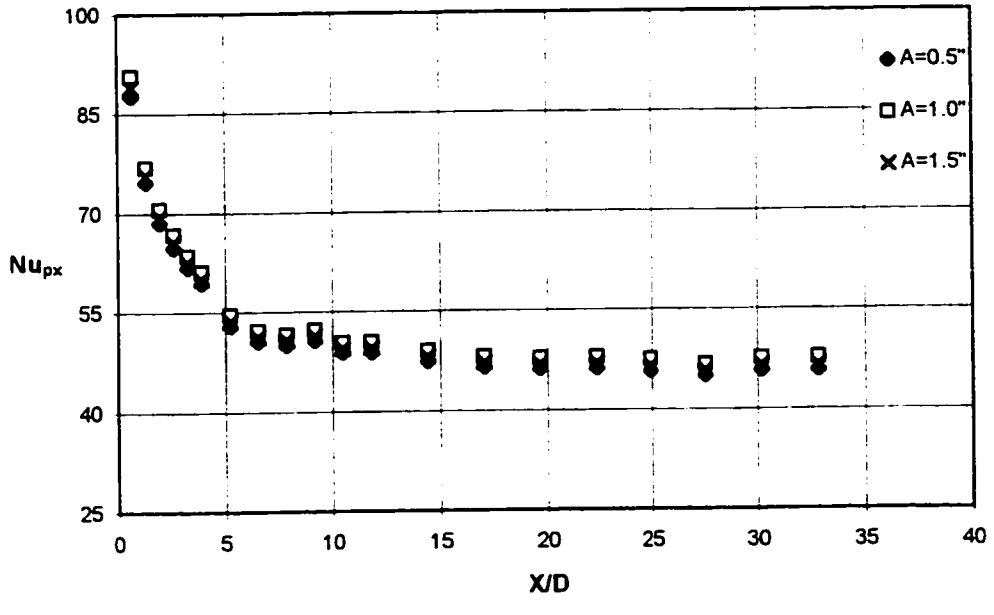

Fig.5.58 Effect of pulsation amplitude on local Nusselt numbers at Re=20,138 and f=8.0 Hz

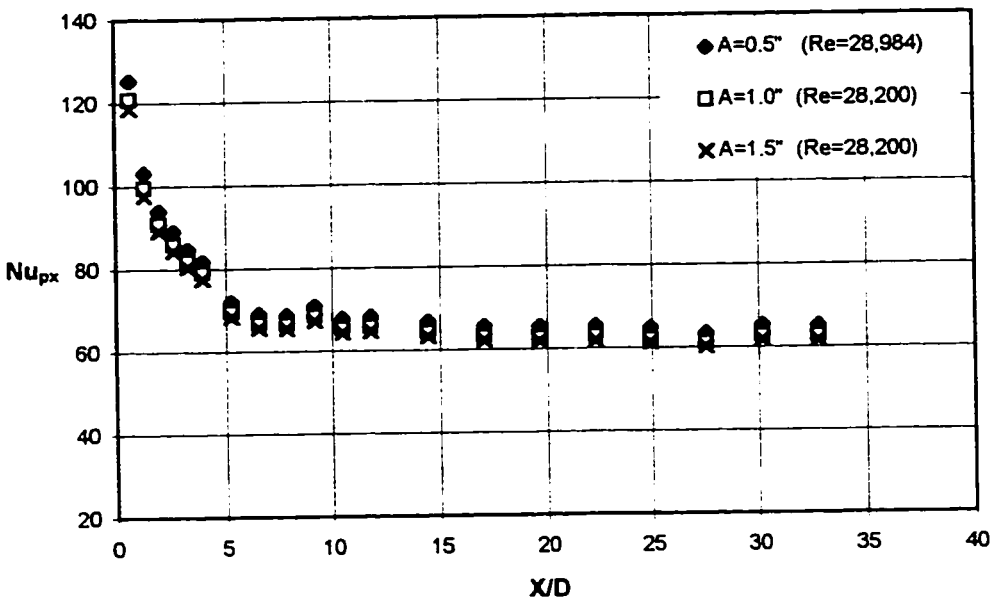

Fig.5.59 Effect of pulsation amplitude on local Nusselt numbers at high Re and f=1.0 Hz

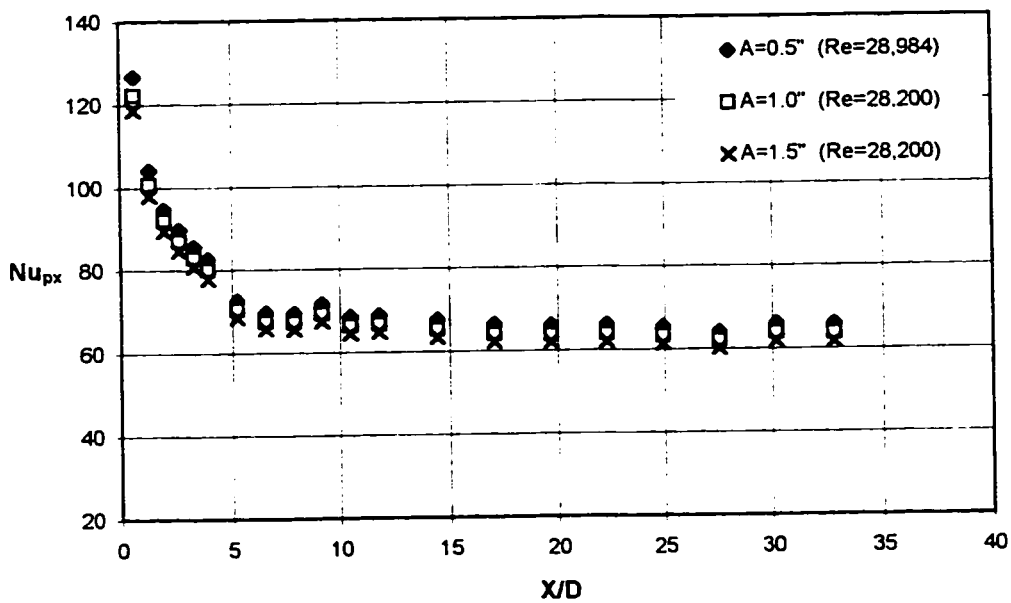

Fig.5.60 Effect of pulsation amplitude on local Nusselt numbers at high Re and f=2.0 Hz

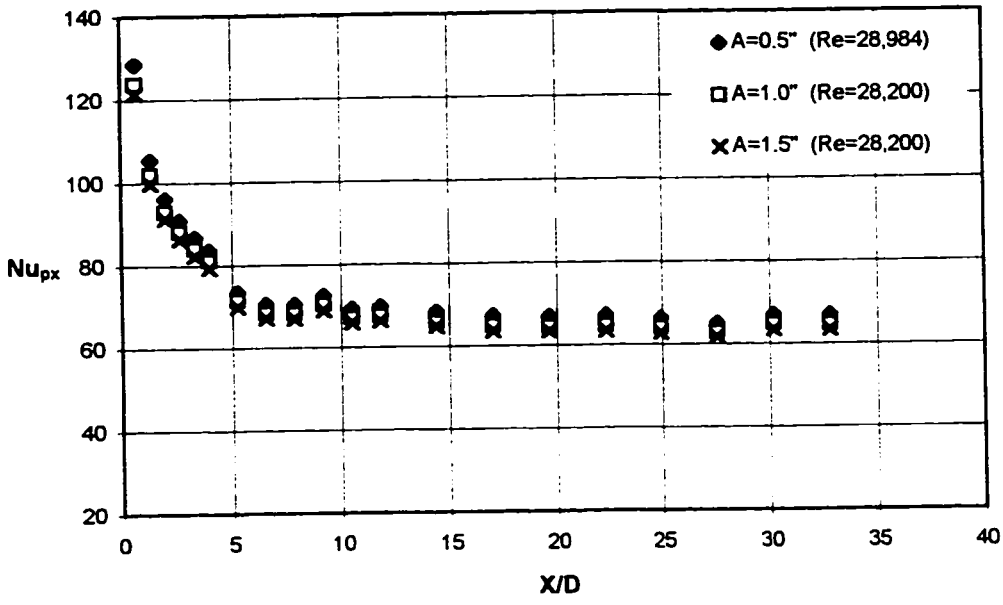

Fig.5.61 Effect of pulsation amplitude on local Nusselt numbers at high Re and f=3.0 Hz

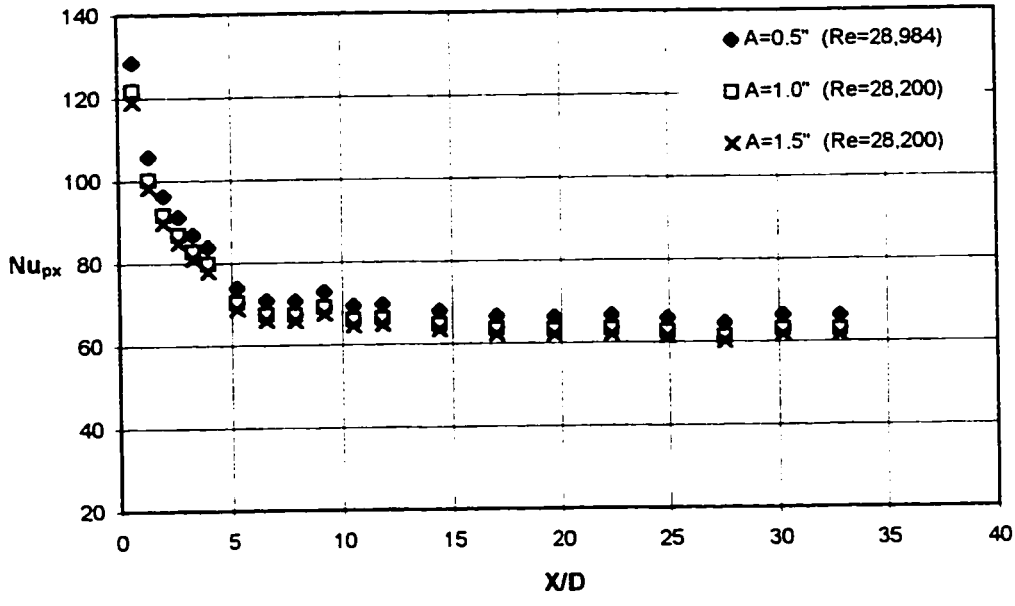

Fig.5.62 Effect of pulsation amplitude on local Nusselt numbers at high Re and f=4.0 Hz

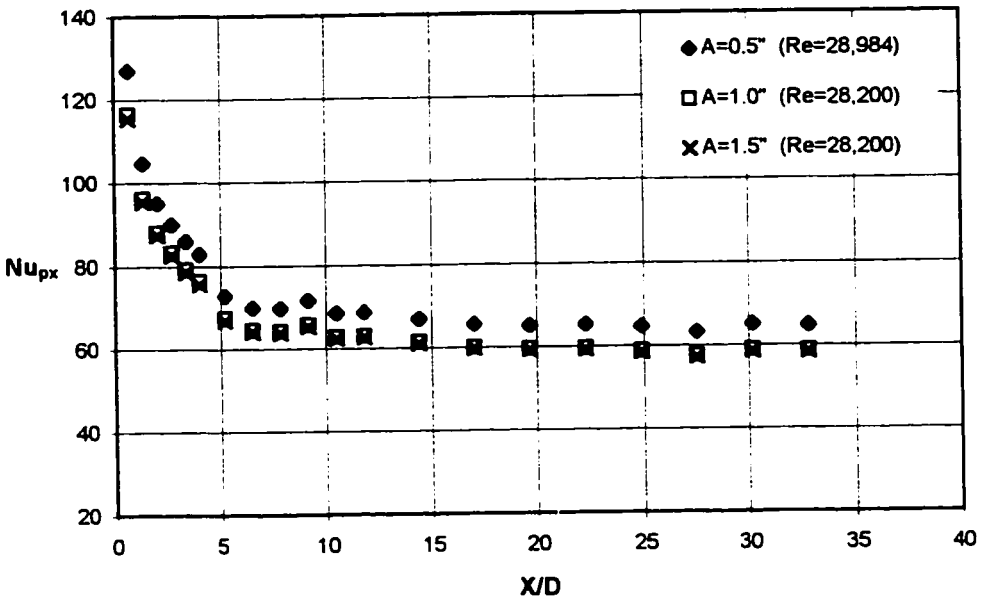

Fig.5.63 Effect of pulsation amplitude on local Nusselt numbers at high Re and f=6.0 Hz

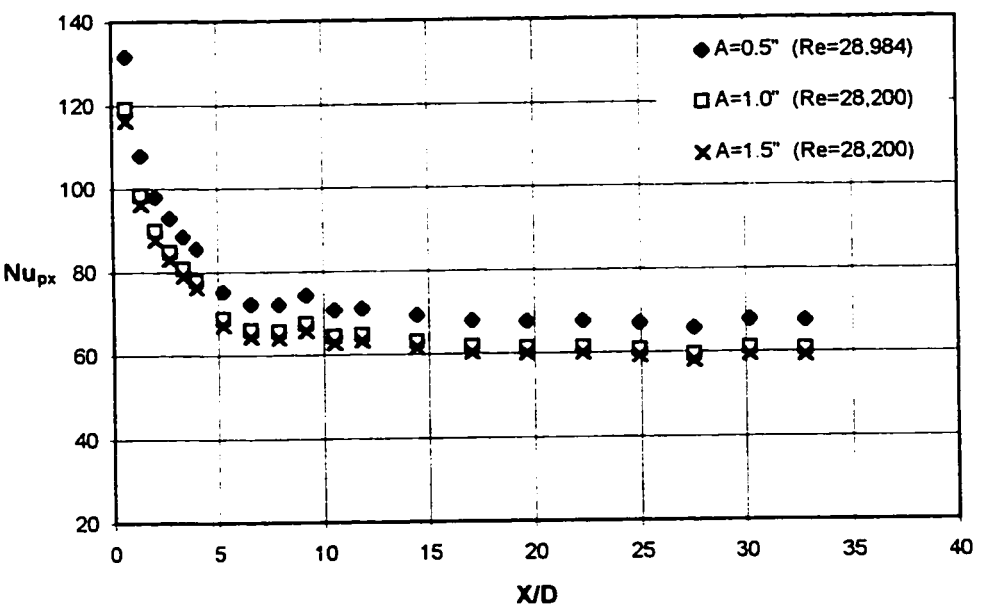

Fig.5.64 Effect of pulsation amplitude on local Nusselt numbers at high Re and f=8.0 Hz

becomes less significant compared to the previous cases. At this Reynolds number the influence of pulsation amplitudes is within ±2% at pulsation frequency of 3 Hz and 4 Hz and within ±3.5% at the other pulsation frequencies . However, at high Reynolds number as shown in Figs. 5.59 to 5.64 the influence of pulsation amplitudes (i.e. $A = 1.0''$ and $A = 1.5''$) is less than ±2% at all pulsation frequencies.The figures also indicate a higher value of local Nusselt numbers at $A = 0.5''$. This difference is due to the difference in Reynolds numbers as explained in the previous section.

5.2.3 The Effect of Pulsation Frequency on the Relative Mean Nusselt Numbers

The mean Nusselt numbers for steady and corresponding pulsating flow at different frequencies and amplitudes considered in the present work are summarized in tables 5.1 to 5.3. The relative mean Nusselt number is defined as the ratio of value of the mean Nusselt number for pulsed flow to the corresponding one for steady flow (without pulsation) at the same Reynolds number.

Figures 5.65 to 5.67 show the overall relative mean Nusselt number as a function of pulsation frequency for Reynolds numbers ranging from 5032 to 28.984 at the three different amplitudes. The figures indicate overall suppression of the heat transfer as a result of pulsating the flow. At low values of the frequency of less than 3 Hz the reduction in the mean Nusselt number is ranging around 4%. In this region of low

Table 5.1 Summary of Experimental Results (A = 0.5")

Re	Mean Nusselt Number						
	Pulsating Flow Frequency f (Hz)						
	Steday Flow	1	2	3	4	6	8
5032	22.312	21.79	21.479	21.434	21.387	21.016	21.348
10,235	34.579	33.598	33.139	33.304	32.575	33.223	33.145
14,460	43.499	41.761	41.653	41.351	41.3	41.461	42.167
20,138	54.133	50.581	53.341	54.009	49.843	49.765	48.788
28,984	71.407	68.276	68.996	69.954	69.638	68.523	70.951

Table 5.2 Summary of Experimental Results (A = 1.0")

Re	Mean Nusselt Number						
	Pulsating Flow Frequency f (Hz)						
	Steday Flow	1	2	3	4	6	8
5032	22.749	21.307	22.194	21.65	20.804	21.169	21.189
10,235	35.477	33.687	33.073	33.567	33.435	33.609	33.274
14,460	43.829	42.838	43.065	42.767	41.669	41.685	42.435
20,138	53.899	52.431	51.357	52.862	50.657	48.024	50.417
28,200	69.999	65.812	66.749	67.587	66.216	62.735	64.391

Table 5.3 Summary of Experimental Results (A = 1.5")

Re	Mean Nusselt Number						
	Pulsating Flow Frequency f (Hz)						
	Steday Flow	1	2	3	4	6	8
5032	21.832	21.598	21.395	21.459	21.298	21.264	21.205
10,235	35.087	34.047	34.119	34.228	33.986	33.953	33.435
14,460	43.779	43.725	42.194	42.416	42.733	43.008	42.357
20,138	54.292	51.449	52.589	52.774	49.728	47.647	49.503
28,200	67.884	64.724	64.855	66.304	64.895	62.292	62.957

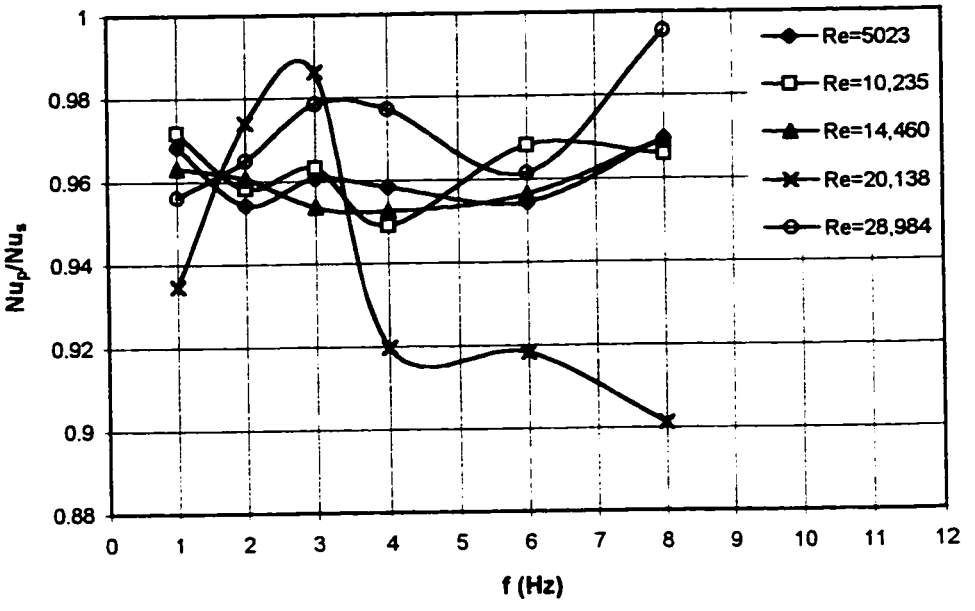

Fig.5.65 Relative mean Nusselt number as a function of pulsation frequency forA=0.5"

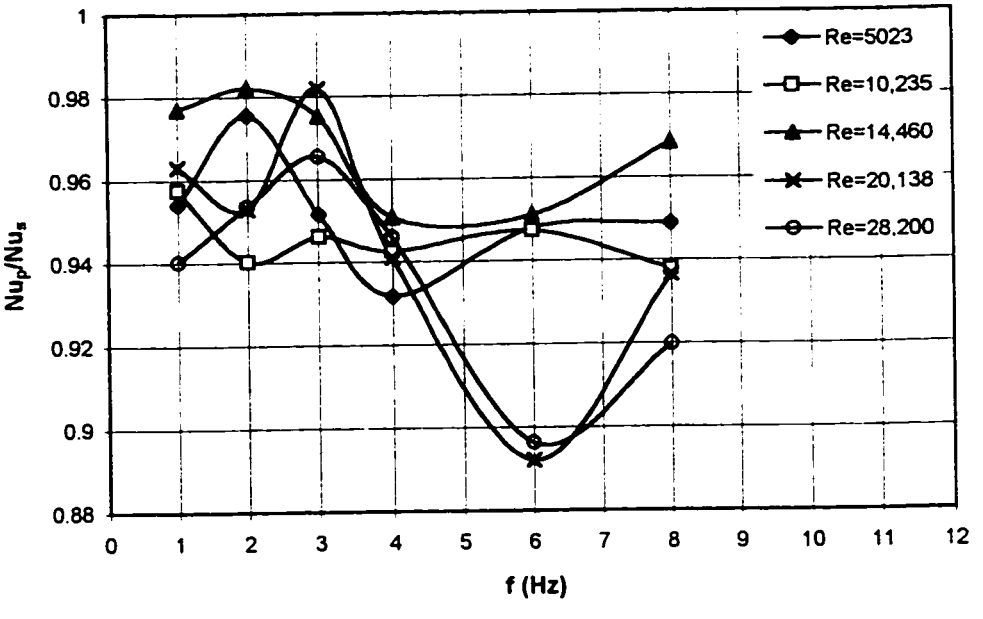

Fig.5.66 Relative mean Nusselt number as a function of pulsation frequency for A=1.0"

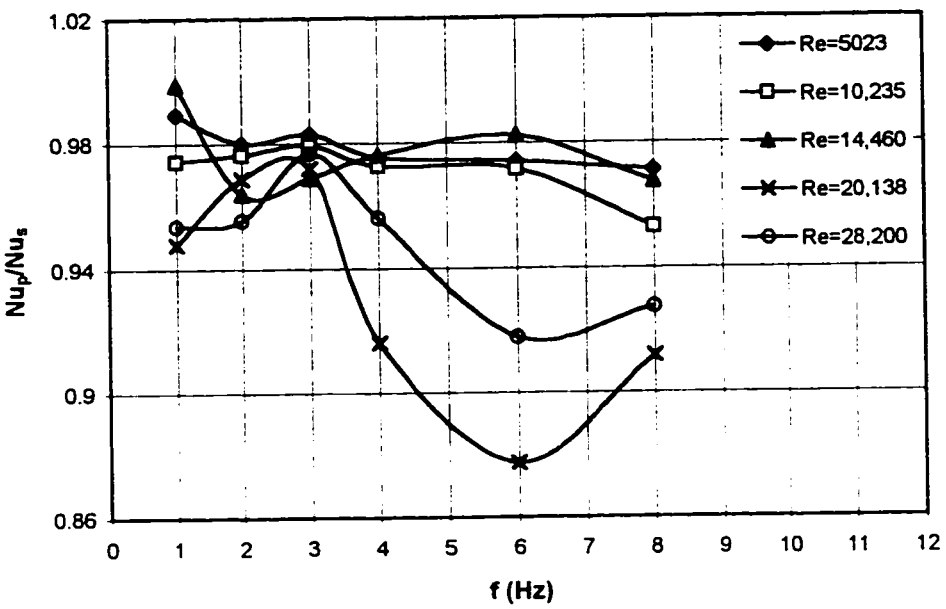

Fig.5.67 Relative mean Nusselt number as a function of pulsation frequency for A=1.5"

frequency the influence of Reynolds number which ranges between 5032 to 28,984 is within ±2%. However, at higher pulsation frequency of excess of 3 Hz the effect of Reynolds is more significant. In this range of high frequency , it can be observed that there is a decrease in the relative mean Nusselt number at pulsation frequency ranged from 3 Hz to 6 Hz at high Reynolds numbers. Also, maximum reduction in the mean Nusselt number due pulsation of around 8% ($A = 0.5''$) to 13% ($A = 1.5''$) at pulsation frequency of 6 Hz is observed at this region of higher frequency. The figures also indicate an insignificant effect of the pulsation amplitude in the distribution of the mean Nusselt numbers.

Figures 5.68 to 5.70 show the plots of relative mean Nusselt number versus the flow Reynolds numbers for different values of pulsation frequencies for the three different amplitudes. These graphs act as prediction charts whereby for a given flow, one can predict the pulsation frequencies at which the maximum or minimum reduction in the heat transfer coefficient (relative to the steady flow values) can be obtained. For example, maximum reduction is achieved at a pulsation frequency of 8 Hz for Reynolds numbers of 20,138 at amplitude of 0.5″. However, for $A = 1.0''$ and $A = 1.5''$ maximum reduction is observed at a pulsation frequency of 6 Hz for Reynolds number of 20,138. Another striking feature of these figures is that at low Reynolds numbers of less than 14,460, the effect of pulsation frequency on the heat transfer coefficient is insignificant. In this region the change in Nu due to frequency

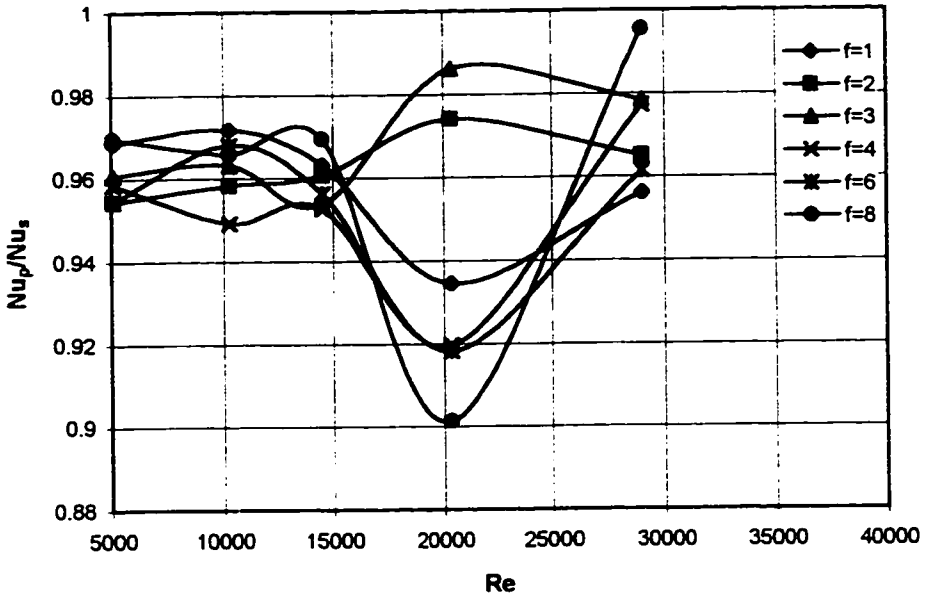

Fig.5.68 Effect of pulsation frequency on relative mean Nusselt numbers at A=0.5"

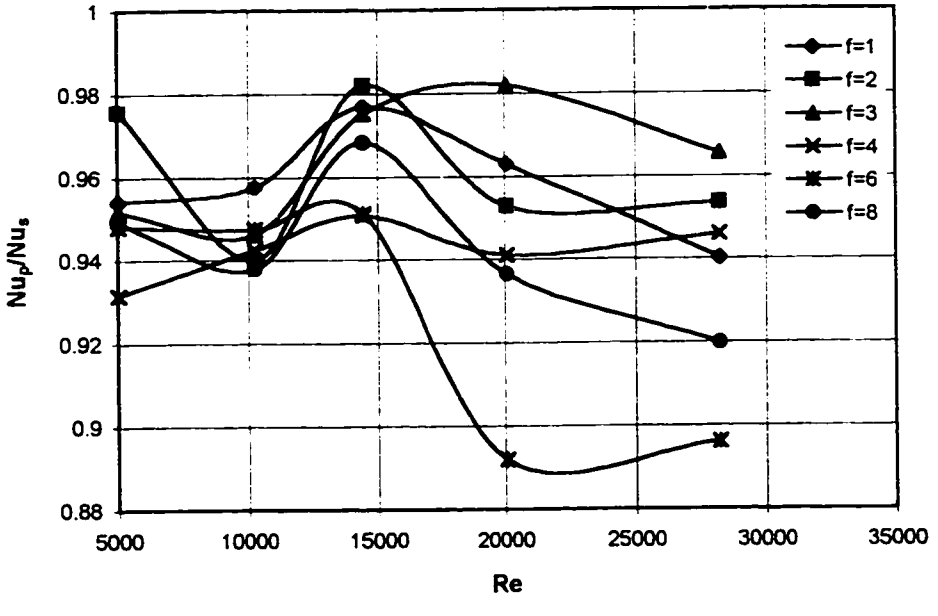

Fig.5.69 Effect of pulsation frequency on relative mean Nusselt numbers at A=1.0"

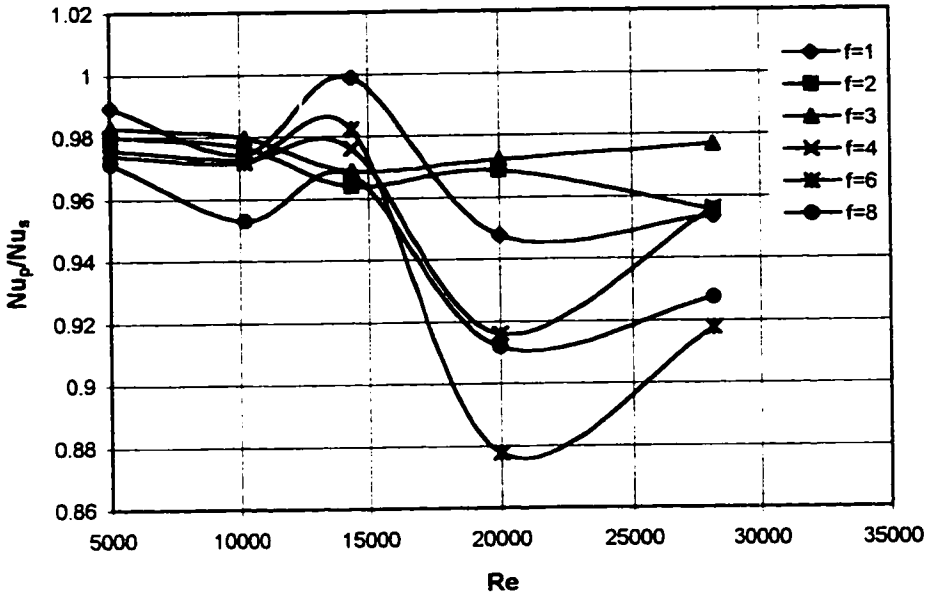

Fig.5.70 Effect of pulsation frequency on relative mean Nusselt numbers at A=1.5"

change from 1 to 8 Hz is limited to ±1% in most cases. However, at higher values of Reynolds numbers the effect of pulsation frequency is shown to be quite significant.In this range of Re, the higher frequency value exhibit higher reduction in Nu values up to 13%. At high Reynolds numbers the low frequency curves indicate a maximum reduction of Nu of about 6% and the change in Nu in this region for this frequency range is within ±3%.

Also, the absolute value of the mean Nusselt numbers for pulsed flow versus Reynolds numbers at different frequencies and amplitudes are plotted as shown in Figs. 5.71 to 5.73. Overall reduction in the mean Nusselt numbers compared to the steady case (without pulsation f = 0) is observed as mentioned above. Another observation from these figures that the values for the mean Nusselt numbers are collapsing at low Reynolds numbers which indicates that the effect of pulsation frequency on the heat transfer coefficient is insignificant at low Reynolds numbers.

5.2.4 The Effect of The Amplitude on The Mean Nusselt Numbers

The mean Nusselt numbers for pulsed flow versus Reynolds numbers for different amplitudes at each pulsation frequency are plotted in Figs 5.74 to 5.79. The figures indicate that the effect of the amplitude on the mean Nusselt numbers is negligible. Same results was reported by Al-Haddad [33].

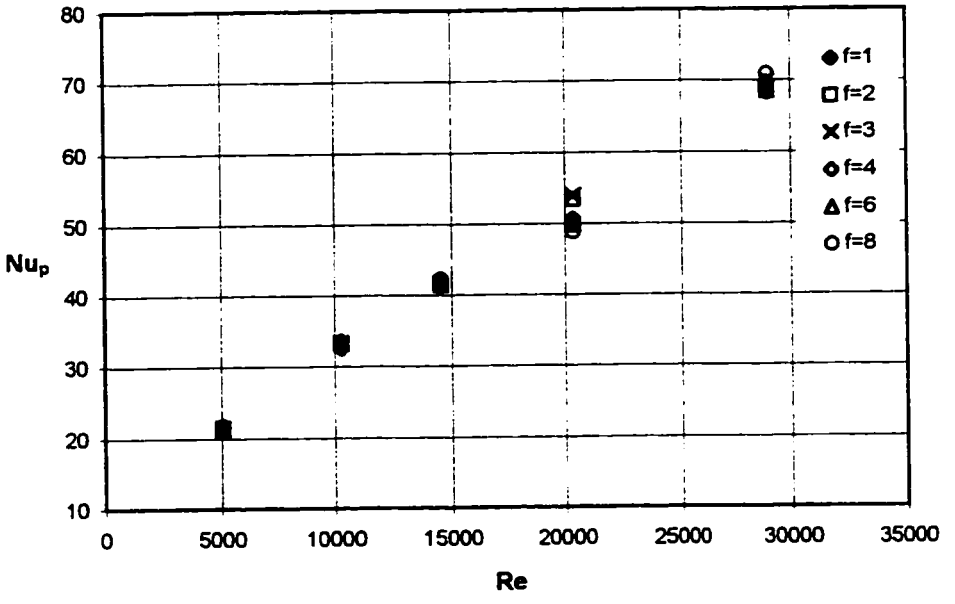

Fig.5.71 Effect of pulsation frequency on mean Nusselt numbers at A=0.5"

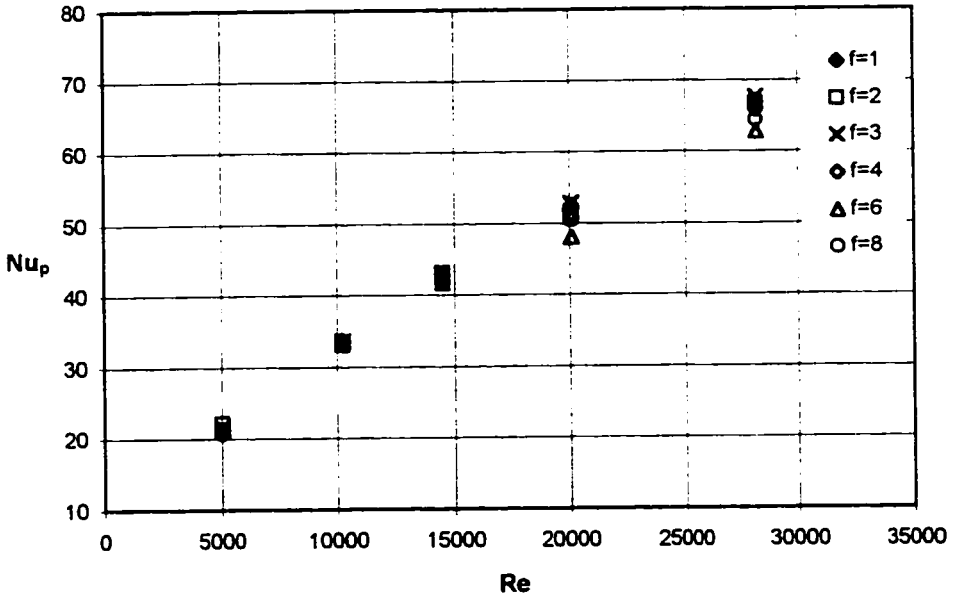

Fig.5.72 Effect of pulsation frequency on mean Nusselt numbers at A=1.0"

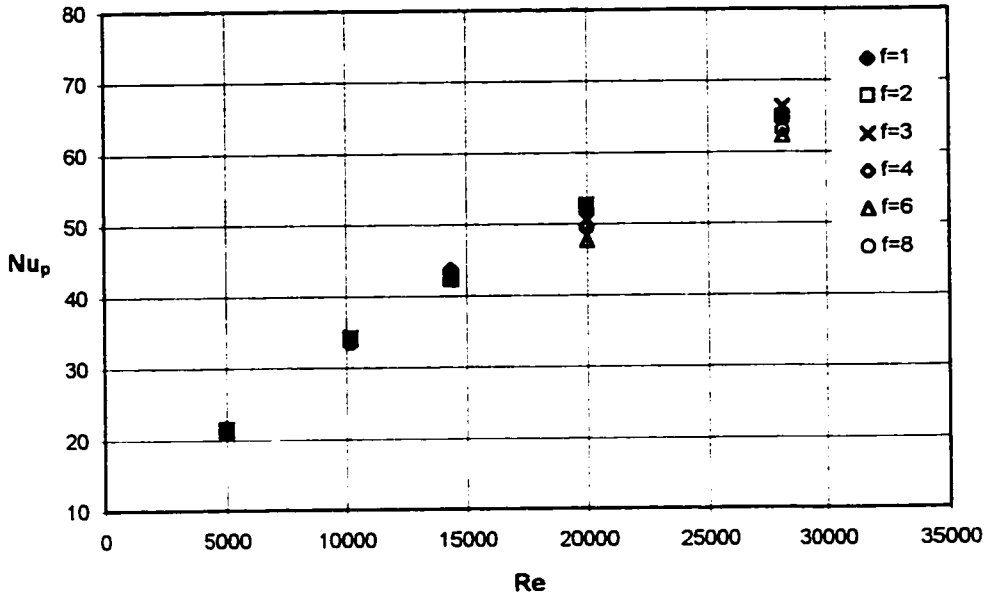

Fig.5.73 Effect of pulsation frequency on mean Nusselt numbers at A=1.5"

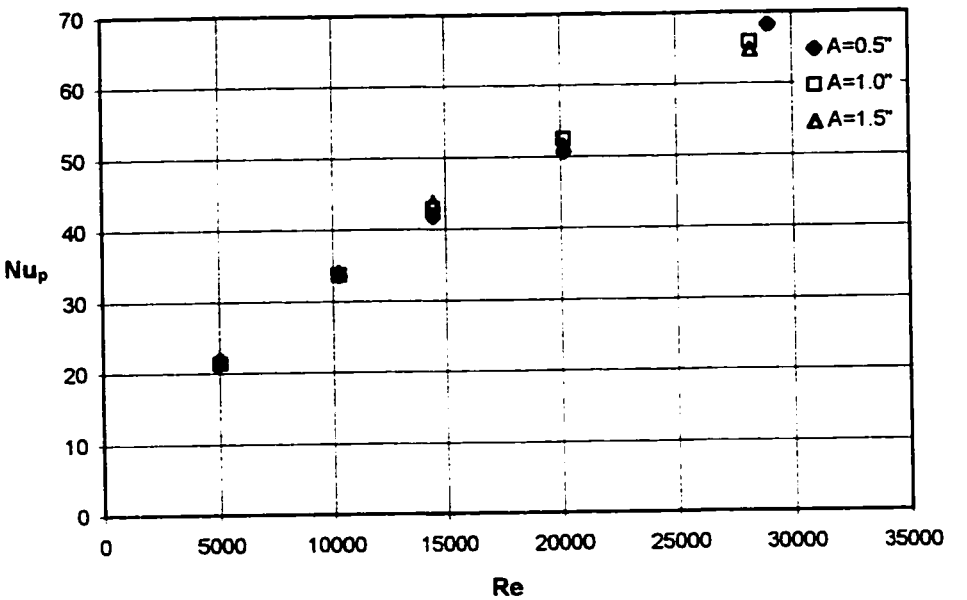

Fig.5.74 Effect of pulsation amplitude on mean Nusselt numbers at f=1.0Hz

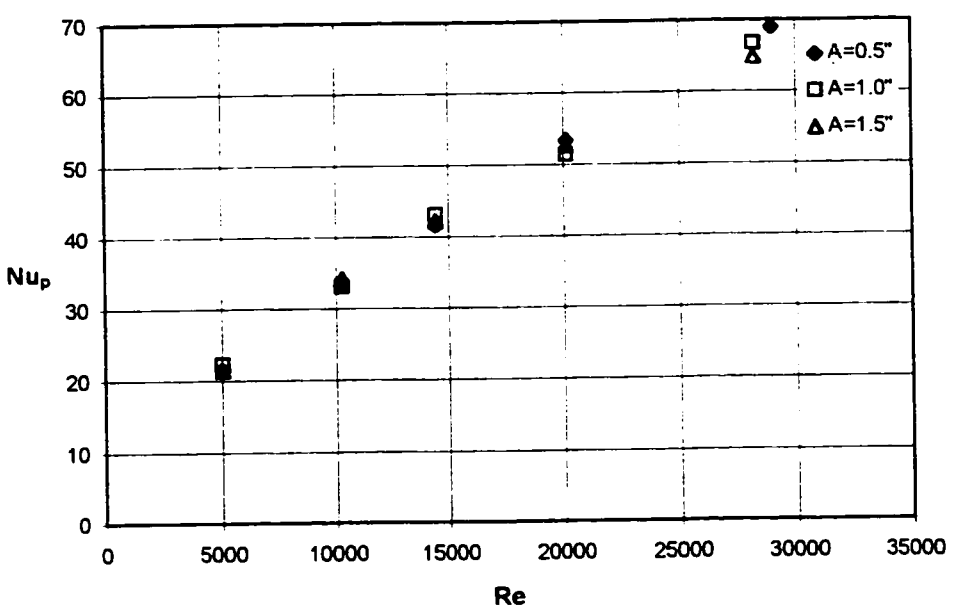

Fig.5.75 Effect of pulsation amplitude on mean Nusselt numbers at f=2.0Hz

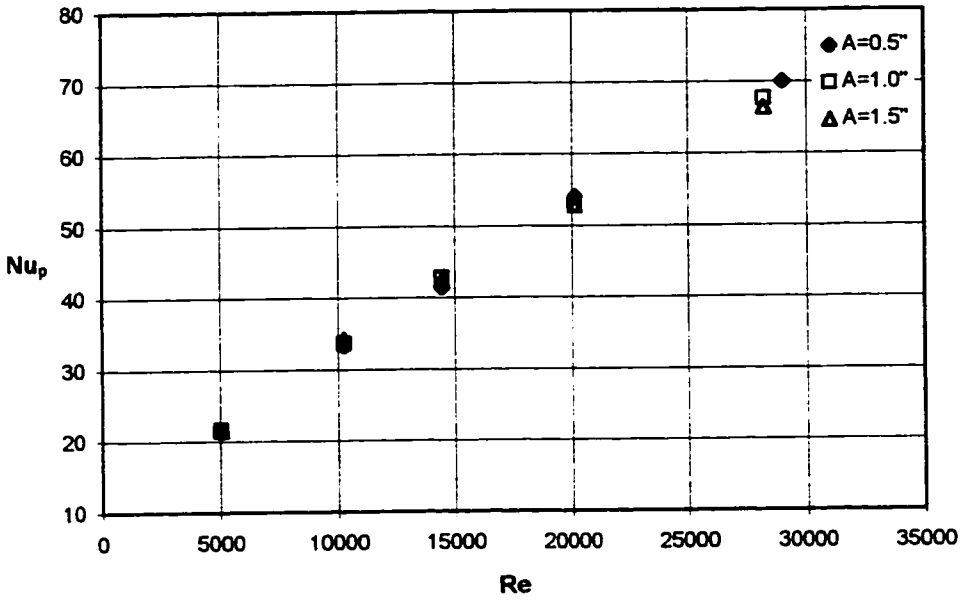

Fig.5.76 Effect of pulsation amplitude on mean Nusselt numbers at f=3.0Hz

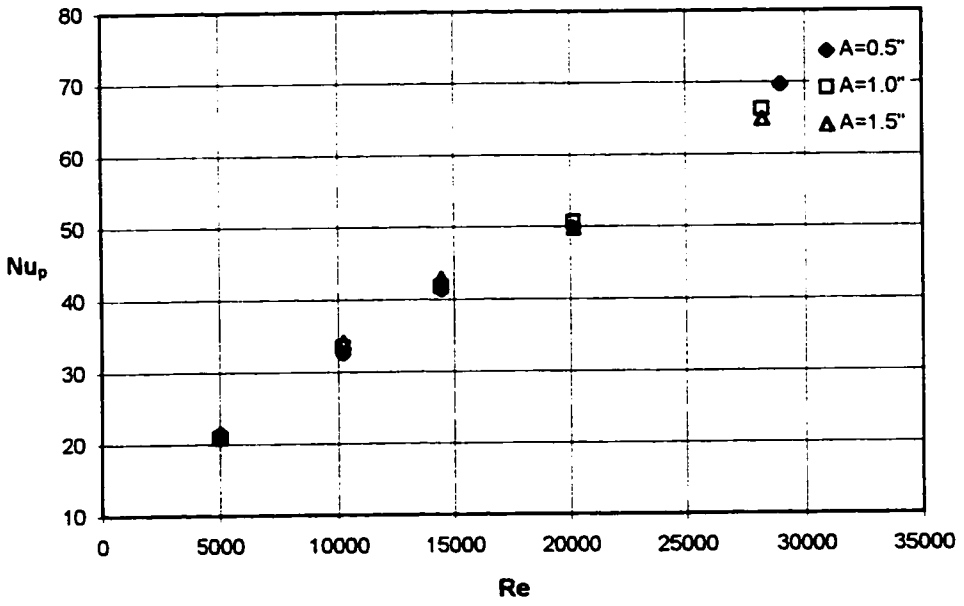

Fig.5.77 Effect of pulsation amplitude on mean Nusselt numbers at f=4.0Hz

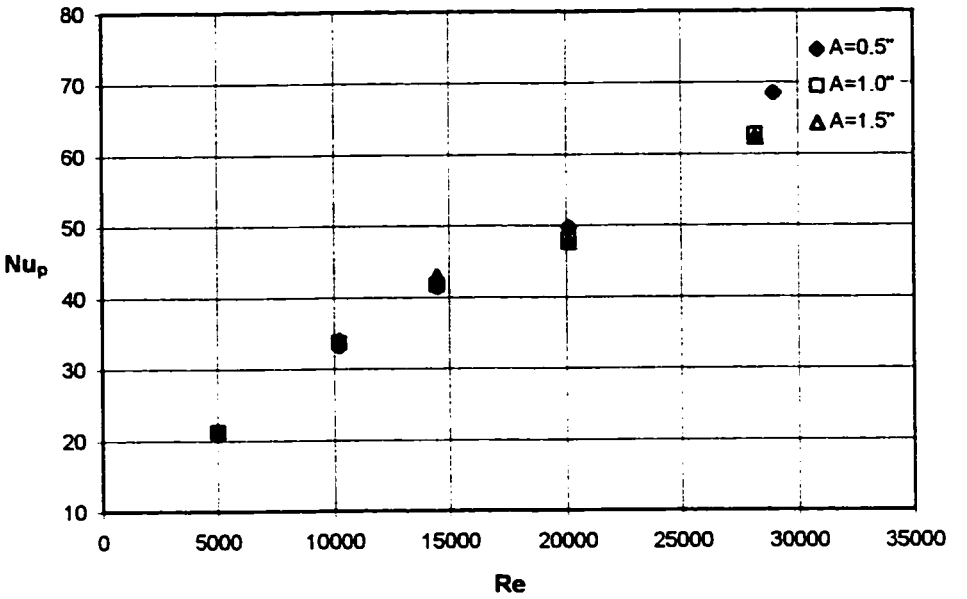

Fig.5.78 Effect of pulsation amplitude on mean Nusselt numbers at f=6.0Hz

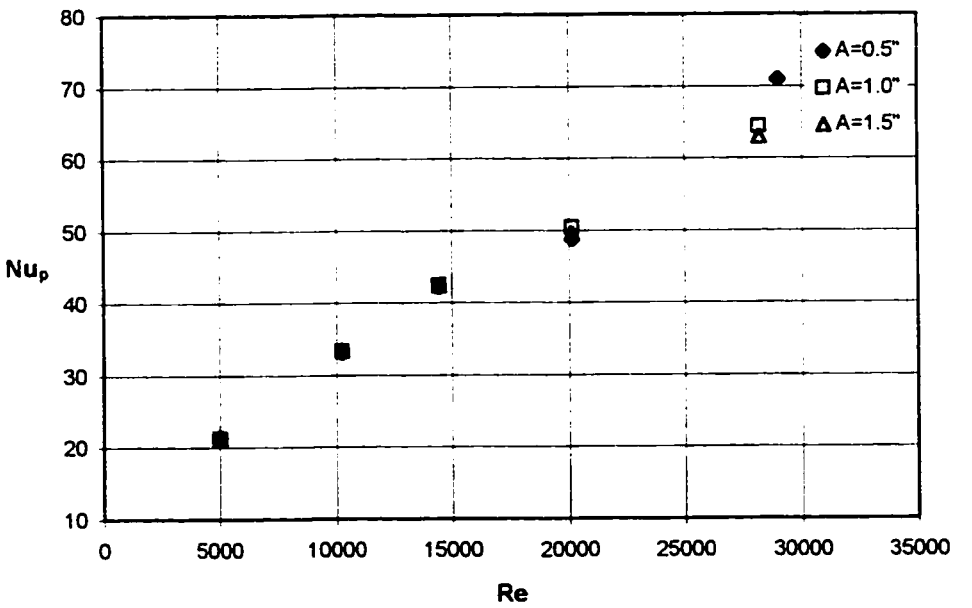

Fig.5.79 Effect of pulsation amplitude on mean Nusselt numbers at f=8.0Hz

5.3 Discussion of Results

5.3.1 Analysis of The Results of Heat Transfer to Pulsatile Flow in light of Bursting Phenomenon

The effect of pulsation on the mass flow rate has been found to be related to the bursting process of turbulent boundary layer [37,38]. As discussed in Chapter 2 the importance of bursting process in turbulent energy production makes it also essential to turbulent heat transfer. With such analogy, data on heat transfer with pulsating flow have been discussed using the turbulent bursting model [14,18]. This model has been able to predict the results of other investigators . Those data (represented by the boundary of the data) as well as the present data are plotted in Fig. 5.80. The data reported by Haveman and Rao [28] lie in the preferred region (regimes II and III) which agrees with their findings that the Nusselt number is increased for pulsation frequency above certain value and is decreased below it. The data reported by Gbadebo [45] fall also in the preferred region and overall enhancement was observed at pulsation frequencies of 2 Hz and 3 Hz. These frequencies centered around the mean bursting frequency. Also, the data reported by Liao et al. [14] fall on the low frequency regime (regime I) outside the preferred regime where the mean bursting frequency is independent of pulsation frequency and as reported their result showed no dependence of frequency as well as reduction in heat transfer coefficient.

However, the data for some other investigators such as Martinelli et al. [27]

and Mamayev et al. [15] did not match this concept. The data of Martinelli et al. [27] fall in the intermediate frequency regime (regime II) of the range of bursting frequencies where the heat transfer is expected to be affected by the imposed pulsation frequencies. However, their results showed that the overall heat transfer coefficient was not effected by pulsation. This might be due to the fact that in their experiments, the flow is periodic given as

$$V = V_{max} sin\theta \qquad 0 < \theta < \pi$$

$$V = 0 \qquad \pi < \theta < 2\pi$$

The heat transfer results of such flow pattern might not be relevant to the present study of pulsating turbulent flow [14]. In the case of Mamayev et al. [15], their data lie outside the preferred range in (regime I) where$\frac{\omega D}{U^*} \ll 1$ as a result, the flow as will the heat transfer is expected to be independent of the frequency of flow pulsation. However, their results showed a strong frequency dependence and an increase in overall heat transfer coefficient. The reason for such results is not clear.

In view of the above, the present experimental data are discussed in relation to the turbulent bursting process. As shown in Fig. 5.80, the bulk of the present data fall in the preferred regime of the bursting frequencies especially in the intermediate

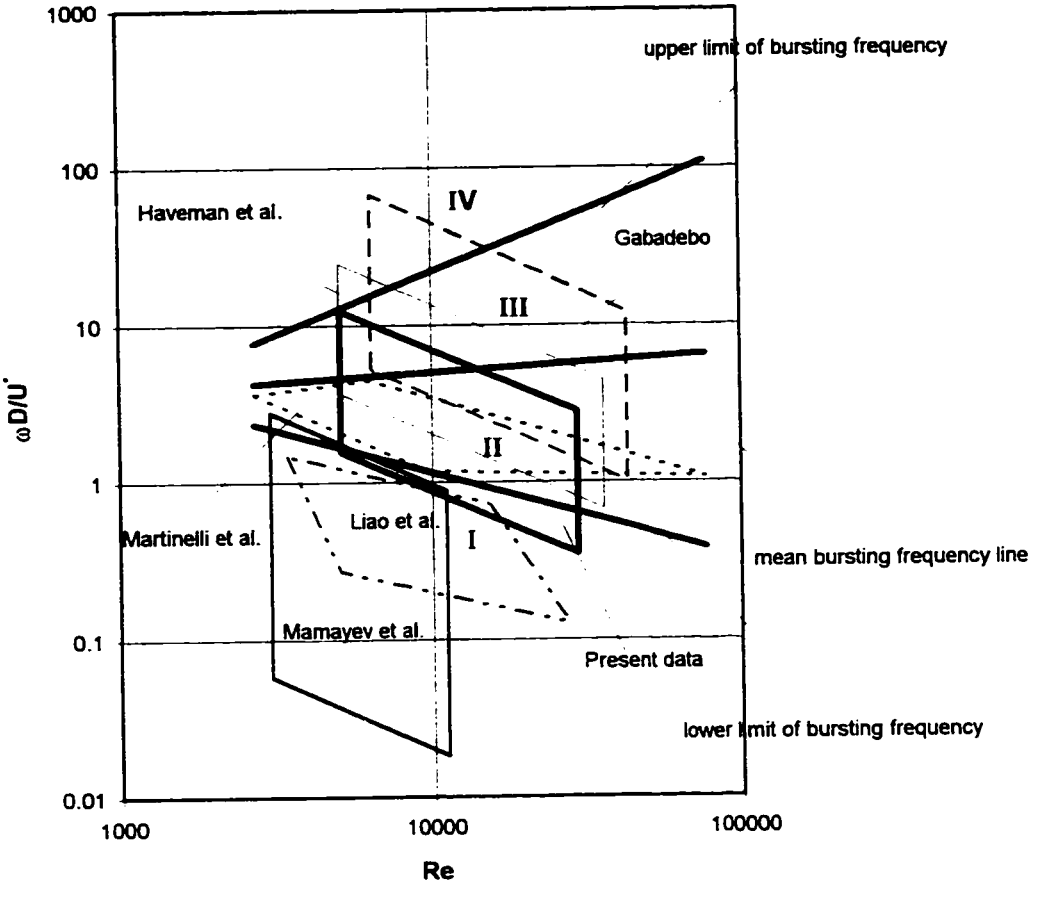

Fig. 5.80 Classification of data on heat transfer with pulsating turbulent flow

frequency regime (regime II). In this regime the mean bursting frequency is subdued as a result of resonance occurring at the pulsation frequency and dependent only on the pulsation frequency. Accordingly, the heat transfer behavior is expected to be affected resulting in either reduction or enhancement .

5.3.2 Local Nusselt Number

The present experimental results, as discussed in the previous subsections, indicate that the enhancement in the heat transfer coefficient due to pulsation is more pronounced in the region of the thermal boundary development ($X/D < 8$). This, in effect, indicates that the improvement is more pronounced for high Prandtl number fluids. In the present study this local enhancement is obtained at Reynolds number of 5032. The reason for this local enhancement close to the inlet may be due to strong agitation of the thermal boundary layer (whose growth has just begun) by the imposed pulsation. At this Reynolds number (Re=5032), based on the turbulent model as shown in Fig. 5.80 the range of pulsation frequencies at which the enhancement occurred are centered around the mean bursting frequency line. This will cause a resonance between the bursting frequency and the pulsation frequency which lead to an enhancement in the heat transfer coefficient. However, a reduction in the local heat transfer coefficient along the test section is observed for the other Reynolds numbers. This reduction is less in the entrance region and compared to

the fully developed region.

It was also observed that the effect of pulsation amplitudes is more significant in the entrance region at Reynolds number of lower than or equal to 14,460 (Figs 5.35 to 5.52). At this range of Re, when the pulsation amplitude increased, the local enhancement on the heat transfer coefficient increased (Re=5032). Also, the reduction in the local heat transfer decreased at the other Reynolds numbers in this range. This may happen because, at a particular frequency, when the displacement amplitudes increased, the pulsation amplitude is also increased. This therefore lead to further enhancement of turbulence which lead to more enhancement or, at least, less reduction in the heat transfer coefficient. This reason is also supported by another observation, that when the Reynolds number increased from 5032 to 14,460 the effect of pulsation amplitudes decreased. Here, the flow is highly turbulent and the turbulent intensity is probably having a more dominant effect on the flow. At high Reynolds numbers of greater than 14,460 the effect of pulsation amplitudes is insignificant (Figs. 5.53 to 5.64). It was also reported in [9] that the turbulent intermittency of the flow at the transition region (which is close to the Re=5032 in the present results) increased with the frequency and amplitude of pulsation. However, at the low range of Reynolds number ($Re < 14,460$) the effect of the amplitudes becomes less significant in the fully developed region unlike the effect in the entrance region.

5.3.3 Mean Nusselt Number

Overall suppression in the mean Nusselt number is observed at the whole range of pulsation parameters and Reynolds numbers (Figs. 5.65 to 5.67). It is also observed that low values of pulsation frequencies of less than 3 Hz the reduction in heat transfer coefficient is ranging around 4%. However, this reduction is small that it comes within the error limits of the experiment (Chapter 4). Also, in this region of low frequency the influence of Reynolds number which range between 5032 to 28,984 is within ±2%. This observation can be explained based on the turbulent bursting model. Figure 5.80 indicates that the data of the low frequency region lie very close to the lower limit of bursting frequency when the Reynolds number is less than 10,235. However, at Reynolds numbers greater than 10,235 for the same low frequency range most of the data fall in to the low frequency regime (regime I). At this regime as discussed in chapter 2, the mean bursting frequency is independent of pulsation frequency and the turbulent structure is not affected. In this regime the heat transfer coefficient is expected to be reduced with pulsation.

At higher frequency of excess to 3 Hz the effect of high Reynolds numbers is significant. Reduction in heat transfer due pulsation of around 8% to 13% is observed. At this range of high frequency the bulk of the present data fall into the intermediate frequency regime. As mentioned before, at this regime the mean bursting frequency

is suppressed due to resonance occurring at pulsation frequency and the heat transfer behavior is expected to be effected resulting in either reduction or enhancement. The negative effect observed in the heat transfer at high Reynolds numbers can be attributed to the reduction in the contribution of induced flow pulsation with increase in the contribution of flow turbulence. Apparently at high frequency, the forced fluctuations somewhat damp out the high-frequency turbulent fluctuations. The present data showed insignificant effect of pulsation amplitudes on the mean Nusselt number. This is quite expected since the bulk of the present data fall in the intermediate frequency regime Fig. 5.80 where the mean bursting frequency dependent only on the pulsation frequency. Accordingly, the present data match to some extents the concept of the bursting model.

In summary, the model of turbulent bursting has been able to provide fairly logical explanation regarding the result of the present study as well as other studies of heat transfer in pulsating flow. However, it should be pointed out that the result classification given here through the model is not the only possible one. Experimental data exist which contradict it [15,27] . From an examination of existing experimental data [14,15,27,28,44], it may be concluded that with pulsating flow, the Nusselt number is affected by the amplitude and the wave form as well as the mean velocity of the flow and the frequency of pulsation. Of course, the theory of the present model does not exhaust all possible variants of the effect of an unsteady

state on the coefficients of turbulent transfer.

Chapter 6

Conclusion and Recommendation

6.1 Summary and Conclusions

The effect of pulsation frequency and amplitude on heat transfer coefficient in the thermal entrance region as well as thermally fully developed region of a hydrodynamically fully developed turbulent air flow in a pipe heated with a uniform heat flux has been studied experimentally . The flow Reynolds number was varied for 5032 to 28,984. A near sinusoidal pulsation with frequency ranging form 1 Hz to 8 Hz was imposed on the flow. For pulsating flow, the results showed similar pattern to that for steady flow regarding variation of the local Nusselt number along the pipe.

Overall reduction on the mean Nusselt number was observed for the whole range of Reynolds numbers that are studied in the present experiment with maximum reduction of about 11% at Re = 20,138. However, there is a local enhancement in the heat transfer coefficient in the entrance region for Reynolds number near 5032 at

frequency range of 2 Hz to 6 Hz with maximum enhancement of about 6% at f = 4 Hz very close to the inlet. For medium to higher Reynolds number a reduction in the local heat transfer coefficient was observed. However, the reduction in the entrance region is less than the reduction in the fully developed region. Also, a negligible effect of pulsation amplitude on heat transfer coefficient is observed. Observation of the local Nusselt number behavior under the influence of pulsation revealed that the improvement in the heat transfer coefficient is more pronounced in the entrance region than in the fully developed region. The same conclusion was reported in [32].

Based on the bursting phenomenon process, it can be concluded that for Reynolds numbers of 5032 the critical frequencies, where resonance interaction between the bursting and pulsation frequencies occur are in the frequency ranges of 2 Hz to 6 Hz.

6.2 Recommendations For Future Work

As an extension to the present work, it is recommended to account for the following flow pulsation parameters:

- Variation in the displacement amplitude of pulsation inducing mechanism especially at very low frequencies of the order $f < 0.5$ Hz. This may have an effect on the heat transfer coefficient observed at such frequency[14].

- Location of the pulsation such as upstream the rest section. This has also been found to have effect on the heat transfer coefficient [30,18,21]

- Mode and pulsation wave form : a tangential rather than axial pulsation may exhibit certain influence on the heat transfer behavior in the test section. Also pulsation of different wave-forms can be devised.

As far as the flow and fluid parameters are concerned the following recommendations are also essential as an extension to the present work:

- Investigation of laminar thermal entrance flow under the influence of pulsation as well as transition and turbulent flows at Reynolds numbers outside the present range.

- Extension of the work to cover the effect of Prandtl number by testing different fluids.

Appendix

DATA REDUCETION SAMPLE PROGRAM AND OUTPUT

```
      Dimension x(26),ts(26),tm(26),h(26),rnu(26)
      Open(unit= 5,file='nusls015.dat')
      Open(unit= 6,file='nusls015.out')
      pi = 3.1415927
      cp = 1007.0
      rmair = 0.000019161368
      rholiq = 827.0
      rhowat = 1000.0
      rhoair =1.1119476
      conduc =0.027399603
      condis =0.035
      dtests =0.0381
      gravty=9.81
      tstlgt=1.674
      Atests=(pi*dtests **2.0)/4.0
*     Enter the mass flow rate reading
      Read(5,*) rmdot
*     Calculate the Reynolds number and the average velocity
      reyno = 4*rmdot/(pi*dtests*rmair)
      vavrg = rmdot/(rhoair*Atests)
*     Enter the heat input and calculate the total heat flux
      Read(5,*) power
      qtotal =3.0*power
      qdotot = qtotal/(pi*din*1.335)
      qtranst = 0.9556*qtotal
*     Enter the surface temperature
      Do 9 i = 1,21
      Read(5,*) x(i),ts(i)
9     continue
*     Calculate the bulk mean temperature
      tbin = ts(1)
      Tbulk = qtranst/(rmdot*cp) + tbin
      Do 15 i = 2,21
      tm(i)=(Tbulk-tbin)*(x(i)-x(1))/1,335+tbin
```

```
15  continue
    qdot = qtranst/(pi*dtests*1.335)
    tqlost = qtotal - qtranst
*   Calculate the local and average heat transfer coefficient
    Do 20 i = 2, 21
    h(i) = qdot/(ts(i) - tm(i))
    rnu(i) = h(i) * dtests/conduc
20  continue
    hm1=(x(2)/2.)*(h(2)+h(7)) + x(2)*(h(3)+h(4)+h(5)+h(6))
    hm2=(x(3)/2.)* (h(7)+h(13)) + x(3)*(h (8)+h (9)+h (10)+
    h(11)+h(12))
    hm3=(x(5)/2.)*(h(13)+h(21)) + x(5)*(h(14)+h(15)+h(16)+
    h(17)+h(18)+& h(19)+ h(20))
    hmean=(hm1+hm2+hm3)/1.25
    rnum = hmean * dtests/conduc write(6,*)'Date: 01/12/96'
    write(6,*)
    Read(5,*) freq
    if (freq.eq.0.0) go to 29
    Write(6,*)'Heat Transfer to Pulsed Flow,Freq. equal to',freq,' Hz'
    Go to 31
29  Write(6,*)'Steady State Solution of Flow without Pulsation'
31  Write(6,*)
    Write(6,*)'Re =',reyno,'  Mean Nusselt No.=',rnum
    Write(6,*)
    Write(6,*)'Inlet Temp.=',tbin,' deg.C'
    Write(6,*)
    Write(6,*)'  x(m) ','Tmean(x)','Tsurf(x)','h(x)'  &,'    Nu(x) '
    Write(6,*)
    Do 25 i = 2, 21
    write(6,30) x(i),tm(i),ts(i),h(i),rnu(i)
30  format (f6.3,3x,4f11.5)
25  continue
    Write(6,*)
    Write(6,*)'Flowrate=',rmdot,' kg/s',' Average veloc=',vavrg,' m/s'
    Write(6,*)
    Write(6,*)'Heat Input=',qtotal,'w',' Heat ransfered=',qtranst,'w'
    Write(6,*)
    Write(6,*)'Average temp. downstream is',Tbulk,' deg.C'
    Write(6,*)
    stop
    end
```

Steady State Solution of Flow without Pulsation

Re = 14493.91 Mean Nusselt No.= 43.85

Inlet Temp.= 23.20 deg.C

x(m)	Tmean(x)	Tsurf(x)	h(x)	Nu(x)
.025	23.83	56.40	53.98	75.38
.050	24.46	61.90	46.96	65.57
.075	25.09	65.90	43.08	60.16
.100	25.72	68.80	40.81	56.99
.125	26.35	71.60	38.85	54.26
.150	26.98	74.00	37.39	52.22
.200	28.24	80.50	33.64	46.98
.250	29.51	84.10	32.20	44.97
.300	30.77	86.10	31.77	44.37
.350	32.03	86.90	32.04	44.74
.400	33.29	89.90	31.06	43.37
.450	34.55	91.10	31.09	43.42
.550	37.08	94.90	30.41	42.46
.650	39.60	98.30	29.95	41.83
.750	42.13	100.90	29.91	41.77
.850	44.65	103.20	30.03	41.93
.950	47.18	105.80	29.99	41.88
1.050	49.70	108.40	29.95	41.82
1.150	52.22	110.40	30.22	42.20
1.250	54.75	112.70	30.34	42.36

Flowrate= 8.27E-03 kg/s Average veloc= 6.5 m/s

Heat Input= 294.00 w Heat transfered= 280.94 w

Average temp. downstream is 56.89 deg.C

Heat Transfer to Pulsed Flow,Freq. equal to 1.0 Hz

Re = 14493.91 Mean Nusselt No.= 42.83

Inlet Temp.= 23.3 deg.C

x(m)	Tmean(x)	Tsurf(x)	h(x)	Nu(x)
.025	23.93	57.10	53.00	74.01
.050	24.56	62.60	46.22	64.54
.075	25.19	66.50	42.56	59.43
.100	25.82	69.60	40.16	56.08
.125	26.45	72.40	38.26	53.43
.150	27.08	74.90	36.77	51.34
.200	28.34	81.50	33.07	46.19
.250	29.61	85.10	31.68	44.24
.300	30.87	87.20	31.21	43.58
.350	32.13	88.00	31.47	43.94
.400	33.39	91.20	30.41	42.47
.450	34.65	92.40	30.44	42.51
.550	37.18	96.40	29.69	41.46
.650	39.70	99.90	29.20	40.78
.750	42.23	102.60	29.12	40.66
.850	44.75	105.00	29.18	40.75
.950	47.28	107.70	29.10	40.63
1.050	49.80	110.20	29.11	40.65
1.150	52.32	112.30	29.31	40.93
1.250	54.85	114.50	29.47	41.16

Flowrate= 8.27E-03 kg/s Average veloc= 6.5 m/s

Heat Input= 294.00 w Heat transfered= 280.94 w

Average temp. downstream is 56.99 deg.C

Nomenclature

a	Crank length of pulsating mechanism (m)
A	Pulsation amplitude
A_o	Area of orifice (m^2)
A_r	Heat transfer area (m^2)
B	Ratio of the orifice diameter to the flow line pipe diameter
b	Length of link 2 of pulsating mechanism (m)
c	Lower part of link 3 of pulsating mechanism (m)
C_d	Orifice discharge coefficient
C_p	Specific heat capacity of fluid (J/Kg.^{o}c)
D	Pipe diameter (m)
e	Upper part of link 3 of pulsating mechanism (m)
f	Frequency of pulsation
f_b	Turbulent bursting frequency
g	Acceleration due to gravity (m/s^2)
Δh	Height of manometer liquid (m)
h_{mean}	Mean heat transfer coefficient (w/m^2 k)
h(x)	Local heat transfer coefficient (w/m^2 k)
I	Electric supplied current (Amps)

k	thermal conductivity
K	Relative velocity oscillation amplitude
L	Length of the test section (m)
L_e	Effective length of test section (m)
L_s	Length of slider of pulsating mechanism (m)
$\dot{m}$	Mass flow rate (kg/s)
n	Characteristic constant for quasi-steady model
Nu_c	Mean Nusselt number calculated from Eqn. (5.1)
Nu_{mean}	Mean Nusselt number (time average)
Nu_p	Mean Nusselt number (Pulsed flow)
Nu_{sx}	Local Nusselt number (steady flow)
Nu_{px}	Local Nusselt number (pulsed flow)
$\frac{Nu_p}{Nu_s}$	Relative mean Nusselt number (time average)
Pr	Prandtl number
q''_{loss}	Heat flux loss in heater segment(w/m^2)
q''	Total heat flux (w/m^2)
q_{trans}	Heat transferred from heater segment (w)
Q_{loss}	Total heat loss (w)
Q_{input}	Heat input (w)

Q_{trans}	Total heat transferred (w)
r	local pipe radius (m)
R_i	Radius of inner surface of insulation (m)
R_o	Radius of outer surface of insulation (m)
Re	Reynolds number
t	Pipe thickness (m)
$T_{os}(x)$	Local outer surface temperature of insulation (^{o}c)
$T_{is}(x)$	Local inner surface temperature of insulation (^{o}c)
T_s	Pipe surface temperature (^{o}c)
T_m	Mean bulk fluid temperature (^{o}c)
T_{in}	Fluid inlet temperature (^{o}c)
U^*	Friction velocity (m/s)
V	Voltage supplied (V)
V_m	Time averaged velocity (m/s)
V_p	Sinusoidal velocity of pulsation inducing piston (m/s)
V_s	Steady velocity component (m/s)
x	Local distance along the test section (m)
x	Displacement of link 2 of pulsation mechanism (m)
Y	Displacement of the slider (link 4) (m)

Greek symbols

α	Angel subtended by the crank (rad)
β	Pivot angle of link 3 (rad)
ϕ	Crank angle (rad)
λ	Coefficient of resistance given by Blasius formula
μ	Dynamic viscosity
θ	Oscillation angle (rad)
ρ	Fluid (air) density
ρ_l	Density of manometer fluid
τ	Time variable (s)
ω_{bU}	Upper bound of bursting circular frequency (rad/s)
ω_{bL}	Lower bound of bursting circular frequency (rad/s)
ω^*	Frequency parameter.

Subscripts

s	steady flow
p	Pulsed flow

Superscripts

$''$	inches

Bibliography

[1] Ede, A.J. (1959) 'Effect of an Abrupt Disturbance of The flow cn the Local Heat Transfer Coefficient in a Pipe.' *Heat 164*, National Eng. Lab. Eastt Kilbride, Glasgow, Scotland.

[2] Zemanick, P.P, and Dougall, R.S (1970) 'Local Heat Transfer Downstream of Abrupt Circular Channel Expansion.' *Journal of Heat Transfer*, Feb., pp. 53-60.

[3] Edwards, R.J, Jambunathan, K and Button B.L (1988) 'Experimental Investigation of turbulent Heat Transfer in Simultaneously Developing Flow in Finned Annuli.' *Experimental Heat Transfer, Fluid Mechanics and Thermodynamics*, pp. 543-549.

[4] Habib, M.A., Mobarak, A.M., Attya, A.M and Aly, A.Z (1993) 'Enhanced Heat Transfer in Channels with Staggered Fins of Different Spacing.' *International Journal of Heat and Fluid flow*, Vol. 14, No. 2, pp. 185-190.

[5] Habib, M.A. and McEligot, D.M (1982) 'Turbulent Heat Transfer in a Swirl Flow Downstream of an Abrupt pipe expansion.' *7th Int. Heat Transfer Conference, Munchem*, Paper FC 29.

[6] Prasad, R.C. and Brown, M.J (1988) 'Effectiveness of Wire-Coils Inserts in Augmentation of Convective Heat Transfer.' *experimental Heat Transfer, Fluid Mechanics an Thermodynamics*, pp. 502- 510

[7] Oppenheim, A.K. and Chilton, E.G. (1953) 'Pulsating- Flow measurement A Literature survey.' *Transaction of the ASME*, Paper No. 53- A - 157, pp. 231 - 248.

[8] Gerrard, J.H. (1971) 'An experimental Investigation of Pulsating Turbulent Water Flow in a Tube.' *Journal of Fluid Mechanics*, Vol. 46, pp. 43 - 64.

[9] Clamen,M. and Minton, P. (1977) 'An Experimental Investigation of Flow in an Oscillating Pipe.' *Journal of Fluid Mechanics*, Vol. 81, pp. 421 - 431.

[10] Shemer, L. , Wygnaski, I. And Kit, E. (1985) 'Pulsating Flow in a Pipe.' *Journal of Fluid Mechanics*, Vol. 153, P. 313 - 337.

[11] Eckmann, D.M. and Grotberg, J.B. (1991) 'Experiments on Transition to Turbulence in Oscillatory Pipe Flow.' *Journal of Fluid Mechanics*, Vol. 222 pp. 329 - 350.

[12] West, F.B. and Taylor A.T. (1952) 'The Effect of Pulsations on Heat Transfer in Turbulent Flow of Water Inside Tubes.' *Chemical Engineering Progress*, Vol. 48, No.1, pp. 39 - 43.

[13] Karamercan, O.E. and Gainer, J.L. (1979) 'The Effect of Pulsation on Heat Transfer.' *Industrial Engineering Chem. Fundamentals*, Vol. 18, pp. 11-15

[14] Liao N.S. and Wang C.C. (1985) 'An Investigation of Heat Transfer in Pulsating Turbulent Pipe Flow.' *Fundamentals of Forced and Mixed Convection*, The 23rd National Heat Transfer Conference, Denver, Co. U.S.A, Aug. 4 -7. pp. 53 - 59.

[15] Mamayev, V.V. Nosov, V.S. and Syromyatnikov, N.I. (1976) 'Investigations of Heat Transfer in Pulsed Flow of Air in the Pipes.' *Heat Transfer- Soviet Research*, Vol. 8, No. 3, pp. 111 - 116.

[16] Ohmi, M. Osui, T., Tanaka, O. and Toyama, M. (1976) 'Pressure and Velocity Distributions in Pulsating Turbulent Pipe Flow.' *Bulletin of Japanese Society of Mechanical Engineers*, Vol. 19, No. 134, pp. 951 - 957.

[17] Iguchi, M. and Miura, H (1989) 'Radial Propagation of Turbulence in Pulsatile Pipe Flow.' *JSME International Journal*, Vol. 32, No.2, pp. 173 - 179.

[18] Genin, L.G., Koval, A.P., Manchkha, S.p and Sviridov, V.g. (1992) 'Hydrodynamics and Heat transfer with Pulsating Fluid flow in Tubes.' *Thermal Engineering*, Vol. 39, No. 5, pp. 30 - 34.

[19] Einav, S. and Sokolov, M. (1993) 'An Experimental Study of Pulsatile Pipe Flow in the Transition Range.' *Transactions of the ASME*, Vol. 115, pp. 404 - 411

[20] Carvalho, J.A. (1995) 'Behavior of Solid Particles in Pulsating Flows.' *Journal of Sound and Vibration*, Vol. 185, No. 4, pp. 581 - 593.

[21] Siegel, R. and Perlmutter, M. (1962) 'Heat Transfer for Pulsating Laminar Duct Flow., *Journal of Heat Transfer*, May, pp. 111 - 123.

[22] Mochizuki, S. (1976) 'Heat Transfer for Pulsating Laminar Flow in a Circular Tube.' *Heat Transfer, Japanese Research*, Vol. 5, N 3, pp. 51 - 74.

[23] Faghri, M., Javdani, K. and Faghri, A. (1979) 'Heat Transfer with Laminar Pulsating Flow in a Pipe.' *Letters in Heat and Mass Transfer*, Vol. 6, No. 4, pp. 259 - 270.

[24] Krishnan, K.N. and Sastri, V.M.K. (1989) 'Heat Transfer in laminar Pulsating Flows of Fluids with Temperature Dependent Viscosities.' *Warme - und Stoffubertragung*,Vol. 24, pp. 37- 42.

[25] Cho, H.W and Hyun, J.M. (1990) 'Numerical Solutions of Pulsating Flow and Heat Transfer Characteristics in a Pipe.' *International Journal of Heat and Fluid Flow.*, Vol. 11, No. 4, pp. 321 - 330.

[26] Kim, S.Y, Kang, B.H. and Hyun, J.M. (1993) 'Heat Transfer in the Thermally Developing Region of a Pulsating Channel Flow.' *International Journal of Heat and mass Transfer*, Vol. 36, No. 17, pp. 4257- 4266.

[27] Martinelli, R.C., Boelter, L.M.K, Weinberg, E. B., and Yakahi, S (1943) 'Heat Transfer to a Fluid Flowing Periodically at Low frequencies in a Vertical Tube.' *Transaction of ASME*, Oct, pp. 789 - 798.

[28] Havemann, H.A. and Rao, N.N. (1954) 'Heat Transfer in Pulsating Flow.' *Nature*, Vol. 7, No. 4418, pp. 41.

[29] Lemlich, R. (1961) 'Vibration and Pulsation Boost Heat Transfer.' *Chemical Engineering*, May, pp. 171 - 176.

[30] Lemlich, R. and Hwu, C. (1961) 'The Effect of Acoustic Vibration on Forced Convective Heat Transfer.' *A.I. Ch. E. Journal*, Vol. 7, No. 1, pp. 102 - 106.

[31] Baird, M.H.I, Duncan, G.J., Smith, J.I and Taylor, J. (1966) 'Heat Transfer in Pulsed Turbulent Flow.' *Chemical Engineering Science*, Vol. 21, pp. 197 - 199.

[32] Krishnan, K.N. and Sastri, V.M.K. (1982) 'Pulsating Flows in Heat Exchangers- an Experimental Study.' *Warme - und Stoffubertragung*, Vol. 16, pp. 169 - 173.

[33] Al- Haddad, A. and Al- Binally, N. (1989) 'Prediction of Heat Transfer coefficient in Pulsating Flow.' *International Journal of Heat and Fluid Flow*, Vol. 10, No. 2, pp. 131 - 133.

[34] Kang, B.H. , Lee, G.T. and Lee, C.S 'Heat transfer Characteristics in an Oscillating Flow of Stirling Engine Heat Exchangers.' *Proceeding of the 2nd JSME-KSME Thermal Engineering Conference*, pp. 19- 21.

[35] Tang, X. And Cheng, P. 'Correlations of the Cycle- Averaged Nusselt Number in a Periodically Reversing Pipe Flow.' *INT. Comm. Heat Mass Transfer*, Vol. 20, pp. 161- 172.

[36] Isshiki, S., Obata, T., Kasagi, N., Hirata, M. (1993) 'Experimental Study on Heat Transfer in a Pulsating Pipe Flow.' *Nipon Kikai Gakkai Ronbunshu, B Hen / Trans. J.S.M.E*, Part B, Vol. 59, No. 563, pp. 145 - 151.

[37] Mizushina, T., Maruyama, T., Shiozaki, Y. (1973) 'Pulsating Turbulent Flow in a Tube.' *Journal of Chemical Engineering*, Japan , Vol. 8, pp. 210- 216.

[38] Ramaprian, B.R. and Tu, S.W. (1983) 'Fully Developed Periodic Turbulent Pipe Flow- Part 2 : The Detailed Structure of the Flow' *Journal of Fluid Mechanics*, Vol. 137, pp. 59 - 81.

[39] Schlitching H. (1991) 'Boundary Layer Theory' , Seventh Edition, *McGraw-Hill Book Company*. N.Y.

[40] Stearns, R.F., Jhonson, R.R., Jackson, R.M. and Larson, C.A. (1951) 'Flow Measurements with Orifice Meters' *D. Van Nostrand Company, Inc.*, New - York.

[41] Babus'haq, R.F. (1993) 'Forced Convection Heat Transfer in The Entrance Region of Pipes.' *International Journal of Heat and Mass Transfer*, Vol. 36, No. 13, pp. 3343 - 3349.

[42] Holman, J.P. (1984) 'Experimental Methods for Engineers', 4th Edition. *McGraw- Hill Book Company*, New York.

[43] Kays, W.M. and Crawford, M.E. (1980) 'Convective Heat Mass Transfer', 2nd Edition. *McGraw- Hill Book Co.*, New-York, U.S.A.

[44] Boelter, L.M.K, Young, G. and Iversen, H.w.,(1975) 'Distribution of Heat Transfer Rate in The Entrance Section of A Circular Tube.' *NACA*, TN No.1451, pp. 1-53.

[45] Gbadebo, S.A. (1996) 'An Experimental Investigation of Heat Transfer in the Thermally Developing Region of a Pulsating Pipe Flow', M.S. Thesis,*KFUPM*, Saudi Arabia, Dhahran 31261.

Vita

- Salem Ahmed Al-Dini
- Received Bachelor's degree in Mechanical Engineering from King Fahd University of Petroleum and Minerals, Dhahran, Saudi Arabia in January, 1994
- Finished all the requirments of the Master degree in Mechanical Engineering from King Fahd University of Petroleum and Minerals, Dhahran, Saudi Arabia in August, 1997.

IMAGE EVALUATION
TEST TARGET (QA-3)

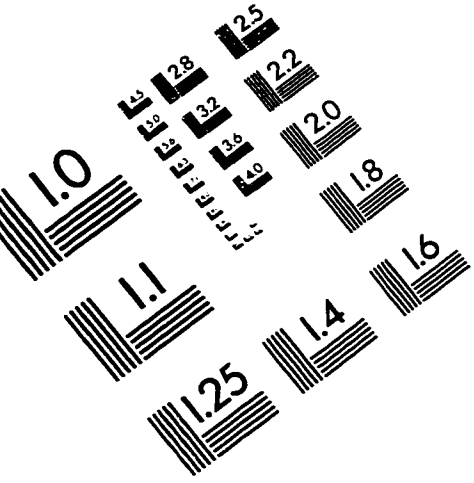

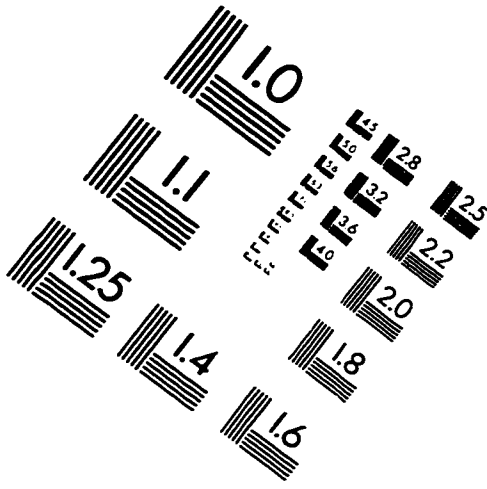

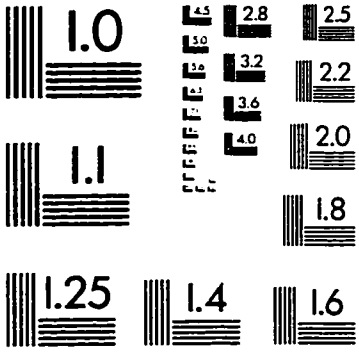

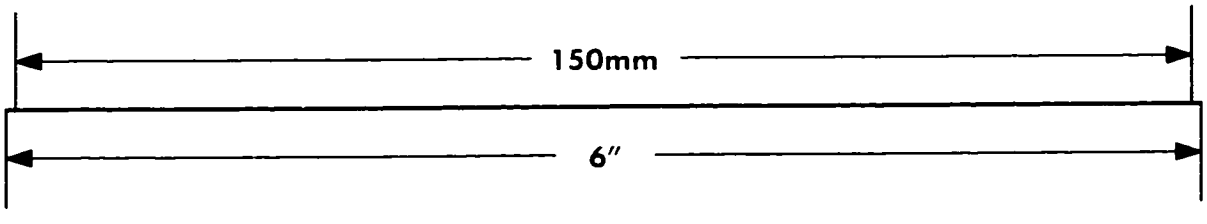

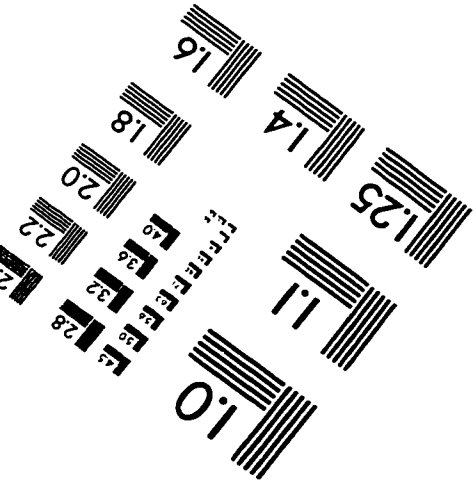

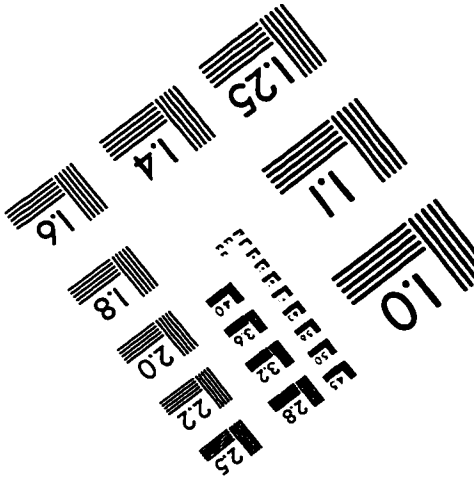

APPLIED IMAGE, Inc
1653 East Main Street
Rochester, NY 14609 USA
Phone: 716/482-0300
Fax: 716/288-5989

© 1993, Applied Image, Inc., All Rights Reserved